CONTRIBUTIONS TO PREDICTING CONTAMINANT LEACHING FROM SECONDARY MATERIALS USED IN ROADS

BY

DEFNE S. APUL

B.S., Boğaziçi University, 1997

M.S., Michigan Technological University, 2000

DISSERTATION

Submitted to the University of New Hampshire
In Partial Fulfillment of
the Requirements for the Degree of

Doctor of Philosophy
in
Civil Engineering

September 2004

This dissertation has been examined and approved.

_____

Dissertation Co-Director, Dr. Taylor T. Eighmy,
Research Professor of Civil Engineering

_____

Dissertation Co-Director, Dr. Kevin H. Gardner,
Research Associate Professor of Civil Engineering

_____

Dr. Tom Ballestero
Associate Professor of Civil Engineering

_____

Dr. Ernst Linder,
Professor of Statistics

_____

Dr. Jean Benoit,
Professor of Civil Engineering

_____

Date

DEDICATION

This dissertation is dedicated to my mom Nuran Demiröz who has throughout my life encouraged me to work hard and to find and realize my potential.

ACKNOWLEDGEMENTS

As a natural extension of my belief in the interconnectedness of the universe my gratitude goes to all the moments others and I have experienced due to countless events and individuals which have paved the way and led to the completion of this dissertation. Included in this acknowledgement are some individuals whose impacts on my Ph.D. work were easily noticeable.

I thank my committee members for their input on my Ph.D. research. Valuable discussions on hydrology with Tom Ballestero, detailed review and input by Jean Benoît on the pavement water movement work were extremely helpful and encouraging for me. I am grateful to Ernst Linder for advising me on the statistical aspects of my research. I have routinely met with Dr. Linder and Ms. Tara Frizzell to develop the method for applying Bayesian statistics to contaminant leaching problems. I truly appreciate their sincerity and the time they spared for this project.

The research outcome of this dissertation is closely linked to several people. Special thanks go to Ruth Roberson for sharing the data and working with me both on data analyses and modeling. I also thank Yannick Mercier, Tom Kurshinsky, and Jirka Simunek for their help on HYDRUS2D simulations.

Many others have indirectly contributed to this dissertation and my teaching career by making me happy through hugs, words of praise, encouragement, and sincerity. Thank you very much Mindy W., Melanie M-D., Jeannie S., Diane D., Süreyya and Serkan, Ayşen and Onur, Jeff M., Gabriel B., Harpa B., Gunvor N., Alison W., Colleen M., Bob, C., Vaso P., Emese H., Lee S. and Nancy K.. I have also truly enjoyed and benefited from being part of the Environmental Research Group and the Recycled Materials Resource Center and thank all of its members for their support and friendly faces and for not discouraging me when I wanted to play games.

My overwhelming thanks go to my immediate family for their support. I am grateful to Mehmet Koca, Asuman Apul, Refik Apul, Güven Apul, Fahrinaz Apul, and Melahat Apul for keeping me in their thoughts. I especially thank my mom, Nuran Demiröz for raising me and for her prayers which have magically helped me a lot. I thank Elifçe Coşar, Ediz Coşar, and Duru Coşar for the fun times we shared last year.

I could not have done without the unconditional love of my dear husband, Tolga. Thank you, Tolgi for making me laugh, thank you for all the support and fun and games, and thank you for picking up the slack when I was always busy with work. You enrich and balance a huge portion of my life.

My Ph.D career has been extremely fulfilling because of my co-advisors Kevin Gardner and Taylor Eighmy. I thank them for being great role models for me both in research and in other aspects of the daily life. They have artistically molded my research and social skills and ethics and have turned me into a self confident scholar with a potentially very promising future. Thank you both for encouraging and supporting me on anything I wanted to do including attending conferences, organizing a workshop, making connections, teaching, and publishing. Thank you, Kevin, for teaching me about priorities and keeping an open door all the time. Thank you, Taylor, for being available when I needed you including the times you cheered me up when I was feeling down. Also, thank you very much for patiently making sure that my capitalization was all correct in anything that I worked on.

TABLE OF CONTENTS

LIST OF TABLES

LIST OF FIGURES

ABSTRACT

CONTRIBUTIONS TO PREDICTING CONTAMINANT LEACHING FROM SECONDARY MATERIALS USED IN ROADS

BY

Defne Apul

University of New Hampshire, September 2004

Slags, coal ashes, and other secondary materials can be used in road construction. Both traditional and secondary materials used in roads may contain contaminants that may leach and pollute the groundwater. The goal of this research was to further the understanding of leaching and transport of contaminants from pavement materials. Towards this goal, a new probabilistic framework was introduced which provided a structured guidance for selecting the appropriate model, incorporating uncertainty, variability, and expert opinion, and interpreting results for decision making. In addition to the framework, specific contributions were made in pavement and embankment hydrology and reactive transport, Bayesian statistics, and aqueous geochemistry of leaching.

Contributions on water movement and reactive transport in highways included probabilistic prediction of leaching in an embankment, and scenario analyses of leaching and transport in pavements using HYDRUS2D, a contaminant fate and transport model. Water flow in a Minnesota highway

embankment was replicated by Bayesian calibration of hydrological parameters against water content data. Extent of leaching of Cd from a coal fly ash was estimated. Two dimensional simulations of various scenarios showed that salts in the base layer of pavements are depleted within the first year whereas the metals may never reach the groundwater if the pavement is built on adsorbing soils. Aqueous concentrations immediately above the groundwater estimated for intact and damaged pavements can be used for regulators to determine the acceptability of various recycled materials.

Contributions in the aqueous geochemistry of leaching included a new modeling approach for leaching of anions and cations from complex matrices such as weathered steel slag. The novelty of the method was its simultaneous inclusion of sorption and solubility controls for multiple analytes. The developed model showed that leaching of SO_4, Cr, As, Si, Ca, Mg, and V were controlled by corresponding soluble solids. Leaching of Pb was controlled by $Pb(VO_4)_3$ solubility at low pHs and by surface precipitation reactions at high pHs. Leaching of Cd and Zn were controlled by surface complexation and surface precipitation, respectively.

CHAPTER 1

INTRODUCTION

OBJECTIVES

Coal ashes, steel making and blast furnace slags, reclaimed asphalt and concrete pavement, municipal solid waste incinerator ash, and roofing shingle waste are examples of secondary materials that have been used in road construction. There is also potential for use of other secondary materials such as contaminated sediments in road construction. Potential leaching of contaminants from secondary materials is a major concern for regulators and sometimes forms a barrier to its widespread use. The goal of this research was to further the understanding of the source term for leaching of contaminants from secondary materials used in roads. More specifically, the objectives were to investigate relevant release and transport processes and develop new approaches for regulators to predict the fluxes of contaminants leaving the secondary materials and entering the groundwater.

DISSERTATION ORGANIZATION

Each chapter of this dissertation was written as a self-contained individual paper focusing on a topic that had not been addressed before. Contributions are in the areas of pavement hydrology (Chapter 2), probabilistic decision making tools for regulators (Chapter 3), Bayesian statistics, hydrology and reactive

transport in embankments (Chapter 4), aqueous geochemistry of leaching (Chapter 5), and two dimensional scenario analyses of unsaturated hydrology and leaching and transport of contaminants from pavements (Chapter 6).

Chapter 2 is a summary of the state of knowledge on water movement in the highway environment. A more extensive version of Chapter 2 is published online at "http://www.rmrc.unh.edu/Research/Rprojects/Project7/review/watermovement.pdf". The major information learned from Chapter 2 is that there exists very limited knowledge about the hydraulic regimes in the pavement and the (unsaturated) hydraulic properties of pavement materials, especially the secondary materials. The needs for research identified in Chapter 2 are addressed in Chapters 4 and 6 which discuss in detail the variably saturated flow in pavements and embankments.

Chapter 3 begins the discussion of contaminant release and transport calculations. Three different areas of research identified are; probabilistic methods, two dimensional modeling, and detailed geochemical modeling. In Chapter 3, a new probabilistic framework for evaluating the environmental acceptability of candidate secondary materials is introduced. The framework developed provides a structured guidance for selecting the appropriate model, incorporating uncertainty, variability, and expert opinion, and interpreting results for decision making. The new framework introduced in Chapter 3 is applied to embankment modeling in Chapter 4, which describes the field hydrology and

leaching from coal fly ash in embankments using a Bayesian approach and a finite element model, HYDRUS2D.

Chapter 5 is an original contribution in the geochemistry of leaching in weathered steel slags. Whereas the remainder of the dissertation emphasizes hydrology, pavement geometry, and probability, in Chapter 5 the leaching mechanisms at the micro scale in local equilibrium conditions are explored. In Chapter 5, a new modeling approach for contaminant release is developed that considers the complex interactions of ions with other ions, sorptive surfaces, and pure precipitates.

Chapter 6 discusses leaching and transport in pavements in two dimensions, in the cross section of a highway, by analyses of HYDRUS2D modeling results. The pioneering aspect of Chapter 6 is its documentation of leaching and transport of contaminants in two dimensions with explicit consideration of spatial and temporal scales including pavement geometry and rain intensity. Chapter 6 also provides a generic tool for regulators for evaluating the acceptability of secondary materials based on source term calculations.

Chapter 2 has been published in a peer-reviewed book whereas the other chapters have been published or submitted for publication in peer-reviewed journals. The appropriate citations are as follows:

Chapter 2:

Apul, D.S., Gardner, K, Eighmy, T., Benoit, J., and Brannaka, L. (2003) “A review of water movement in the highway environment: Implications for recycled

materials use," *in Beneficial Use of Recycled Materials in Transportation Applications,* T.T. Eighmy Ed., Air and Waste Management Association Press, p195-204.

Chapter 3:

Apul, D.S., Gardner, K., and Eighmy, T. (2003) "A probabilistic source assessment framework for leaching from recycled materials in highway applications," Clean Technologies and Environmental Policy, 5(2), p120-127.

Chapter 4:

Apul, D.S., Gardner, K., Eighmy, T., Linder, E., Frizzell, T., and Roberson, R. "Probabilistic modeling of one dimensional water movement and leaching from highway embankments containing secondary materials," in press Environmental Engineering Science.

Chapter 5:

Apul, D.S., Gardner, K., Eighmy, T., Comans R., and Fallman A-M. "Simultaneous application of dissolution/precipitation and surface complexation / precipitation modeling to contaminant leaching from weathered steel slag," submitted to Environmental Science and Technology.

Chapter 6:

Apul, D.S., Gardner, K., and Eighmy, T. "Modeling hydrology and reactive transport in roads: The effect of cracks, the edge, and contaminant properties," in preparation for Waste Management.

CHAPTER 2

A REVIEW OF WATER MOVEMENT IN THE HIGHWAY ENVIRONMENT: IMPLICATIONS FOR RECYCLED MATERIALS USE

ABSTRACT

Both traditional and recycled materials used in pavements may contain contaminants that have the potential to leach and pollute the groundwater. To assess the environmental impact of traditional and recycled materials the hydraulic regimes within the pavement need to be known. The purpose of this study was to review the literature and determine the state of knowledge on water movement in the highway environment, so that this knowledge may be incorporated in studies examining the potential of leaching and transport of organic and inorganic contaminants. The information compiled and presented in this paper includes water routes, water content, and saturated and unsaturated hydraulic conductivity of pavement materials.

INTRODUCTION

Water movement in pavements has been traditionally studied by pavement engineers to understand the relationship between moisture in the pavement and pavement integrity. It is well accepted that moisture shortens pavement life. Water pumping and freeze-thaw phenomena are two examples causing pavement damage in the form of cracking, rutting, and stripping. To examine damaging effects of moisture, water regimes in pavements need to be known. Thus, most of the information about water movement in pavements in the literature has been reported with the intent to understand the moisture removal and moisture damage in pavements.

A new interest in water movement in pavements has stemmed from researchers interested in assessing the environmental impact of beneficial use of recycled materials in roadways. The potential for leaching of inorganic and organic contaminants in materials used in roadways or wastes disposed of in landfills needs to be determined to assess the risk posed by utilization or disposal. However, the contaminant release mechanism and contaminant transport depends on the hydraulic regime. Thus, a rigorous study on field leaching and environmental impact assessment should incorporate knowledge on hydraulic regimes.

Contaminant release depends on contaminant solubility, diffusion, and advection. As contaminants solubilize, they diffuse within the particle pore space

and across the aqueous boundary layer that surrounds the particle. The contaminant release continues until the aqueous solution is saturated with that particular contaminant. If the hydraulic regime is governed by “fast” fluxes, advection will quickly remove the released contaminant from the source, thereby leaving the solution unsaturated and allowing more release. If advection is slow, such as in a slow percolation system across unbounded materials, then the solubility may govern the maximum concentration of release. In granular materials (base course, embankments) the release is more often controlled by solubility. In monolithic systems (asphalt concrete, Portland cement concrete(PCC)), the rate limiting step in release of contaminants is more typically diffusion. Researchers examining contaminant release from waste materials often assume that release is either solubility/availability limited or diffusion limited. However, in real life, the limiting factor may vary temporally depending on the hydraulic regime. Considering that leaching cannot be fully described without the knowledge on the hydraulic regimes, development of studies in water movement in roadways will grow and take a new path with involvement of environmental researchers in addition to transportation engineers.

A limited volume of literature exists on water movement in pavements, particularly ones containing recycled materials. A literature review was conducted to compile all information available on water movement in pavements for the purpose of understanding hydraulic regimes dictating leaching. This paper summarizes the information available about water movement in

pavements. First ingress and egress routes of water and water content are discussed. Then, a summary of the hydraulic conductivity of asphalt concrete, PCC, and base/subbase layers is presented. Considerably less information was available on recycled materials than traditional materials. The hydraulic conductivity of concrete and embankments containing recycled materials is discussed briefly. Finally, the importance of unsaturated hydraulic conductivity is discussed.

WATER ROUTES AND WATER CONTENT

Current engineering practice in the U.S. is predicated on the fact that water enters the pavement despite efforts to prevent it. Elsayed and Lindly[1] note that until the study by Ridgeway,[2] high water table and capillary water were thought to be the primary causes of excess water in pavements. Recently, crack and shoulder infiltration, and to some extent subgrade capillary action, are considered to be the major routes of water entry to the pavement.[1,3] Van Sambeek[4] reported that surface water infiltration could account for as much as 90 to 95 percent of the total moisture in a pavement system. Van Sambeek[4] and Ahmed et al.[5] identified transverse and longitudinal joints as major routes of water ingress and surface infiltration. For routes of egress, Dawson and Hill[3] note that the lateral or median drain is the most significant route. Thus, infiltration through cracks and joints is thought to be the major ingress route and engineered drainage is believed to be the major egress route.

The volumetric water content in the pavement varies considerably (3-45%) not only because of material or design differences but also because of spatial differences such as lateral variability including edge effects along the shoulders or wheel path location[6,7] or vertical variability.[8] Temporal variability of water content in the field in the short term based on precipitation events[9] or in the long term based on seasons[10] or time passed after construction[11] has also been reported. The high variability in water content indicates that both saturated and unsaturated conditions occur in the field.

SATURATED HYDRAULIC CONDUCTIVITY

The wide range of hydraulic conductivity values reported in the literature for pavement sections and embankments can be attributed to differences in designs and measurement techniques. The measurements should be done at small hydraulic gradients (less than 0.05 or 0.075) to better simulate field conditions.[12,13] Considering that bases and subbases may be predominantly subject to horizontal flow rather than vertical flow, measurement of the horizontal hydraulic conductivity in addition to the vertical hydraulic conductivity may be appropriate.[14,15,16]

Many researchers showed that it is difficult to establish a linear relationship between porosity and hydraulic conductivity[17-19] because many factors such as interconnectivity (e.g. some air voids are trapped by asphalt and mineral fillers), shape, and size of voids affect the hydraulic conductivity.[20] Still,

the porosity of asphalt concrete has been used to categorize it as impermeable (below 6-7 percent porosity) or free draining (>15 percent porosity).[21] Terrel and Alswailmi[17] note that both the impermeable and the free draining asphalt concrete have significant advantages such as higher strength and less susceptibility to moisture damage over the medium void range asphalt concrete, which is typically used in the United States. Porous asphalt pavements with better skid resistance in wet weather are common in Europe and are also in use in the United States. For these types of pavements, susceptibility of porous asphalt mixtures to clogging may be of concern if the road is used by vehicles that have dirty wheels or carry earth.[22]

In PCC, the pores exist in the cementitious matrix of concrete and in the interfacial regions with aggregate.[23] Similar to the asphaltic concrete, the hydraulic conductivity of PCC is also more complex than a simple function of porosity. There is some evidence that the hydraulic conductivity of concrete may be more closely related to the pore volume over a certain threshold value of diameter (e.g. 500 or 1000nm) rather than to the mean diameter of pores or total porosity.[24] The hydraulic conductivity of concrete, which depends on the size, distribution and continuity of pores and total porosity is modified during the hardening of concrete. Bakker[25] describes the fresh concrete as a granular structure with continuous capillary pores. During the hardening period the hydration products glue the particles together and block the capillary pores. These processes increase the strength of the material and decrease the

hydraulic conductivity. The hydraulic conductivity of hardened concrete also depends on the temperature during hydration. Higher curing temperatures increase the hydraulic conductivity of PCC if traditional (as opposed to recycled) materials are used.[25] Thus, the type of raw materials (cementitious materials and chemical admixtures) used, the type and extent of chemical reactions during hardening, and curing temperature affect pore size distribution and hydraulic conductivity of PCC.

The hydraulic conductivity of asphalt concrete and PCC may vary eight orders of magnitude because of different designs.[17-20,22,26-29] Typically, the hydraulic conductivity of PCC ($<10^{-7}$cm/s) is less than the hydraulic conductivity of dense graded asphalt (10^{-2}-10^{-4}cm/s), Superpave asphalt (10^{-5}-10^{-1}cm/s), and porous asphalt concrete (10^{-2}-10^{1}cm/s). Less data was found on the hydraulic conductivity of PCC possibly because PCC is assumed to be essentially impermeable. However, if there is cracking, the hydraulic conductivity of the asphalt concrete or PCC may vary significantly depending on the width, depth, and spacing of the cracks.

For adequate drainage, many sources agree that the hydraulic conductivity of the base layer should be at least 0.34cm/s.[30-33] The compiled hydraulic conductivity data of base/subbase layers varied almost four orders of magnitude both below and above this value because both free draining and impermeable bases are currently used.[1,5,,9,12,15,34-39] The hydraulic conductivity values reported for stabilized base layers (10^{-4}-10^{3}cm/s) were not necessarily

always higher or lower than the hydraulic conductivity of unstabilized base layers (10^{-4}-10^{2}cm/s).

If the hydraulic conductivity of the base material cannot be measured, one approach to estimate the hydraulic conductivity is to examine the gradation curve of the material (percent passing as a function of sieve size). The gradation is important because the extent of fines in the material considerably affect the hydraulic conductivity.[40] Cedergren charts and Moulton nomographs, the two common methods for estimating the hydraulic conductivity of aggregate base layers from the gradation curve, have been updated by another empirical relationship given by Lindly and Elsayed.[37] To estimate the hydraulic conductivity of asphalt or Portland cement stabilized bases, Lindly and Elsayed provide a regression that uses the percent asphalt cement and porosity information in addition to the gradation curve.[37] However, the correlation is for open-graded materials and may not be useful for dense-graded asphalt-treated bases. Yet, since the addition of two to three percent asphalt cement has markedly less effect on hydraulic conductivity than the aggregate gradation, approaches used for untreated bases may closely approximate the coefficient of hydraulic conductivity for treated bases.[41]

It is difficult to generalize the effect of recycled materials on hydraulic conductivity of pavement layers or embankments. Compared to Portland cement paste, introduction of mineral by-products results in different hydraulic conductivity and pore structure in the concrete. Before and during hardening, the

hydraulic conductivity of concretes containing slag or fly ash is greater than that of Portland cement concrete. However, once the reactions are complete the reverse is observed.[42] Similarly, laboratory studies by Feldman,[43] Ozyildirim,[44] and Bakker,[25] respectively show that (1) hydrated blended cement has lower hydraulic conductivity than hydrated Portland cement and that (2) concretes containing a pozzolan or slag have lower long-term hydraulic conductivity than the control, and (3) that blast furnace cement and cement containing fly-ash has lower hydraulic conductivity than Portland cement. Virtanen[45] and Pigeon and Regourd[46] note that the air content of concrete containing slag, fly ash or silica fume is smaller relative to the air content of pure cement mixes. On the contrary, laboratory experiments by Nakamoto[24] suggest (1) that higher slag content in PCC may result in increased porosity and hydraulic conductivity, and (2) that the water tightness may be improved by utilizing more fine slag. With the exception of Nakamoto's[24] results, these studies suggest that addition of mineral by-products to Portland cement mix decreases the hydraulic conductivity of the concrete. Fineness of the by-product may also affect hydraulic conductivity.

There is some literature on the use of recycled materials in embankments, however most of these focus on strength and workability of the material rather than its hydraulic conductivity. Kim et al.[47] present a knowledge-based expert system for utilization of solid flue gas desulfurization by-product (a coal combustion by-product) in highway embankments and note that the hydraulic conductivity of solid flue gas desulfurization by-product may range from 3.1×10^{-9}

to 1.6×10^{-4} cm/s at 28-day curing while its hydraulic conductivity in place may gradually decrease with aging. Partridge et al.[48] note that compacted waste foundry sand used in embankments is not a free draining material. Its laboratory and field hydraulic conductivity ranges from 0.1×10^{-5} to 7.1×10^{-5} cm/s. Bhat and Lovell[49] examine the design of flowable fill by using waste foundry sand as a fine aggregate. They note that the hydraulic conductivity of flowable fill is low (2.6×10^{-6} – 1.2×10^{-5} cm/s) and that the hydraulic conductivity does not necessarily decrease with increasing contents of fly ash possibly because the advantage from the fine particle size of fly ash is outweighed by the uniform spherical shape of these particles.

UNSATURATED HYDRAULIC CONDUCTIVITY

The constitutive equation used in water flow models for variably saturated media is the well known Richards equation, which is based on a mass balance of water over a unit volume with Darcy's law substituted for water flux. However, the hydraulic conductivity in Darcy's law is not a single value but is a nonlinear function of water content or pressure head. Thus, to model variably saturated water flow using Richards equation the relation between hydraulic conductivity and water content should be known. Another soil specific property is the soil moisture retention curve, which describes the relation between the water content and pressure head. If a general mathematical model for soil moisture retention curve is established for a specific porous medium, estimation of unsaturated

hydraulic conductivity as a function of water content or pressure head is made easier. Thus, for estimation of unsaturated hydraulic conductivity, characterization of the soil moisture retention curve is essential.

Many empirical relationships have been derived for a general description of the soil moisture retention curve.[50-53] Typically, these empirical equations relating water content to pressure head involve residual water content, saturated water content, and some fitting parameters. The most common equation that is often implemented in numerical variably saturated water flow models is the one derived by van Genuchten.[52] However, to the authors' knowledge, applicability of this model or any other models to recycled materials has not been tested. In addition, parameters needed for these models have been documented for various soil types but not for recycled materials. Determination of the fitting parameters by measuring the soil moisture retention curve is time consuming and thus costly. However, forward modeling of unsaturated water flow through recycled materials is almost impossible without any information on these parameters. Preliminary modeling results using HYDRUS2D to predict edgedrain outflow and water content in a pavement test cell section in Minnesota also suggested that the model was highly sensitive to the fitting parameters (unpublished data). Thus, prerequisite to understanding water flow through pavements containing recycled materials is the knowledge on soil moisture retention curve and the fitting parameters for recycled materials.

CONCLUSIONS

The lack of information on water movement through pavements with and without recycled materials needs to be compensated to be able to accurately assess the environmental impact of traditional and recycled materials. The literature review on water movement identified infiltration through cracks and joints as the major ingress routes and engineered drainage as the major egress route. The literature review showed that both saturated and unsaturated conditions occur in the field and the variability in water content can be attributed to spatial and temporal differences. To be able to model the variably saturated water flow through pavements, knowledge on hydraulic conductivity of the medium is necessary. Saturated hydraulic conductivity of asphalt concrete, PCC, base and subbase layers vary significantly (from less than 10^{-7}cm/s to 10^{3}cm/s) because of different designs. Use of recycled materials in PCC and embankments may lower the hydraulic conductivity of the material. In addition to saturated hydraulic conductivity, unsaturated hydraulic conductivity of pavement materials should also be investigated. There is a significant need for determination of soil moisture retention curves of both traditional and recycled materials.

ACKNOWLEDGMENTS

This work was funded through a cooperative agreement (DTFH61-98-X-00095) between FHWA and the University of New Hampshire.

REFERENCES

1. Elsayed, A. S., and Lindly, J. K. (1996). "Estimating permeability of untreated roadway bases." *Transportation Research Record*, 1519, 11-18.

2. Ridgeway, H. H. (1982). "National Cooperative Highway Research Program Synthesis of Highway Practice 96: Pavement Drainage Systems.", NCHRP.

3. Dawson, A. R., and Hill, A. R.(1998) "Prediction and implication of water regimes in granular bases and subbases." *International Symposium on Subdrainage in Roadway Pavements and Subgrades*, Granada, Spain, 121-129.

4. van Sambeek, R. J. (1989). "Synthesis on subsurface drainage of water infiltrating a pavement structure.", Braun Pavement Technologies, St. Paul.

5. Ahmed, Z., White, T. D., and Kuczek, T. (1997). "Comparative field performance of subdrainage systems." *Journal of Irrigation and Drainage Engineering*, 123(3), 194-201.

6. Gordon, R. G., and Waters, T. J. "A Case study of performance of pavements on an expansive soil subgrade." *5th International Conference on Expansive Soils*, Adelaide, South Australia, 263-269.

7. Houston, S. L., Houston, W. N., and Anderson, T. W. (1995). "Moisture and strength variability in some Arizona subgrades." *Transportation Research Record*, 1481, 35-46.

8. Rainwater, N. R., and Yoder, R. E. (1999). "Comprehensive monitoring systems for measuring subgrade moisture conditions." *Journal of Transportation Engineering*, 125(5), 439-448.

9. Birgisson, B., and Roberson, R. (2000). "Drainage of pavement base material: Design and construction issues." *Transportation Research Record*, 1709, 11-18.

10. Andrew, J. W., Jackson, N. M., and Drumm, E. C. (1998) "Measurement of seasonal variations in subgrade properties." *Application of geotechnical principles in pavement engineering*, Boston, MA, USA, 13-38.

11. Look, B. G., Reeves, I. N., and Williams, D. J. "Application of time domain reflectometry in the design and construction of road embankments." *Symposium and Workshop on Time Domain Reflectometry in Environmental, Infrastructure, and Mining Applications*, Evanston, IL, 410-421.

12. Tandon, V., and Picornell, M. (1997). "Proposed evaluation of base materials for drainability." *Transportation Research Record*, 1596, 62-69.

13. Jones, J. A., and Jones, R. H. "Granular drainage layers in pavement foundations." *UNBAR3, Unbound Aggregates in Roads*, 55-69.

14. Moynahan, T. J., and Sternberg, Y. M. (1974). "Maryland Drainage Study: Vol. VII - An Investigation of vertical and horizontal hydraulic conductivities in base courses.", University of Maryland, College Park.

15. Randolph, B. W., Steinauser, E. P., Heydinger, A. G., and Gupta, J. D. (1996). "In situ test for hydraulic conductivity of drainable bases." *Transportation Research Record*, 1519, 36-40.

16. Li, Z., and Chau, C.-K. (2000). "New water permeability test scheme for concrete." *ACI Materials Journal*, 97(1), 84-90.

17. Terrel, R. L., and Al-Swailmi, S. (1993). "Role of pessimum voids concept in understanding moisture damage to asphalt concrete mixtures." *Transportation Research Record*, 1386, 31-37.

18. Choubane, B., Page, G. C., and Musselman, j. A. (1998). "Investigation of water permeability of coarse graded superpave pavements." *Asphalt Paving Technology*, 67, 254-276.

19. Cooley, L. A., and Brown, E. R. (2000). "Selection and evaluation of field permeability device for asphalt pavements." *Transportation Research Record*, 1723, 73-82.

20. Huang, B., Mohammad, L. N., Raghavendra, A., and Abadie, C. (1999). "Fundamentals of permeability in asphalt mixtures." *Asphalt Paving Technology*, 68, 479-500.

21. Kennedy, T. W. "Prevention of water damage in asphalt mixtures." *Evaluation and prevention of water damage to asphalt pavement materials*, Philadelphia, 119-133.

22. Fwa, T. F., Tan, S. A., and Guwe, Y. K. (1999). "Laboratory evaluation of clogging potential of porous asphalt mixtures." *Transportation Research Record*, 1681, 43-49.

23. Roy, D. M., Shi, D., Scheetz, B., and Brown, P. W. "Concrete microstructure and its relationships to pore structure, permeability, and general durability." *Durability of Concrete - G. M. Idorn International Symposium*, 139-152.

24. Nakamoto, J., Togawa, K., Miyagawa, T., and Fujii, M.(1998) "Water permeability of high slag content concrete." *Fly ash, silica fume, slag and natural pozzolans in concrete*, Bangkok, 779-798.

25. Bakker, R. F. M. "Permeability of blended cement concretes." *Fly Ash, Silica Fume, Slag and Other Mineral By-Products in Concrete*, Detroit, 589-605.

26. Lynn, T. A., Brown, E. R., and Cooley, L. A. (1999). "Evaluation of aggregate size characteristics in stone matrix asphalt and superpave mixtures." *Transportation Research Record*, 1681, 19-27.

27. Cooley, L. A., Brown, E. R., and Watson, D. E. (2000). "Evaluation of open-graded friction course mixtures containing cellulose fibers." *Transportation Research Record*, 1723, 19-25.

28. Cramer, S. M., and Carpenter, A. J. (1999). "Influence of total aggregate gradation on freeze-thaw durability and other performance measures of paving concrete." *Transportation Research Record*, 1668, 1-8.

29. Aldea, C.-M., Shah, S. P., and Karb, A. (1999). "Effect of microcracking on durability of high-strength concrete." *Transportation Research Record*, 1668, 86-90.

30. Baumgardner, R. H. (1992). "Overview of permeable bases." Materials:performance and prevention of deficiencies and failure, New York, 275-287.

31. FHWA. (1990). "Technical paper on subsurface pavement drainage." *Technical Paper 90-01*, Office of Engineering, Pavement Division, Federal Highway Administration, Washington.

32. Freeman, R. B., and Anderton, G. L. "Permeability versus unsurfaced stability." *Proceedings of the Materials Engineerng Conference Infrasturcture*, 685-692.

33. Mallela, J., Titus-Glover, L., and Darter, M. I. (2000). "Considerations for providing subsurface drainage in jointed concrete pavements." *Transportation Research Record*, 1709, 1-10.

34. Randolph, B. W., Cai, J., Heydinger, A. G., and Gupta, J. D. (1996). "Laboratory study of hydraulic conductivity for coarse aggregate bases." *Transportation Research Record*, 1519, 19-27.

35. Biczysko, S. J. "Permeable sub-bases in highway pavement construction." *2nd Symp. UNBAR*, Univ. of Nottingham, Dept. of Civil Eng., 81-82.

36. Kazmierowski, T. J., Bradbury, A., and Hajek, J. (1994). "Field evaluation of various types of open-graded drainage layers." *Transportation Research Record*, 1434, 29-36.

37. Lindly, J. K., and Elsayed, A. S. (1995). "Estimating permeability of asphalt-treated bases." *Transportation Research Record*, 1504, 103-111.

38. Manion, W. P., Humphrey, D. N., and Garder, P. E. (1995). "Evaluation of existing aggregate base drainage performance.", Maine Department of Transportation.

39. Koch, P. B., and Sandford, T. C. (1998). "Infiltration rate of water through pavement cracks.", Dept. of Civil and Env. Eng., University of Maine, Orono, Maine.

40. Lytton, R. L., Pufahl, D. E., Michalak, C. H., Lian, H. S., and Dempsey, B. J. (1993). "An integrated model of the climatic effects on pavements.", Texas Transportation Institute, Texas A&M University, Texas.

41. Mathis, D. M. (1990). "Permeable bases prolong pavement, studies show." *Roads & Bridges*, 28(5), 33-35.

42. Berry, E. E., and Malhotra, V. M. (1978). "Fly ash for use in concrete, Part II - A critical review of the effects of fly ash on the properties of concrete." *CANMET Report 78-16*, Canada Center for Mineral and Energy Technology.

43. Feldman, R. F. "Significance of porosity measurements on blended cement performance." *Fly Ash, Silica Fume, Slag and Other Mineral By-Products in Concrete*, Detroit, 415-433.

44. Ozyildirim, C. (1998). "Effects of temperature on the development of low permeability in concretes.", Virginia Transportation Research Council, Charlottesville.

45. Virtanen, J. "Freeze-thaw resistance of concrete containing blast-furnace slag, fly ash or condensed silica fume." *Fly Ash, Silica Fume, Slag and Other Mineral By-Products in Concrete*, Detroit, 923-41.

46. Pigeon, M., and Regourd, M. "Freezing and thawing durability of three cements with various granulated blast furnace slag contents." *Fly Ash, Silica Fume, Slag and Other Mineral By-Products in Concrete*, Detroit, 979-997.

47. Kim, S.-H., Wolfe, W. E., and Hadipriono, F. C. (1992). "The development of a knowledge-based expert system for utilization of coal combustion by-product in highway embankment." *Civil Engineering Systems*, 9, 41-57.

48. Partridge, B. K., Fox, P. J., Alleman, J. E., and Mast, D. G. (1999). "Field demonstration of highway embankment construction using waste foundry sand." *Transportation Research Record*, 1670, 98-105.

49. Bhat, S. T., and Lovell, C. W. (1996). "Design of flowable fill: waste foundry sand as a fine aggregate." *Transportation Research Record*, 1546, 70-78.

50. Gardner, W. R. (1958). "Some steady state solutions of the unsaturated moisture flow equation with application to evaporation from a water-table." *Soil Science*, 85, 228-232.

51. Brooks, R. H., and Corey, A. T. (1964). "Hydraulic properties of porous medium, Hydrology paper 3.", Colorado State University, Fort Collins.

52. van Genuchten, M. T. (1980). "A closed form equation for predicting the hydraulic conductivity of unsaturated soils." *Soil Science Society of America*, 44, 892-898.

53. Fredlund, D. G., Xing, A., and Huang, S. (1994). "Predicting the permeability function for unsaturated soils using the soil-water characteristic curve." *Can. Geotech. J.*, 31, 533-546.

CHAPTER 3

A PROBABILISTIC SOURCE ASSESSMENT FRAMEWORK FOR LEACHING FROM RECYCLED MATERIALS IN HIGHWAY APPLICATIONS

ABSTRACT

Recovered materials from the transportation sector or secondary or by-product materials from the industrial, municipal, or mining sector can be used as substitutes for natural materials in the construction of highway infrastructure. The environmental impact of traditional and newer secondary materials needs to be determined for the conditions of their expected use. The purpose of this paper is to introduce a probabilistic framework for evaluating the environmental acceptability of candidate secondary materials based on the risk of soil and groundwater contamination from leached metals and organics from the pavement. The proposed framework provides a structured guidance for selecting the appropriate model, incorporating uncertainty, variability, and expert opinion, and interpreting results for decision making. This new approach is illustrated by a probabilistic analysis of arsenic leaching from portland cement concrete and asphalt concrete materials that were constructed using virgin and secondary products.

RECYCLING IN THE TRANSPORTATION SECTOR

There are nearly six million kilometers of roads in the U.S. (FHWA, 1999). Construction and maintenance of these roadways require use of large volumes of materials. Problems with quarrying of natural materials in environmentally sensitive areas and the importance of promoting sustainable construction measures have increased interest in recycling (Eighmy and Magee, 2001; Schimmoller et al., 2000). There are promising results for equal or better engineering performance of recycled materials at comparable or less costs and without significant environmental impact (Deschamps, 1997; Pandey et al., 1995; Humphrey and Katz, 2000; Mahboub and Massie, 1996; Mulder, 1996; Partridge et al., 1999).

Numerous by-product and waste materials, produced in millions of metric tons per year, have the potential to be reutilized in roadway applications (Table 3.1). Among materials listed in Table 3.1, the U.S. has a history of use of recycled asphalt pavement, reclaimed concrete pavement, coal fly ash, coal bottom ash, blast furnace slag, and scrap tires. Other materials listed in Table 3.1 are not as commonly used even though there is significant potential for utilizing these materials in various roadway applications such as structural layers (asphalt concrete or Portland cement concrete, base, and subbase), embankments, landscape materials, and appurtenances (e.g. fences, signs, sound barricades, and drain pipes). This paper is concerned with secondary material use in

structural layers and embankments because much greater volumes are used in these applications than in appurtenances and landscaping.

Resources exist to aid in decision-making for use of secondary materials in construction and maintenance projects (Hyman and Johnson, 2000; Eighmy and Chesner, 2001). Yet, compared to Europe, there is still less than optimum recycling and reutilization in the roadway environment. For example, reclaimed asphalt pavement, blast furnace slag, coal bottom ash, coal fly ash, and municipal solid waste ash are completely being reutilized in the Netherlands and only partially or not at all reutilized in the U.S. (Schimmoller et al., 2000). A survey study of 50 state environmental protection agencies revealed that sparsity of environmental impact assessments for recycled materials is one major barrier to recycling (ASTSWMO, 2000)(Figure 3.1). Evaluation of environmental impact of relatively new secondary materials is especially important to determine if it is worthwhile to invest time and research in developing high quality engineering products out of these less traditional candidate materials. Environmental impact assessments may show which proposed beneficial uses are not appropriate and which are acceptable.

Table 3.1. Annual production and use of recycled materials (adapted from Collins and Ciesielski, 1994[(a)]; Schroeder, 1994[(b)]; Chesner et al., 1998[(c)]). U= Undetermined, MF = mineral filler, ACM = asphalt cement modifier, A = aggregate, CM = cementitious material, E = embankment or fill, and F = flowable fill.

Waste Materials	Production (million metric tons)	Recycled (million metric tons)	% Recycled	Highway Applications				
				Asphalt concrete	Portland cement concrete	Granular Base	Stabilized base	Other
Agricultural								
Crop wastes	362[a]	U	U	CM				
Lumber and wood wastes	64[a]	U	U					E
Domestic								
Incinerator ash	7.8[a] 7.3[b] 8[c]	<0.7[b] 0[c]	0-10	A		A	A	E
Sewage sludge ash	0.5-0.9[a,c]	U	U	MF,A	A			
Scrap tires	2.2[a] 2.3[b]	U	U	ACM,A				E
Glass and ceramics	11.3[a]12[b, c]	2.4[b] 3.2[c]	20-27	A		A		
Plastic waste	13.1[a] 14.7[b]	0.3[b]	2	ACM				
Industrial								
Coal ash – Fly ash	43.5[a] 45[b]	11[b]	24	CM	CM		CM	F, E
Coal ash - Bottom ash	12.7[a] 16[b] 14.5[c]	5.0[b] 4.3[c]	31	A		A	A	F, E
Coal ash – Boiler slag	3.6[a] 2.3[c]	2.1[c]	91	A		A	A	
Advanced SO_2 control by-products	4.5[a] 18.0[b] 21.4[c]	>1[c]	>5				A	E
Construction and demolition debris	22.7[a]	U	U			A		E
Blast furnace slag	14.1[a,c]	14.1[b,c]	100	A	CM, A	A		
Steel making slag	7.2[a] 7.5[b]	7.0-7.5[c]	96-100	A		A		E
Non ferrous slags	9.1[a] 7.6-8.1[c]	U	U	A	A	A		E
Cement and lime kiln dusts	12.9[c]	U	U	MF, A			CM	F
Bag house fines	5.4-7.2[c]	U	U	MF				
Reclaimed asphalt and concrete pavements	45[a,c] 94[b]	33[c]	73	A, ACM	A	A	A	E
Foundry sand	9.1[a] 9.0-13.6[c]	U	U	A				F
Roofing shingle waste	9.1[a] 8.1[b]10[c]	U	U	ACM, A				
Lime waste	1.8	U	U	MF				F
Petroleum contaminated soils, contaminated sediments	U	U	U	A, CM			ACM	
Mineral processing wastes	1 600[c]	U	U	A		A		

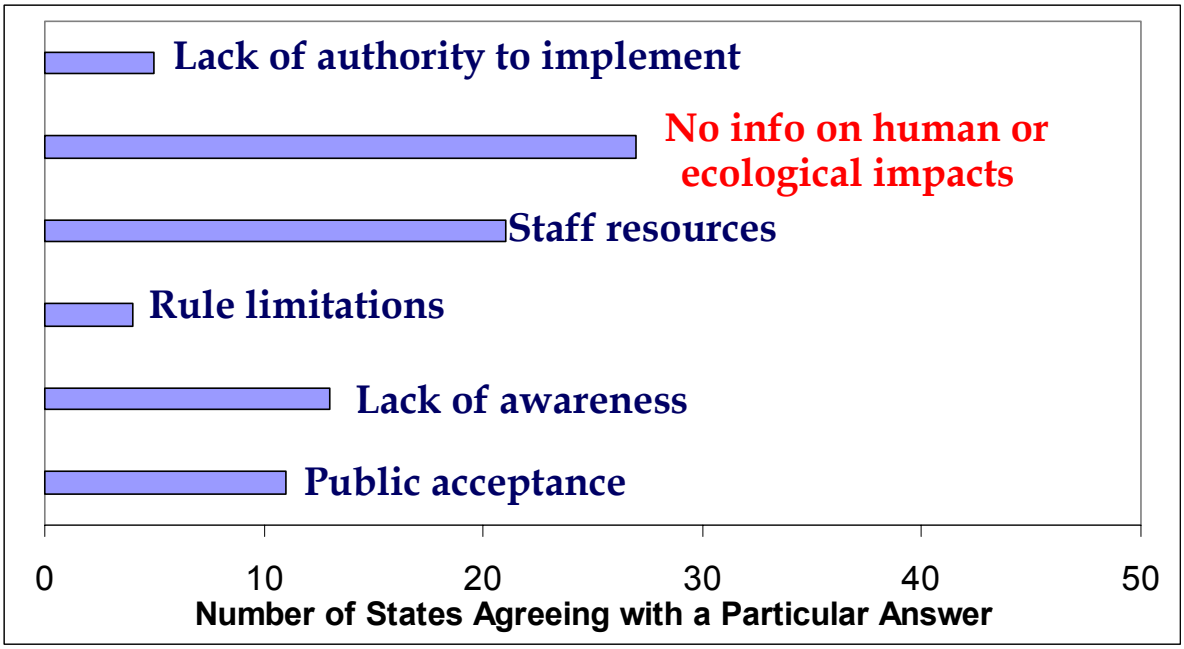

Figure 3.1. Barriers to recycling. 40 states and 2 territories responded to the survey (ASTSWMO, 2000).

SCOPE

The purpose of this paper is to introduce a new source-term framework for evaluating the acceptability of candidate secondary materials for their use in roadways. Evaluation of pavement materials is based on potential risk from contamination of soil and groundwater with leached metals, salts, and organics from secondary or even traditional materials in pavement structural layers and embankments. Risks of surface water contamination from leaching, other risks from relatively smaller volume uses (e.g. ceramic and plastic wastes in

appurtenances), and risks from exposures of workers to fugitive dust during construction are not considered in this paper.

In accordance with the definition of risk as the probability of an adverse outcome, this paper proposes a probabilistic approach that honors the unavoidable presence of uncertainty and variability in soil and groundwater contamination. Probability is emphasized in this framework because point estimates of outputs (e.g. of cumulative leaching and transport of a single metal species) may considerably overestimate or underestimate reality and no knowledge will be available to determine the confidence in this output unless a probabilistic approach is taken. Probabilistic methods have been commonly used in various steps of human health and ecological health risk assessments but rarely has the source term been described probabilistically. A probabilistic approach to leaching is also new in the waste leaching realm.

The probabilistic approach for estimating contaminant release fluxes from pavement materials is shown in Figure 3.2. The framework is explained step by step along with application of each step to an example that compares leaching of arsenic from bound materials (portland cement concrete and asphalt concrete) in the presence and absence of secondary materials (coal neutral fly ash, coal basic fly ash, and municipal solid waste incinerator bottom ash).

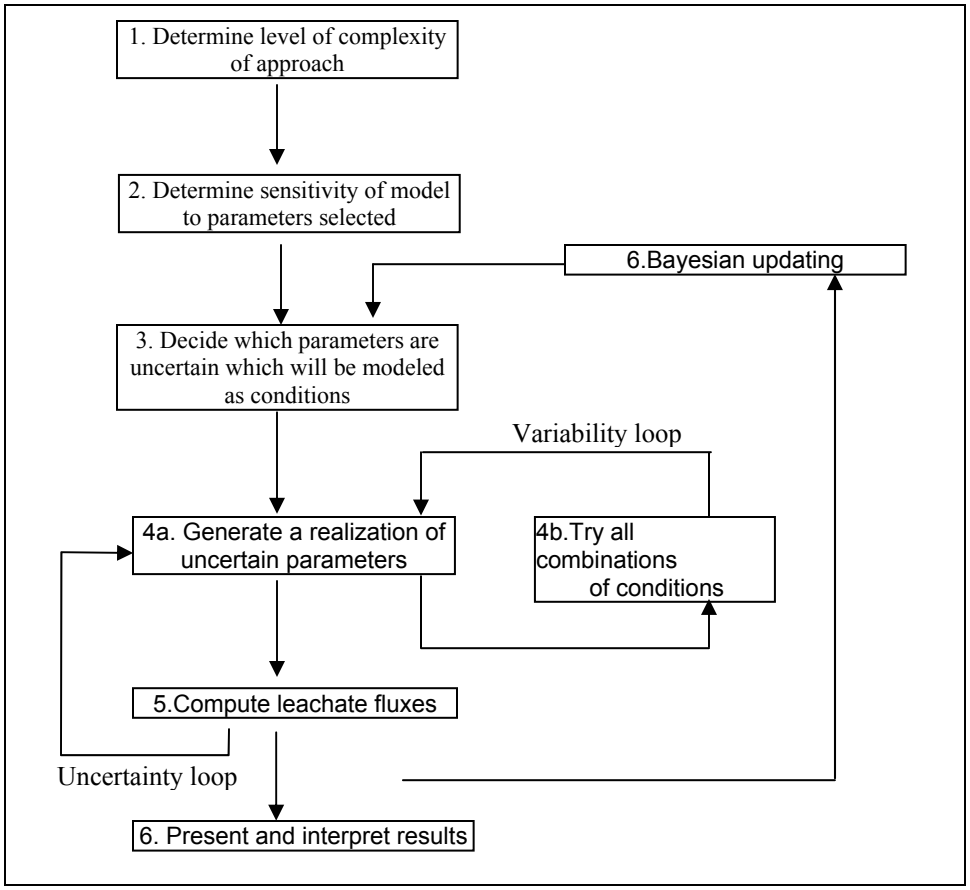

Figure 3.2. Proposed framework

PROPOSED FRAMEWORK

Step 1: Level of Complexity of Approach

The first step is to decide on the complexity of the approach that will be used for release estimates. The model selected and the extent of incorporation of probabilistic methods will determine the level of complexity. Model complexity varies widely from calculation of the release using one equation for the entire system to use of a finite element code for unsteady variably saturated fluid and

contaminant transport. Probabilistic complexity is low if only uncertainty or only variability (uncertainty or variability loop) is propagated; medium if uncertainty and variability are jointly incorporated; and high if Bayesian statistics is used. In medium probabilistic complexity, the variability and uncertainty are either separated within the same parameter or distributed to different parameters or both. I suggest starting with a simple approach and increasing the model complexity and probabilistic treatment of the approach as warranted. A site-specific, detailed analysis may be expensive, however, the benefits and cost savings from not disposing of the material may outweigh the cost of a more comprehensive approach.

To determine the acceptability of the portland cement concrete and asphalt concrete to be used as surface layers in a pavement, the first step is to measure the total content of the contaminants in the materials. If the total content is low enough then there is no need for release estimates. In my example, total concentrations of arsenic in all the materials are assumed to be high requiring prediction of potential release.

Three models are included in this paper (Table 3.2) although other models can also be used within the proposed framework to probabilistically predict the release fluxes (Nelson et al., 2001; Park and Batchelor, 2002; EPA, 1999). Monolith and percolation approaches have been discussed in detail in Kosson et al. (1996 and 2002) and currently form the basis for release estimates in Europe (BMD, 1995). These two approaches yield more realistic and typically less

conservative results than the TCLP test (Sanchez et al., 2002). Monolith and percolation approaches are practical to use because only a single equation is calculated and a small number of parameters is required. However, monolith and percolation equations are based on the assumption that the pavement material is completely saturated for the times it is considered “wet“. In reality, the saturation of the different parts of the pavement material may vary based on the design, the extent of cracking, and the climate. Considering that without water, there is no leaching, and that the extent of leaching and transport is dictated by the degree of saturation of the medium with water, incorporating hydraulic regimes in a two dimensional or three dimensional medium is crucial if there is room for further rigor. Incorporation of spatial and temporal variability in hydraulic regimes and consequent leaching forms the basis for the third model discussed in this paper. As expected, incorporation of spatial and temporal scales in water and contaminant movement adds considerable complexity and parameters to the model (Table 3.2).

Table 3.2: Single equation modeling approaches and the rigorous approach

Approach	Diffusion	Percolation	Variably saturated transport
Complexity of approach	Single equation	Single equation	Multiple equations and temporal and spatial scales
Material type	Monolith	Granular	Monolith and/or granular
Process modeled	Mass transfer limited: diffusion	Solubility limited: percolation	Adsorption and mass transfer limited: diffusion and advection
Decisions	• Parameter selection	• Parameter selection	• Unsaturated water flow and contaminant transport model selection • Parameter selection • Pavement design and climate selection
Characteristic equations	• One dimensional diffusion equation $M_t = \frac{4 \times C_{ini}}{H}\left(\frac{t \times D_{obs}}{\pi}\right)^{\frac{1}{2}}$	• Solubility multiplied by liquid to solid ratio $M_t = \frac{I \times t \times S}{\rho \times H}$	• Variable saturated water movement: Richards' equation • Hydraulic properties: empirical models (e.g. van Genuchten, Brooks and Corey equations) • Solute transport: Common convection dispersion equation
Output	Cumulative contaminant release	Cumulative contaminant release	Spatial and temporal water content and water fluxes Spatial and temporal contaminant concentration and fluxes Temporal edgedrain water and contaminant fluxes
Parameters	D_{obs}, H, t, C_{ini}	ρ, , C_{ini},, S, I, H, t	θ_{sat};, θ_{res}, K_{sat}, α, n, ρ, Disp, T, C_{ini}, D, K_d, Depth, P, H, Cracking, Edgedrain pipe/No edgedrain pipe, paved/unpaved shoulder, geo, t

θ_{sat}: saturated water content
θ_{res}: residual water content
α, n: Hydraulic fitting parameters for the van Genuchten soil moisture retention curve,
ρ: density
C_{ini}: initial contaminant concentration
D: diffusion coefficient
geo: geometry of the pavement design
Disp: dispersion
D_{obs}: observed diffusivity
H: height of material of concern
I: infiltration
K_d: adsorption coefficient
K_{sat}: saturated hydraulic conductivity
M_t: contaminant mass released
P: precipitation
S: solubility at field pH
T: tortuosity
t: lifetime of the pavement

For the arsenic release example, the appropriate first stage modeling is the monolith approach. Even though the monolith approach has been used for more than a decade, its probabilistic application is new. In selecting the monolith approach it was assumed that the arsenic release rate from both portland cement concrete and asphalt concrete is limited by mass transfer. For this example the probabilistic complexity was set to low for simplicity.

Step 2: Parameter Sensitivity

Whenever possible, a sensitivity analysis is encouraged to save time and focus efforts. If the model selected is not sensitive to certain parameters, then less effort should be directed to determining those parameters. Conversely, the parameters that significantly affect the model results should be more carefully handled. Parameter sensitivity is important not only before modeling; interpretation of model results is more thorough if the effect of each parameter on the model output is well characterized.

There are many local and global sensitivity analysis methods (Cronin et al., 1995; Boateng, 2001; Chang et al., 1993; Saltelli et al, 2000). A practical sensitivity analysis using @Risk is multivariate stepwise regression between the input parameters and the output. This method is useful if the R^2 value of the regression is greater than ~60 % suggesting that the linear regression sufficiently explains the relationship between the inputs and outputs. In the arsenic

example, regressing input parameters, D_{obs}, H, t, and C_{ini} against the release estimates showed that more than 80% (R^2>0.80 for all four simulations) of the output variation could be explained by the linear relationship between the inputs and the output (Table 3.3). The sensitivity is expressed as the normalized regression coefficients associated with each input parameter (Table 3.3). A regression value of 0 indicates that there is no significant relationship between the input and the output, while a regression value of 1 or –1 indicates a 1 or –1 standard deviation change in the output for a 1 standard deviation change in the input. In the arsenic example, both with and without secondary materials, one standard deviation of any input caused at least 0.2 standard deviation change in the output. The output had higher sensitivity to H and D_{obs} than t and C_{ini} in the presence of secondary materials. A more rigorous sensitivity analysis for the arsenic example would include the sensitivity of distribution parameters (lower and upper limits for uniform distributions and mean and standard deviation for normal and lognormal distributions) to the release estimates.

Table 3.3. Normalized regression coefficients and the R^2 value for the sensitivity analysis using regression.

	Portland Cement Concrete		Asphalt Concrete	
	w/ secondary materials	w/o secondary materials	w/ secondary materials	w/o secondary materials
H	-0.588	-0.846	-0.647	-0.839
t	0.268	0.38	0.305	0.388
C_{ini}	0.221	-	0.372	-
D_{obs}	0.596	-	0.466	-
R^2	0.84	0.87	0.83	0.87

Step 3: Conditions and Uncertainty

Uncertainty represents the degree of ignorance about the precise value of a particular parameter whereas variability is the inherent variation in the value of a particular parameter within the population of interest. Clear distinctions between the uncertain and variable nature of parameters have been made in risk assessment studies (Hatis and Burmaster, 1994; Rai et al., 1996; Hoffman and Hammonds; 1994; Bogen, 1995) and much less frequently in fate and transport models (Frey and Rhodes, 1996). A similar distinction is made in the proposed framework because the release information from this source assessment framework is to be used for risk analysis, which relies on propagating uncertainty and variability for decision making. In the proposed framework variability can be thought of as “conditions“. The variability in this context represents different scenarios for pavement designs or spatial or temporal variability in climate. Parameters with low ignorance level (i.e. accurately and precisely known parameters) can be treated as conditions.

In the arsenic example, there are four parameters (ρ, D_{obs}, H, and t) in the diffusion model. These parameters were represented as possible release conditions, which can be considered to be different pavement design scenarios. In common deterministic calculations, conservative estimates of these parameters are used or several different scenarios are calculated to represent variability. In this new framework, parameters were represented as probability

density functions that were more representative of what is fully known about the parameters. Using @Risk, stratified random samples (Latin Hypercube sampling) were then drawn from these distributions to propagate variability. Latin Hypercube sampling was arbitrarily selected since a comparison of output distributions from Latin Hypercube and Monte Carlo (unstratified sampling) sampling techniques yielded similar results at two thousand iterations. In other problems, Latin Hypercube sampling might be preferred over Monte Carlo sampling for computing efficiency (fewer iterations due to stratification) and better representation of low probability outcomes. The iteration number (number of samples from each distribution) in these Monte Carlo experiments was set to two thousand based on convergence. In other words, the shape and statistics of the output distribution did not markedly change by additional iterations.

Selection of parameter values and distributions are shown in Table 3.4. Based on my judgment, the knowledge of the lifetime of the pavement was represented with a normal distribution with a mean of 15 years and a standard deviation of five years. Assuming that the pavement would last at least one year, the lower tail of the distribution was truncated at one year. This distribution was selected to account for variability in the climate (i.e. different geographical locations with varying degrees of pavement performance), volume and type of traffic, and the pavement design. The height of the surface layer in pavements may vary from 10 cm to 40 cm in the presence of overlays. Thus, a uniform distribution from 0.1m to 0.4m was selected to represent the variability in height

of the application in existing and future designs. Variability in pavement materials was accounted for by the variability in observed diffusivity and the initial available concentration. For asphalt concrete and portland cement concrete with secondary materials, observed diffusivity was represented by lognormal distributions, and initial available concentrations were represented as uniform distributions based on data from de Groot et al (1990). The observed diffusivity and initial available concentration of arsenic in asphalt concrete and Portland cement concrete without secondary materials were not modeled probabilistically because there was not available data to define a probability density function. For pavements containing recycled materials, a uniform distribution was selected for initial available concentrations because there was no basis to select a different distribution.

Table 3.4. Observed diffusivity and initial available concentrations*.

	Portland Cement Concrete		Asphalt Concrete	
	w/ secondary materials	w/o secondary materials	w/ secondary materials	w/o secondary materials
D_{obs} (m^2/s)	Lognormal ($3.16\ 10^{-10}$,$2.76\ 10^{-10}$)	$8.51\ 10^{-12}$	Lognormal ($8.42\ 10^{-13}$, $5.4\ 10^{-13}$)	$6.31\ 10^{-12}$
C_{ini} (mg/kg)	Uniform (0.03, 0.05)	0.012	Uniform (0.04, 0.09)	0.03

*The values in parentheses represent mean and standard deviation for lognormal distribution, and upper and lower values for uniform distribution.

Step 4: Propagating Uncertainty in Presence of Different Conditions

The purpose of the arsenic example was to analyze different conditions only and thus uncertainty was not explicitly included in the model. However,

there may be other cases when this distinction becomes meaningful and medium probabilistic complexity is more appropriate. For example, if the goal is to predict leaching from a pavement made of the same unbound material and constructed throughout a region using the same design, the percolation model can be used and the parameters H and ρ can be modeled as constants (design is constant), I can be modeled as a variable parameter (based on variation of the climate within the region), and S can be modeled as an uncertain parameter with the distribution constructed from available leaching test results for different liquid to solid ratios.

An embedded Monte Carlo nest is used for joint propagation of uncertainty and conditions. Random samples are drawn from the probability density distributions of uncertain variables (S in this case). A random parameter sample is matched with a sample from a probability density function of the condition. Then, the sampled uncertain parameter is kept constant and matched with however many samples (number of rounds of variability loop) are collected from the condition distribution. If the condition is represented as a set number of different scenarios (e.g. a total of four infiltration values in the percolation example), then the total iterations in the variability loop is equal to that number. This process is repeated for the other random samples from the probability distributions of uncertain variables.

In addition to describing the uncertainty and variability in different parameters, many studies have also propagated the uncertainty and the

variability within the same parameter using the embedded Monte Carlo nest (Moschandreas and Karuchit, 2002; Cohen et al., 1996; Hoffman and Hammonds; 1994). However, in leaching models, unambiguous representation of joint uncertainty and variability in the same parameter may be difficult. An example is the parameter adsorption coefficient that would be needed if the rigorous approach had been selected in Step 1. Pavement material adsorption parameters for metals abound in the literature; however, the release is a complex mechanism that depends on pH and liquid to solid ratio. Both of these conditions will change in the field in time and in space (variability) in a less predictable manner (uncertainty). A convenient representation that is also realistic is to represent the adsorption coefficient as a probabilistic variable where the probability encompasses both uncertainty and variability since these two cannot be clearly distinguished for this particular parameter. Thus, in unclear situations, a single probability density function should be preferred over forced inclusion of both uncertainty and variability within the same parameter.

Step 5: Release Calculations

In this step, the model selected is run to calculate release of contaminants from recycled materials. In the arsenic example, the number of samples collected from each distribution was two thousand. Thus, the monolith equation was calculated two thousand times.

If a modeling approach that involves variably saturated contaminant transport has been selected, then the simulation would involve significant computation. The model for the this approach is a two or three dimensional finite element or finite difference code that simulates the variably saturated hydraulic regimes and the solute transport (e.g. HYDRUS2D, FEFLOW). Such a model brings not only computational burden but also greater difficulty in determining parameter values or probability distributions due to a greater number of parameters required for the model. In addition, use of such complicated codes (as opposed to single equations) requires some expertise in defining boundary conditions and initial conditions, and working with mesh designs. However, the spatial and temporal leaching information specific to existing hydraulic regimes and the pavement design (i.e. thickness and width of surface layers, base/subbase layers, shoulders, drainage pipes) may be valuable. For example, if infiltration occurs only under cracks and joints, and is collected adequately by drainage pipes, then placement of recycled materials away from joints and possible location of cracks would yield significantly smaller risks. Similarly, if there is leaching from the pavement materials but if this leachate is collected in the drainage pipes, then the path of the leachate after it exits the outlet of the edgedrain should be of concern (i.e. not the contamination of the groundwater directly under the pavement). The only way to simulate and predict the outcome of such more detailed scenarios is to use a variably saturated water movement and solute transport model.

Step 6: Bayesian Modeling

For the purpose of the arsenic example, Bayesian updating was unnecessary because uncertainty was not considered and thus the probabilistic complexity was set to low. In high probabilistic complexity, the emphasis is on uncertainty and the goal is to reduce the uncertainty by incorporating a weighted average of all available information using Bayesian statistics. For example, if the release analysis is for a specific design and if measured values are available then these can be used to represent the uncertainty of the parameters. However, these measurements can be biased or may contain significant noise in which case other information from literature data, expert judgment, past experience, and intuition can be used to reach an updated information state. The proposed framework includes the Bayesian approach because a lot of uncertainty exists with many of the parameters needed for release estimates and this alternative approach to classical statistics provides the means to make best use of the data.

Step 7: Presentation and Interpretation of Results for Decision Making

Arsenic Leaching: Presentation of a Low Probabilistic Complexity Example

The probabilistic output in the arsenic example can be presented in the form of cumulative probability where the arsenic release at 100% variability represents the worst case scenario among all design parameters (Figures 3.3

and 3.4). If the model is assumed to represent reality, one can say that 90% of all existing pavement designs would release no more than 0.023mg/kg arsenic for asphalt concrete pavements and no more than 0.272mg/kg arsenic for Portland cement concrete pavements. This approach can also be used to determine what percent of designs may exceed a given contaminant release limit. In this example, at 50% and 90% variability, there was almost twice as much release in the presence of recycled materials from both Portland cement concrete and asphalt concrete.

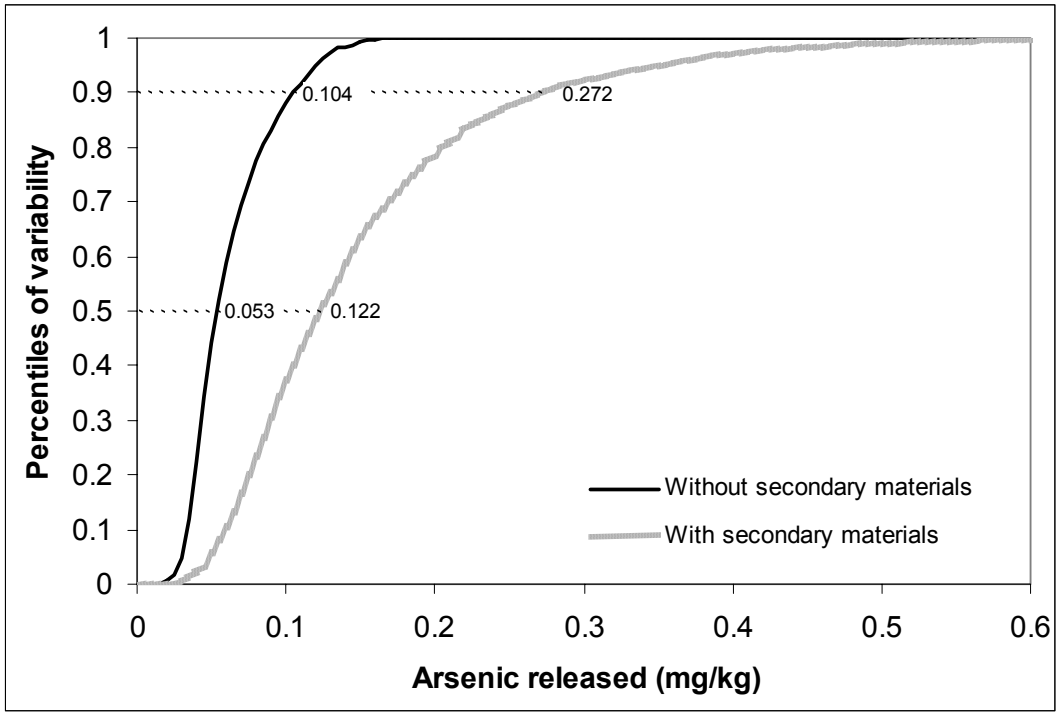

Figure 3.3: Arsenic release from portland cement concrete for different designs.

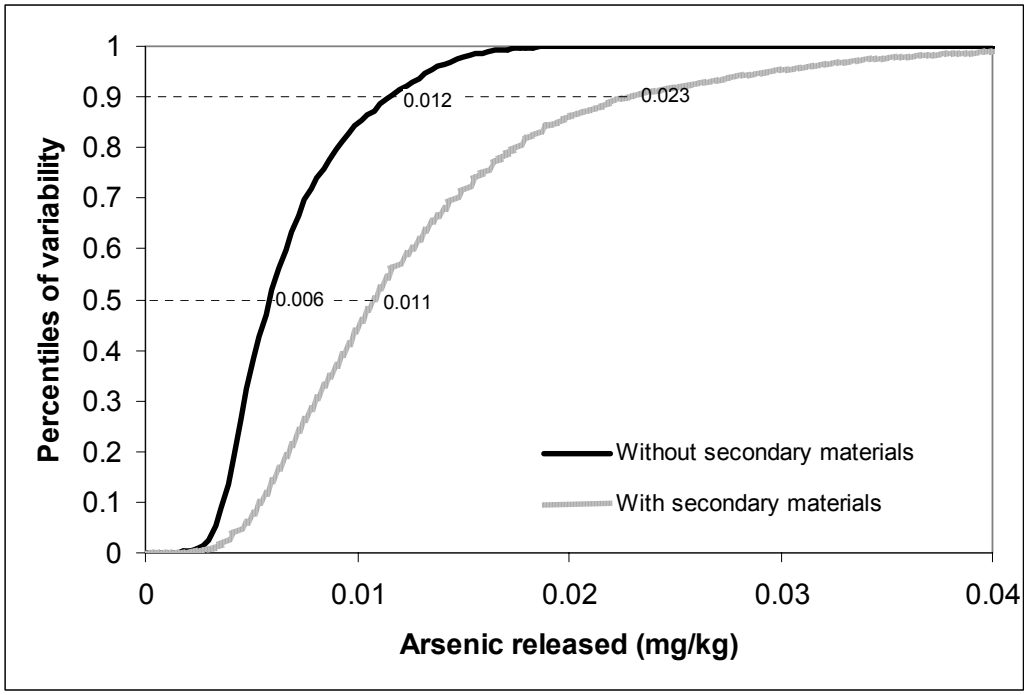

Figure 3.4. Arsenic release from asphalt concrete for different designs.

Interpretation

Regulatory agencies need to decide how much leaching constitutes an unacceptable risk using a straightforward method that does not lead to unclear situations. One approach is to forward calculate the risk based on exposure and dose-response relationships using probabilistic risk models (Batchelor et al., 1998). Another practical approach may be to follow the Dutch Building Materials Decree, which is based on soil protection (BMD, 1995). Dutch regulations specify that use of any material (primary or recycled) should not increase the target soil concentrations more than one percent within 100 years in one meter of the underlying soil (assuming 100 percent retention). The target values

represent concentrations at which the risks to human health and the environment are considered negligible. By specifying that materials should be at least 0.5m above the groundwater table, the regulations also assume that this criterion protects the groundwater. The American or the Danish system provides another option for evaluating the contaminant burden on the groundwater by modeling contaminant transport to groundwater using a dilution factor (Hartlen et al., 1999; EPA, 1996).

Alternatively, estimates of contaminant release from the pavement can be compared to background soil concentrations (Figure 3.5). The results of the arsenic example show that depending on the location of the road, the release may be a very small burden to the soil. For example, in Colorado, the total release from the road is expected to be 15 times less than the lower value of arsenic found in the soil. (This analysis assumes that all arsenic released is retained in the upper soil horizon, with a depth equal to the depth of recycled material application above the soil.)

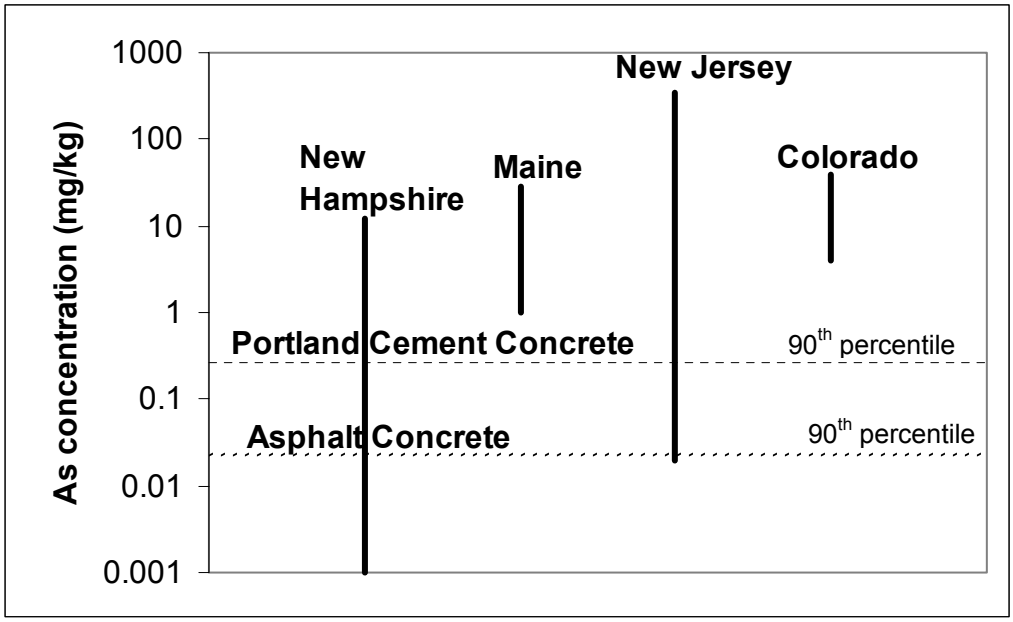

Figure 3.5. Background soil concentrations (Baldwin and McCreary; 1998).

In addition to, or in lieu of, comparison of estimates of contaminant burden on soil and groundwater, a comparative risk assessment can be employed. For evaluation of the use of secondary materials in roadway environments, appropriate cases of comparison are estimates of contaminant flux leached from highways with recycled materials, highways without recycled materials, and landfills if the material is disposed of instead of recycled. For example, the arsenic release analysis allows the decision maker to compare environmental acceptability of PCC and asphalt concrete in the presence and absence of secondary materials. For example, use of recycled materials in asphalt concrete is estimated to release 0.023 mg/kg of arsenic at 90% variability; PCC constructed with virgin materials releases 0.104 mg/kg at the same variability level. Comparative risk assessment is a powerful method because it places risks

due to recycling in an appropriate context of other likely disposal options for materials and inherent risks of using virgin materials.

EVALUATION OF PROPOSED FRAMEWORK AS A POLICY TOOL

In the proposed framework, increasing levels of probabilistic and model specific alternatives for characterizing the contaminant fluxes offers flexibility for the risk manager to tailor the modeling approach to the problem and resources at hand. The probabilistic output from the framework allows for easier interpretation and use of the results because the output includes all the information known and not known about the analysis. The major implied complexity of acceptance of probabilistic information is the need for the risk assessor, manager, communicator, and the public to comprehend probability. Communicating probabilistic output to people not familiar with probability may be difficult but perhaps not more so than having to deal with the problem in ignorance of all information available about the variability and the uncertainty.

CONCLUSIONS

This paper is based on the hypothesis that use of secondary materials may be advantageous and more common if a methodology was available to characterize the environmental impact for decision makers. Thus, a new framework is proposed which provides the much needed tool for the decision maker to evaluate possible designs with secondary materials and also compare the risks with risks from use of traditional materials. With more rigorous description of the input parameters, the framework is a new approach (instead of best case or worst case designs) for prediction of the “correct“ range of release concentrations along with their frequency of occurrence as demonstrated in the arsenic example. A major strength of the framework is that it provides guidance on how to incorporate different levels of ignorance and knowledge in contaminant release estimates. The probabilistic approaches that have almost become standard in other components of risk assessment can now be used for source term estimates as explained in this paper.

ACKNOWLEDGEMENTS

This work was funded through a cooperative agreement (DTFH61-98-X-00095) between FHWA and the University of New Hampshire. The comments of anonymous reviewers were valuable in helping to focus and improve this paper.

REFERENCES

1. ASTSWMO (2000). "ASTSWMO Beneficial Use Survey.", Association of State and Territorial Solid Waste Management Officials, Washington, D.C.

2. Baldwin L, McCreary H., (1998) Study of State Soil Arsenic Regulations, Conducted by the Association for the Environmental Health of Soils.

3. Batchelor, B., Valdes, J., and Araganth, V. (1998). "Stochastic risk assessment of sites contaminated by hazardous wastes." *Journal of Environmental Engineering*, 124(4), 380-388.

4. BMD (1995) Building Materials Decree. Bulletin of acts, orders and decrees, no 567, available in English from Ministry VROM, Direction of Soil Protection (ipc 625), PO Box 20945, 2500 GX The Hague, The Netherlands, fax: +31-70-3391290

5. Boateng, S. (2001). "Evaluation of probabilistic flow in two unsaturated soils." *Hydrogeology Journal,* 9(6), 543-554

6. Bogen, K.T. (1995). "Methods to approximate joint uncertainty and variability in risk." *Risk Analysis*, 15(3), 411-419

7. Chang, C. -H., Yang, J.C., and Tung, Y.-K. (1993). "Sensitivity and uncertainty analysis of a sediment transport model: a global approach." *Stochastic Hydrology and Hydraulics*,7, 299-314

8. Chesner, W. H., Collins, R. J., and MacKay, M. H. (1998). "User guidelines for waste and by-product materials in pavement construction.", Chesner Engineering, New York.

9. Cohen, J.T., Lampson, M.A., and Bowers, T.S. (1996). " The use of two-stage Monte Carlo simulation techniques to characterize variability and uncertainty in risk analysis" *Human and Ecological Risk Assessment*, 2(4), 939-971

10. Collins, R. J. and Ciesielski, S. K. (1994). " Recycling and use of waste materials and by-products in highway construction.", Transportation Research Board, Washington D.C.

11. Cronin W.J., Oswald, E.J., Shelley, M.L., Fisher, J.F., and Flemming, C.D. (1995). "A Trichloroethylene risk assessment using a Monte Carlo analysis

of parameter uncertainty in conjuntion with physiologically-based pharmacokinetic modeling.", *Risk Analysis*, 15(5), 555-565

12. de Groot, G.J., van der Sloot, H.A., Bonouvrie, P., and Wijkstra, J. (1990) Karakterisering van het uitlooggedrag van intacte produkten, ECN-C—90-007, Netherlands Energy Research Foundation ECN, Petten, The Netherlands

13. Deschamps, R. J. (1997). "Geotechnical and environmental characteristics of atmospheric fluidized bed combustion ash and stoker ash." *Transportation Research Record*, 1577, 90-95.

14. Eighmy, T. T. and Magee, B. J. (2001). "The Road to Reuse." *Civil Engineering*, 66-81.

15. Eighmy, T.T. and Chesner, W.H. (2001) "Framework for Evaluating Use of Recycled Materials in the Highway Environment", *Report No. FHWA-RD-00-140*, U.S. DOT, Washington, D.C.

16. EPA (1996) Soil Screening Guidance: User's guide, http://www.epa.gov/superfund/resources/soil/ssg496.pdf

17. EPA (1999) A framework for finite-source multimedia multipathway, and multireceptor risk assessment, 3MRA, http://www.epa.gov/epaoswer/hazwaste/id/hwirwste/pdf/risk/reports/s0538.pdf

18. FHWA (1999) http://wwwcf.fhwa.dot.gov/ohim/hs99/tables/hm10.pdf

19. Frey, H.C. and Rhodes, D.S. (1996). "Characterizing, simulation, and analyzing variability and uncertainty: an illustration of methods using an air toxics emissions example." *Human and Ecological Risk Assessment*, 2(4), 762-797

20. Hartlen, J., Fallman, A.-M., Back, P.-E., and Jones, C. (1999). "Principles for risk assessment of secondary materials in civil engineering work.", Swedish Environmental Protection Agency, Stockholm.

21. Hatis, D. and Burmaster, D.E. (1994). "Assessment of variability and uncertainty distributions for practical risk analyses." *Risk Analysis*,14(5), 713-730

22. Hoffman, O.F. and Hammonds, J.S. (1994). "Propagation of uncertainty in risk assessments: the need to distinguish between uncertainty due to lack

of knowledge and uncertainty due to variability." *Risk Analysis*, 14(5), 707-712

23. Humphrey, D. N. and Katz, L. E. (2000). "Water-quality effects of tire shreds placed above the water table." *Transportation Research Record*, 1714, 18-24.

24. Hyman, W. A. and Johnson, B. L. (2000). "Assessing public benefits of reusing waste materials in highway projects." *Transportation Research Record*, 1702, 97-107.

25. Kosson, D. S., Sloor, H. A. v. d., and Eighmy, T. T. (1996). "An approach for estimation of contaminant release during utilization and disposal of municipal waste combustion residues." *Journal of Hazardous Materials*, 47, 43-75.

26. Kosson, D. S., H. A. van der Sloot, et al. (2002). “An integrated framework for evaluating leaching in waste management and utilization of secondary materials.” *Environmental Engineering Science* 19(3), 159-204.

27. Mahboub, K. C. and Massie, P. R. (1996). "Use of scrap tire chips in asphaltic membrane." *Transportation Research Record*, 1530, 59-63.

28. Moschandreas, D.J., and Karuchit, S. (2002). "Scenario-model-parameter: a new method of cumulative risk uncertainty analysis." *Environment International*, 28, 247-261

29. Mulder, E. (1996). "A mixture of fly ashes as road base construction material." *Waste Management*, 16(1-3), 15-20.

30. Nelson, P. O., Huber, W. C., Eldin, N. N., Williamson, K. J., Lundy, J. R., Azizian, M. F., Thayumanavan, P., Quigley, M. M., Hesse, E. T., Frey, K. M., and Leahy, R. B. (2001). "Environmental Impact of Construction and Repair Materials on Surface and Ground Waters: Summary of Methodology, Laboratory Results, and Model Development." *NCHRP Report 448*, Oregon State University.

31. Pandey, K. K., Canty, G. A., Atalay, A., Robertson, J. M., and Laguros, J. G. (1995) "Fluidized bed ash as a soil stabilizer in highway construction." *Geotechnical Special Publication No. 46 -Characterization, containment, remediation, and performance in environmental geotechnics*, New Orleans, Louisiana, 1422-1436.

32. Park, J. -Y. and Batchelor, B. (2002). " A multi-component numerical leach model coupled with a general chemical speciation code." *Water Research*, 36, 156-166

33. Partridge, B. K., Fox, P. J., Alleman, J. E., and Mast, D. G. (1999). "Field demonstration of highway embankment construction using waste foundry sand." *Transportation Research Record*, 1670, 98-105.

34. Rai, S.N., Krewski, D., and Bartlett, S. (1996). "A general framework for the analysis of uncertainty and variability in risk assessment." *Human and Ecological Risk Assessment*, 2(4), 972-989

35. Saltelli, A., Chan, K., and Scott, M. (2000). Sensitivity Analysis, Probability and Stataistics Series. John Wiley & Sons publishers, New York

36. Sanchez, F., Mattus, C.H., Morris, M.I., and Kosson, D.S. (2002). "Use of a new leaching test framework for evaluating alternative treatment processes for mercury contaminated soils." *Environmental Engineering Science 19(4), 251-269*

37. Schimmoller, V., Holtz, K., Eighmy, T., Wiles, C., Smith, M., Malasheskie, G., and Rohrbach, G. J. (2000). "Recycled Materials in European Highway Environments: Uses, Technologies, and Policies.", American Trade Initiatives

38. Schroeder, R. L. (1994). "The use of recycled materials in highway construction." *Road & Transport Research*, 3(4), 12-27.

CHAPTER 4

PROBABILISTIC MODELING OF ONE DIMENSIONAL WATER MOVEMENT AND LEACHING FROM HIGHWAY EMBANKMENTS CONTAINING SECONDARY MATERIALS

ABSTRACT

Predictive methods for contaminant release from virgin and secondary road construction materials are important for evaluating potential long-term soil and groundwater contamination from highways. The objective of this research was to describe the field hydrology in a highway embankment and to investigate leaching under unsaturated conditions by use of a contaminant fate and transport model. The HYDRUS2D code was used to solve the Richards equation and the advection-dispersion equation with retardation. Water flow in a Minnesota highway embankment was successfully modeled in one dimension for several rain events after Bayesian calibration of the hydraulic parameters against water content data at a point 0.32 m below the surface of the embankment. The hypothetical leaching of Cadmium from coal fly ash was probabilistically simulated in a scenario where the top 0.50 m of the embankment was replaced by coal fly ash. Simulation results were compared to the percolation equation method where the solubility is multiplied by the liquid to solid ratio to estimate total release. If a low solubility value is used for Cadmium, the release estimates obtained using the percolation/equilibrium model are close to those predicted from HYDRUS2D simulations (~ 10^{-4}-10^{-2} mg Cd/kg ash). If high solubility is used, the percolation equation over predicts the actual release (0.1-1.0 mg Cd/kg ash). At the 90th percentile of uncertainty, the ten-year liquid to solid ratio for the

coal fly ash embankment was 9.48 L/kg, and the fraction of precipitation that infiltrated the coal fly ash embankment was 92 percent. Probabilistic modeling with HYDRUS2D appears to be a promising realistic approach to predicting field hydrology and subsequent leaching in embankments.

INTRODUCTION

Highway embankments and pavement structural layers such as base/subbase layers, shoulders, asphalt concrete, and Portland cement concrete provide suitable settings to utilize large volumes of secondary materials such as coal fly ash, steel slag, reclaimed asphalt pavement, and recycled concrete (Apul et al., 2003). A major environmental concern for use of secondary materials in the highway environment is the potential long-term leaching of contaminants, which may result in widespread soil and groundwater contamination. Leaching from embankments may pose an even greater problem than leaching from structural components of the highway considering that much larger volumes of material are used in uncovered embankments. If predictive methods for contaminant release are available, more informed decisions can be made about the use of secondary materials in the highway environment.

Physical and chemical factors dictating leaching from secondary materials are complex and many studies have focused on various aspects of leaching. For example, a significant portion of the leaching literature discusses laboratory experiments under varying liquid to solid ratios and pHs (Kosson et al., 1996; Kosson et al, 2002). Some researchers have modeled the pH dependent leaching behavior by equilibrium dissolution/precipitation reactions (Kida et al., 1996; Fallman, 2000) and more recently by sorption reactions (surface complexation and surface precipitation) (Meima and Comans, 1998; Dijkstra et

al., 2002). Others have coupled diffusion with chemical equilibrium to model leaching behavior in the laboratory (Ganguly et al., 1998; Park and Batchelor, 2002; Gardner et al., 2002). Kosson et al. (1996, 2002) suggested use of a percolation and a diffusion equation to extend laboratory results to field leaching conditions. Most of these studies have assumed that the water flow through the secondary material was uniform and constant and did not consider unsaturated flow in their analyses.

Modeling and field studies show that the highway environment remains unsaturated most of the time (Birgisson and Ruth, 2003; Birgisson and Roberson, 2000). An accurate description of this unsaturated flow would be helpful for understanding contaminant release in field conditions. In unsaturated conditions, carbonation and oxidation reactions may affect the contaminant release by modifying the matrix pH and chemistry (Townsend et al., 1999; Sanchez et al., 2002). Details of pavement hydrology are also needed to determine the dominant physical release and transport processes of contaminants in the field. Either diffusion or solubility may limit contaminant release in the field and the relative importance of these processes may depend on water flow conditions, which will vary spatially (e.g., below cracks/joints, unpaved shoulders versus below intact pavement sections) and temporally (e.g., dry and wet periods).

Some of the recent modeling work in highway environments includes advective and diffusive transport of contaminants and spatial variability of the

hydraulic regimes in two dimensions. For example, de Haan et al. (2003) investigated variably saturated water flow in highway pavements using laboratory and field experiments as well as numerical simulations using HYDRUS2D. Experimental data and two-dimensional modeling results suggested that there might be lateral water movement from the shoulder to the area below a relatively impermeable pavement. Using HYDRUS2D, Bin-Shafique et al. (2002) reproduced concentration measurements from coal fly ash in full-scale field studies and laboratory column experiments. Huber et al. (2001) developed the IMPACT model specifically for predicting the impact of beneficial use of secondary materials in roads. While unsaturated flow was not considered for simplicity, multiple transport, removal and retardation processes (e.g., advection, dispersion, sorption, biodegradation, photolysis, and volatilization) were included in the IMPACT model. Pagotto et al. (2003) used CESAR and PHREEQC codes to model leaching from municipal solid waste incinerator ash and the 3FLO code for mass transfer in the underlying soil. The model was one-dimensional and considered variably saturated flow, advection and diffusion, as well as precipitation/dissolution reactions.

This paper describes the probabilistic application of a finite element model to simulate variably saturated flow and contaminant leaching in one dimension in a highway embankment. The goal of the research was to develop a probabilistic model for water movement in an existing highway embankment and to evaluate the hydrological and leaching response of the embankment if part of the

embankment was replaced by a secondary material, coal fly ash. A probabilistic approach was used because the confidence in release estimates can be expressed by explicitly considering the variability and uncertainty in the complex physical and chemical factors affecting leaching. Many authors have treated uncertainty and variability separately (Frey and Rhodes, 1996; Rai et al., 1996; Maxwell and Kastenberg, 1999); in this paper, I do not make that distinction and assume that the probability distributions I use represent the combined true uncertainty and variability. If a probabilistic approach had not been taken, point estimates from deterministic modeling might have considerably overestimated or underestimated the reality and provided no information on the confidence of the output.

Water movement was simulated in an embankment at the Minnesota Department of Transportation's (MnDOT) MnROAD instrumented, outdoor test facility. Unsaturated hydraulic parameters of the model are often not known for many virgin and secondary pavement materials. Thus, a Bayesian approach was taken where the uncertainty in unsaturated parameters was propagated through the model and then updated using Bayes' theorem and embankment water content data for 14,641 simulations. This updated information was combined with literature data to investigate a hypothetical leaching scenario for Cadmium when coal fly ash is used in the embankment.

METHODS

Field Site

The MnROAD test facility consists of 40, 152-m-long hot mix asphalt and Portland cement concrete test sections with varying structural designs. Each test section is instrumented to monitor strength and hydraulic properties. The hydraulic properties of the embankment were predicted from water content measurements made in the embankment of test section 12, a Portland cement concrete pavement with an asphalt shoulder (Figure 4.1a). Water content was measured every three hours using an automated time domain reflectometry (TDR) waveguide. The Ledieu et al. (1986) calibration equation was used to convert dielectric values to volumetric water content. A 16-day period (23 July-8 August 1997) was used for Bayesian uncertainty analysis of the parameters. This period was selected because (1) no major rain events had occurred for the previous three days, (2) the water contents had been constant for days, and (3) it included several rain events of varying intensities.

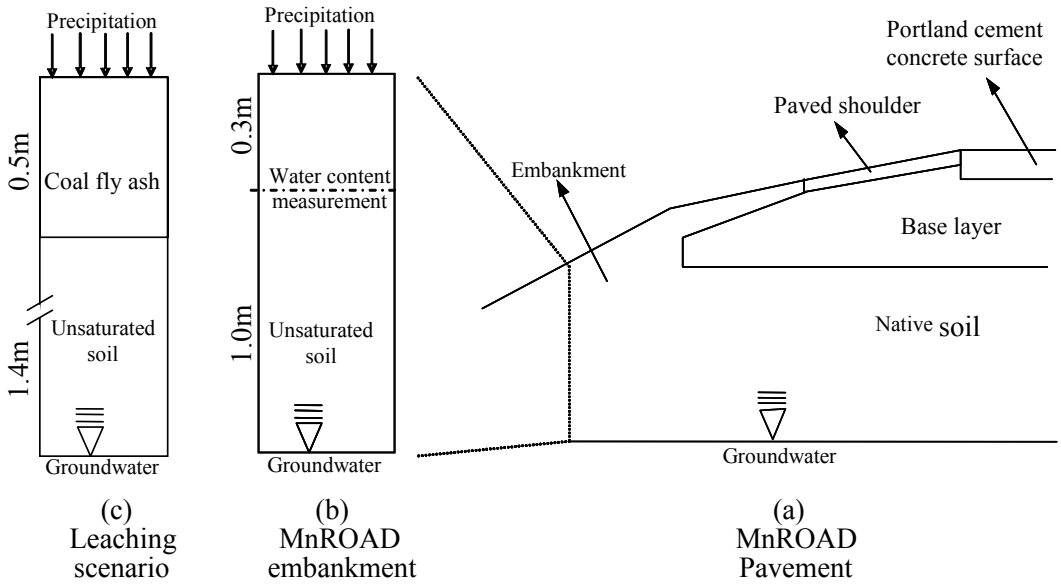

Figure 4.1 Cross section of MnROAD test section 12 (a), conceptual model of the MnROAD embankment (b), and coal fly ash scenario (c).

Finite Element Model

HYDRUS2D, a Windows-based finite element code, was used for all simulations (Simunek et al., 1999). HYDRUS2D numerically solves the following equations for variably saturated water movement and solute movement:

- Advection-dispersion equation with retardation for unsaturated medium:

$$\frac{\partial(\theta C)}{\partial t} + \rho_b \frac{\partial(K_d C)}{\partial t} = \frac{\partial}{\partial z}\left(\theta \frac{\partial C}{\partial z}(\tau D_m + \theta v D_i)\right) - \frac{\partial(vC)}{\partial z} \qquad [4.1]$$

where ρ_b is bulk density [M/L^3), K_d [L^3/M] is the partition coefficient, τ is the tortuosity factor [-], θ is volumetric water content [-], C is aqueous concentration [M/V], D_m is the molecular diffusion of the metal in free water [L^2/T], D_i is the dispersivity [L], t is time [T], z is the vertical location [L], and ν is the advective velocity [L/T]. The assumptions of this equation are local equilibrium and linear sorption.

- Richards' equation for water movement in unsaturated media:

$$\frac{\partial \theta}{\partial t} = \frac{\partial}{\partial z}\left[K(h)\left(\frac{\partial h}{\partial z} - 1 \right) \right] \qquad [4.2]$$

where h is pressure head [L].

- Closed form expression of the van Genuchten (1980) formulation for the soil moisture retention curve:

$$\theta = \theta_r + \frac{\theta_s - \theta_r}{(1 + |\alpha h|^n)^{1-1/n}} \qquad [4.3]$$

where θ_r [-] is (volumetric) residual water content, θ_s [-] is (volumetric) saturated water content and α [1/L] and n [-] are fitting parameters.

- Variation of hydraulic conductivity with water content:

$$S_e = \frac{\theta - \theta_r}{\theta_s - \theta_r} \qquad [4.4]$$

$$K(\theta) = K_{sat} S_e^{0.5} [1 - (1 - S_e^{n/(n-1)})^{1-1/n}]^2 \qquad [4.5]$$

where S_e is effective water content [-], and K_{sat} [L/T] is saturated hydraulic conductivity. Equations 4.3 and 4.4 assume that the (non-hysteretic) soil

moisture retention curve and the hydraulic conductivity curve for a soil can be estimated using five parameters (α, n, θ_s, θ_r, and K_{sat}).

Embankment Infiltration Model

Precipitation was input in to the model in 15 minute intervals as a time-varying-flux boundary condition at the surface of the embankment (Figure 4.1b). Maximum pressure head at the embankment surface was set to 2 mm to allow for runoff. The effect of groundwater was modeled by setting a constant zero pressure head at 1.3 m below ground surface, which is the actual depth to groundwater at the time of the data. Time varying water content values at 0.32 m from the surface were stored for each simulation for posterior probability calculations. Ground freezing and evaporation were not considered.

The initial water content distribution was specified to be as close to steady state conditions as possible. In HYDRUS2D, equilibrium conditions can be specified based on the pressure at the bottom of the mesh. When equilibrium pressures are assigned, the initial water content at the measurement depth may be considerably higher or lower than the first measured water content value. To overcome this problem, initial conditions were set at equilibrium pressure and these pressure values were converted to water content values based on the most likely parameter set of preliminary modeling exercises.

Probabilistic Calibration of Unsaturated Parameters

There were two major criteria for selecting a model for calibrating the hydraulic parameters: to be able to incorporate all available information on the system, and to be able to present the results in a probabilistic way such that the confidence in results would be explicit. A Bayesian approach satisfies both criteria because Bayes' theorem can statistically weight and thus update the prior information about the model parameters (e.g. from literature values, preliminary modeling exercises), with the degree of agreement between model predictions and observed field water content data. Bayesian approaches differ from classical statistics by allowing use of a subjective probability distribution, which represents the information on the system prior to new data collection. In this research, each simulation was assumed to have equal probability prior to comparison of simulations results with the field data. Through a Bayesian updating procedure, the probability of each simulation and the probability distributions of the parameters were re-calculated.

The Bayesian approach used in this research for probabilistic calibration of hydraulic parameters (θ_r, θ_s, K_{sat}, α, and n) was adopted from Sohn et al. (2000). Uniform prior probability distributions were assigned to the unsaturated parameters based on literature data (Bigl and Berg, 1996) and previous embankment modeling experience. Uniform prior distributions were selected because the prior available information suggested that the parameters could take

any value within the expected ranges. The parameter θ_r was kept constant at 0.25 based on values reported by Bigl and Berg (1996) and water content observations of the embankment in the field. The ranges of the remaining parameters are shown in Table 4.1. Parameters were grid sampled (11 samples each) from uniform distributions and HYDRUS2D was run for all combinations of the parameters (11^4=14,641 simulations). Visual basic code was used to sequentially run HYDRUS2D for each parameter combination and store the necessary output in a designated folder. The simulated output from HYDRUS2D was compared to field measurements of water content at a depth of 0.32 m into the embankment by calculating the likelihood of each simulation. Posterior probabilities of each simulation were obtained from Bayes' theorem.

Table 4.1 Prior and posterior mean and standard deviations of the updated parameters.

Parameters/ranges	Prior		Posterior		% Change in Standard Deviation
	Mean	Standard Deviation	Mean	Standard Deviation	
θ_s (0.33-0.43) (m^3/m^3)	0.380	0.029	0.356	0.011	-60.7
α (2.7-4.7) (1/m)	3.700	0.577	3.788	0.673	16.5
n (2.6-4.1) (-)	3.350	0.433	3.854	0.215	-50.4
K_{sat} (0.3-4.3)(m/day)	2.300	1.155	0.353	0.246	-78.7

Assuming the error is distributed normally, the likelihood for any observation in time for the u'th simulation was calculated using the following equation:

$$L(O(t)|Y(t)) = \frac{1}{\sqrt{2\pi}\sigma_u} \exp\left(-\frac{1}{2}\left[\frac{O(t) - Y(t)_u}{\sigma_u}\right]^2\right) \quad [4.6]$$

where σ_u is the variance of the difference between measured and modeled water content values in time; O(t) is observed and Y(t) is modeled water content value at 0.32 m below ground surface.

Each of the data points in time in the measured data set was assumed to be independent. In other words, for simplicity, the temporal correlation between consecutive water content measurements was not included in the statistical model. The likelihood of observing all data points in time (129 observations for 16 days) and thus the likelihood for the u'th simulation is given by the product of likelihood of each observation which quantifies the difference between the observations and the model output:

$$L(O \mid Y_u) = \prod_{t=1}^{T} L(O(t) \mid Y(t)_u) \qquad [4.7]$$

The variance of each simulation was calculated as:

$$\sigma_u{}^2 = \frac{1}{T} \sum_{t=1}^{T} (O(t) - Y(t))^2 \qquad [4.8]$$

where t is 3-hour intervals up to 16 days.

The posterior probability of each simulation, p'_u, was calculated from the likelihood using Bayes theorem:

$$p'_u = p'(Y_u|O) = \frac{L(O|Y_u)p(Y_u)}{\sum_{u=1}^{U} L(O|Y_u)p(Y_u)} \qquad [4.9]$$

The prior distribution for the simulations was uniform (each simulation had equal probability initially) resulting in a constant $p(Y_u)$ value, which was canceled

out from the denominator and the numerator. Thus, the posterior probability of each simulation was the normalized likelihood value.

Once the posterior probabilities were calculated for each simulation, the profile likelihood ratio concept (Kalbfleish and Sprott, 1970; Vrugt and Bouten, 2002) was used to determine the confidence intervals of the posterior parameters. Chi square significance of $p<0.05$ was chosen as a cut off for deciding which parameter combinations (simulations) were significant.

Probability weighted mean and variance of the unsaturated parameters were calculated from the posterior probabilities that passed the likelihood ratio test and the corresponding parameter value using:

$$\mu'_{\theta} = \sum_{u=1}^{U} \theta_u \cdot p_u' \qquad [4.10]$$

$$\sigma'^{2}_{\theta} = \sum_{i=1}^{U} (\theta_u - \mu'_{\theta})^2 \cdot p'_u \qquad [4.11]$$

where θ_u is one of the four parameters investigated and U is the total number of simulations (14,641).

Coal Fly Ash Scenario Model

Contaminant leaching was simulated for 10 years for a hypothetical coal fly ash embankment scenario where top 0.50 m of the MnROAD embankment was replaced with coal fly ash (Figure 4.1c). The groundwater table was set at 1.9 m, which is within the range (1.3 to 4.6m) observed at the MnROAD test site.

An entire year's precipitation data repeated ten times was input as the variable flux boundary condition. The molecular diffusion coefficient of Cadmium in free water was input in the model as a constant (6.2×10^{-5} m^2/day) (Li and Gregory, 1974) and tortuosity factor was calculated within HYDRUS2D as a function of the water content using Millington and Quirk's (1961) equation ($\tau = \theta^{7/3}/\theta_s^2$).

The probability distributions of unsaturated hydraulic properties of the embankment soil, given in Table 4.3, were determined from parameter posterior probabilities obtained from embankment infiltration simulations. Probability distributions were fit to the four parameters (θ_s, α, n, K_{sat}) based on the posterior probabilities generated from HYDRUS2D simulations that passed the profile likelihood ratio test. Weighted moment equations were applied to calculate the means and standard deviations for the normal distributions (Table 4.2). Saturated hydraulic conductivity and saturated water content were assigned joint lognormal distributions with correlation ($\log(\theta_s)$,$\log(K_{sat})$) = 0.87.

Table 4.2 Probability distributions for unsaturated parameters.

Coal fly ash	MnROAD Embankment
Log (θ_r) ~Normal (-2.881, 0.559)	θ_r = 0.25
θ_s ~ Normal (0.455,0.035)	Log (θ_s) ~ normal (1.033, 0.031)
α ~Uniform (0.08,0.45)	α ~Normal (3.788, 0.673)
n ~Normal (2.567,0.378)	Log (5 - n) ~ normal (0.113, 0.186)
Log (K_{sat}) ~Normal (-3.18,0.96)	Log (K_{sat}) ~ normal (-1.125, 0.315)
K_d ~ Uniform (0.3, 2000)	K_d ~ Uniform (1, 4000)
ρ_b ~ Normal (1.303, 0.109)	ρ_b ~ Normal (1.756, 0.074)
τ ~Uniform (0.1, 0.5)	
D_i ~ Uniform (0.05, 0.36)	

Probability distributions for all other parameters were based on literature data. Probability distributions for α, n, θ_s, θ_r, K_{sat}, and bulk density of the coal fly ash were based on six sources of coal fly ash with measurements on both drying and wetting of the samples (Young, 1993). The saturated hydraulic conductivities reported in Young (1993; 10^{-2}-10^{-1} m/day) are similar to those reported by Bowders et al. (1987; 10^{-2} m/day) but higher than those reported in Vesperman et al. (1985; 10^{-7} m/day) and Creek and Shackelford (1992; 10^{-5}-10^{-3} m/day). The bulk density distribution for the embankment was estimated by measurement of the subgrade material in this research (1.88 kg/L) and by Bigl and Berg (1996) (1.74, 1.69, 1.84 kg/L).

Partition coefficients reported in soil and coal fly ash vary three to four orders of magnitude for different conditions of pH and liquid to solid ratios. In unsaturated conditions, the pH of secondary materials during leaching may vary more than in saturated conditions (Townsend et al., 1999). To account for the variability, uniform distributions (Table 4.2) were assigned to partition coefficients based on the values reported by U.S. EPA (1999) and van der Sloot et al. (1992) for soil and coal fly ash, respectively. The temporal and spatial variability of K_d that would be expected in the field was incorporated in the modeling approach by keeping the K_d values of the subgrade and the coal fly ash constant in a given simulation but probabilistically varying them from simulation to simulation. The value of K_d is often considered as a measure of the strength of the adsorption of a contaminant on the soil. In this research, K_d is the lumped parameter for

multiple processes such as dissolution/precipitation, surface complexation, surface precipitation, and diffusive transfer from particle core to the bulk solution. Use of K_d in the finite element model can be viewed as a method for interpreting pH and liquid to solid specific leachate data.

My decision to use K_d values for predicting contaminant release is supported by the work of Bin-Shafique et al. (2002) on another metal; selenium. Bin-Shafique et al. (2002) estimated material specific K_d values from laboratory column studies and then used these estimates in HYDRUS2D to predict leaching from coal fly ash stabilized pavements. Field data was available for only two years; yet a deterministic HYDRUS2D simulation accurately predicted field release for Selenium for this short period.

Uncertainty in parameters was propagated through the model by running HYDRUS2D with parameters randomly sampled from the parameter probability distributions. To be able to run consecutive automated simulations randomly sampled from probability distributions, the initial aqueous concentration assigned to the coal fly ash was set to unity. HYDRUS2D allows input of initial aqueous concentration and calculates the equilibrium solid concentration of the contaminant based on the K_d value. As long as the simulation results can be normalized, the absolute value of the concentration is not important since the concentration term appears throughout the advection dispersion equation. Contaminant leaching was evaluated by comparing the total mass of Cadmium

leached across a point 0.01 m below the coal fly ash to the initial Cadmium mass input in the HYDRUS2D.

RESULTS AND DISCUSSION

Updating of Uncertainty

A majority of the posterior probabilities were insignificantly low suggesting that many of the parameter combinations were unlikely to be representative of the system modeled (Figure 4.2). Applying the likelihood ratio criteria, simulations with posterior probabilities less than 10^{-6} were eliminated leaving 510 simulations (with total posterior probability of 0.999345) that were further analyzed statistically. Only three simulations had posterior probabilities greater than 0.1.

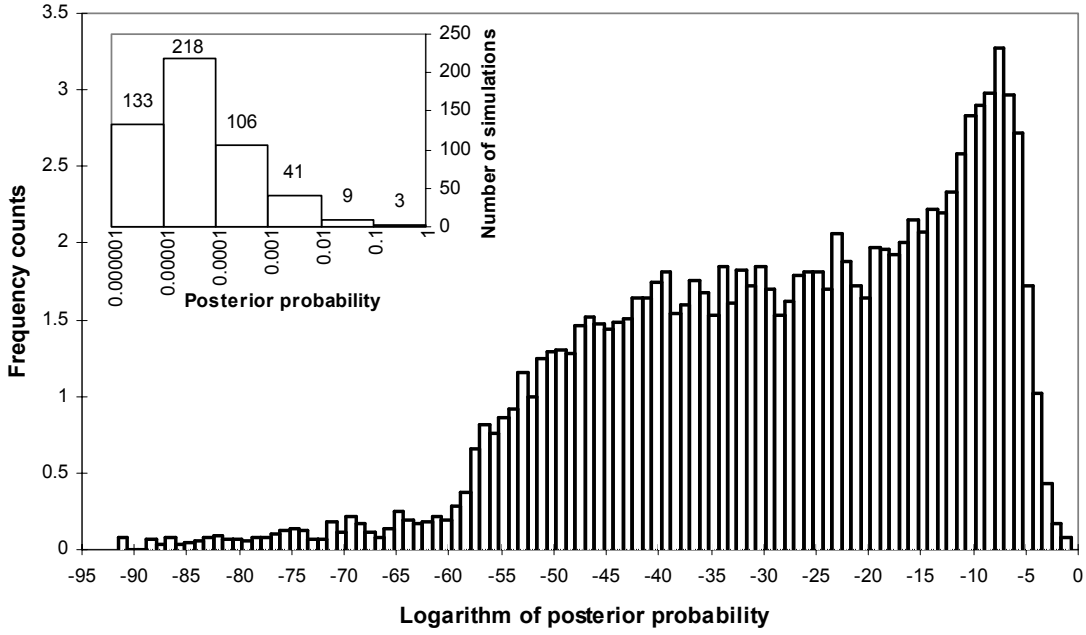

Figure 4.2 Histogram of posterior probabilities of all simulations and distribution of accepted posterior probabilities (inset).

The summary statistics of the prior and posterior distributions are shown in Table 4.1. The mean of the distribution of n increased, while its standard deviation decreased in the posterior estimates. The standard deviation of α increased suggesting that the prior distribution assigned to this parameter was too tight. The mean and the standard deviations of K_{sat} and θ_r distributions decreased after Bayesian updating. The posterior mean of K_{sat} is very close to the lower end of the range of the prior distribution. Laboratory measured values by Bigl and Berg (1996) (0.0002-0.003m/day) also included much lower values for K_{sat}. However, K_{sat} is probably not much lower than 0.03 m/day since preliminary Bayesian analysis of this problem done with fewer grid samples but wider ranges for K_{sat} (including 0.00035, 0.0035, and 0.035) had eliminated the possibility of these low values representing field saturated hydraulic conductivity. The results of the Bayesian analysis suggest that embankment hydraulic conductivity may be higher than laboratory measured values, possibly due to preferential flow paths.

Many authors noted that calibrated parameters may not be unique (Lambot et al., 2002; Poeter and Hill, 1997; Valota et al., 2002). The Bayesian updating technique inherently addresses this concern by probabilistic conceptualization of the calibration problem. Firstly, all parameters were varied (except θ_r) simultaneously since the parameter space was sampled in all four dimensions. The updated parameters are representative of all combinations within the parameter ranges sampled from. This approach is more

representative of the parameter space than varying one parameter at a time. Secondly, the updated parameter values are not viewed as unique solutions where the possibility of other parameters representing the system is mainly ignored. In the Bayesian updating approach, the possibility of other values of the parameters is viewed as the uncertainty related to the model, model parameters, and the modeler. Bayesian posteriors, which define the most relevant regions of the multidimensional parameter space for this particular problem, contain all information about the system such as prior expectations of the parameters and the measured field water content data.

The posterior means of the parameters provide a reasonable match between the measured and simulated water content data (Figure 4.3) and similar results were observed when the posterior means were tested on another set of time series available for the same embankment (Figure 4.4). Presence of only a single data point for calibration is one weakness of the current research compared to other studies where close matches between measured and modeled water contents were also observed in controlled field and laboratory experiments (Jacques et al., 2000; Lambot et al., 2002). In this research, overall, the model adequately reproduced water content for precipitation events exceeding 0.01 m, but under predicted the response of smaller rain events. Multiple factors may be the cause of the minor deviations between the model output and field data. Presence of lateral flow, limitations of the van Genuchten model, evaporation, and hysterisis may have contributed to the deviations

between measured and modeled output. Acting as an impermeable boundary, the TDR rod might also affect the local distribution of water content (Ferre et al. 2002). The impermeable volume of the TDR rod was not considered in the HYDRUS2D model.

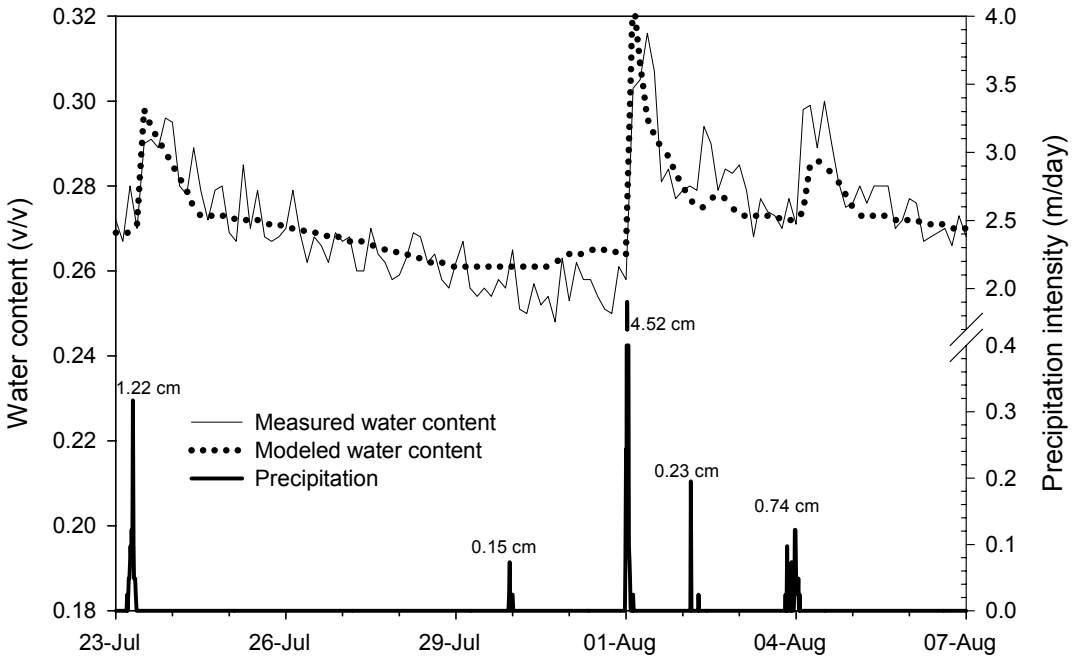

Figure 4.3 Modeled and measured water content data at 0.32m from the surface and the corresponding precipitation quantity and intensity for a 16 day period in 1997.

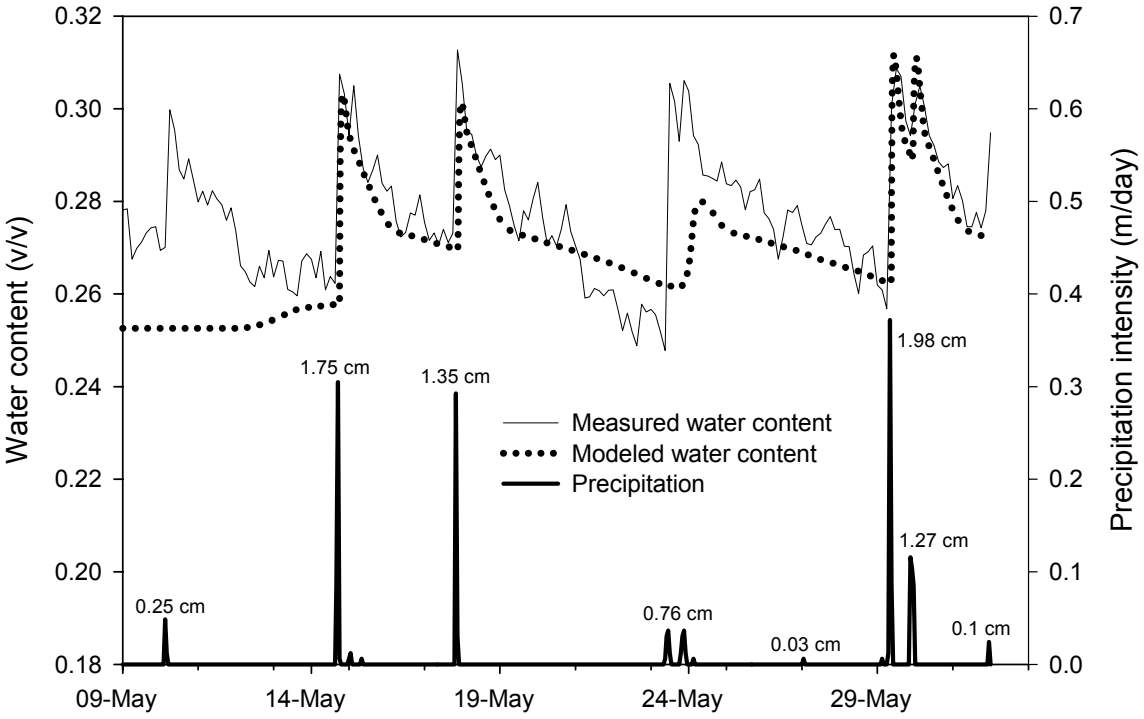

Figure 4.4 Modeled and measured water content data at 0.32 m from the surface and the corresponding precipitation quantity and intensity for a 23 day period in 1998.

Coal Fly Ash Simulations

Infiltration and Liquid to Solid Ratio

Water and Cadmium mass balance errors in the 113 randomly sampled simulations were less than 2.7 and 1.0 percent, respectively. The total potential infiltration (annual precipitation) was 0.65m/year and 92 percent (0.60 m/year) of this flux actually infiltrated into the embankment at the 90^{th} percentile of uncertainty. Simulation results showed that the actual infiltration could be as low as 34 percent (0.22 m/year) of the potential infiltration, while the mean infiltration was 71 percent (0.46 m/year). Hjelmar (1990) measured percentage of precipitation passing through large-scale lysimeters filled with slightly compacted coal fly ash. The values reported by Hjelmar (58, 53, 55, 42, 46, 59, 61 percent) for multiple lysimeters and two different types of fly ashes are slightly lower than the mean value estimated in this research possibly due to differences in site conditions.

The liquid to solid ratio is a measure of the amount of water that has passed through the secondary material application and is calculated by dividing the product of time [T] and flux of water [L^3/T] through the material by the mass of the material [M]. The mass of the secondary material varied among simulations due to randomly sampled bulk density values. The liquid to solid ratio in ten years was 7.15 L/kg and 9.48 L/kg on average and at the 90^{th} percentile of uncertainty,

respectively (Figure 4.5). The liquid to solid ratios measured by Hjelmar (1990) normalized to 10 years and 0.50 m of coal fly ash are 4.6, 4.85, and 3.92 L/kg. Higher liquid to solid ratios estimated in this research may be due to differences in climate, groundwater table depth, and hydraulic conductivity.

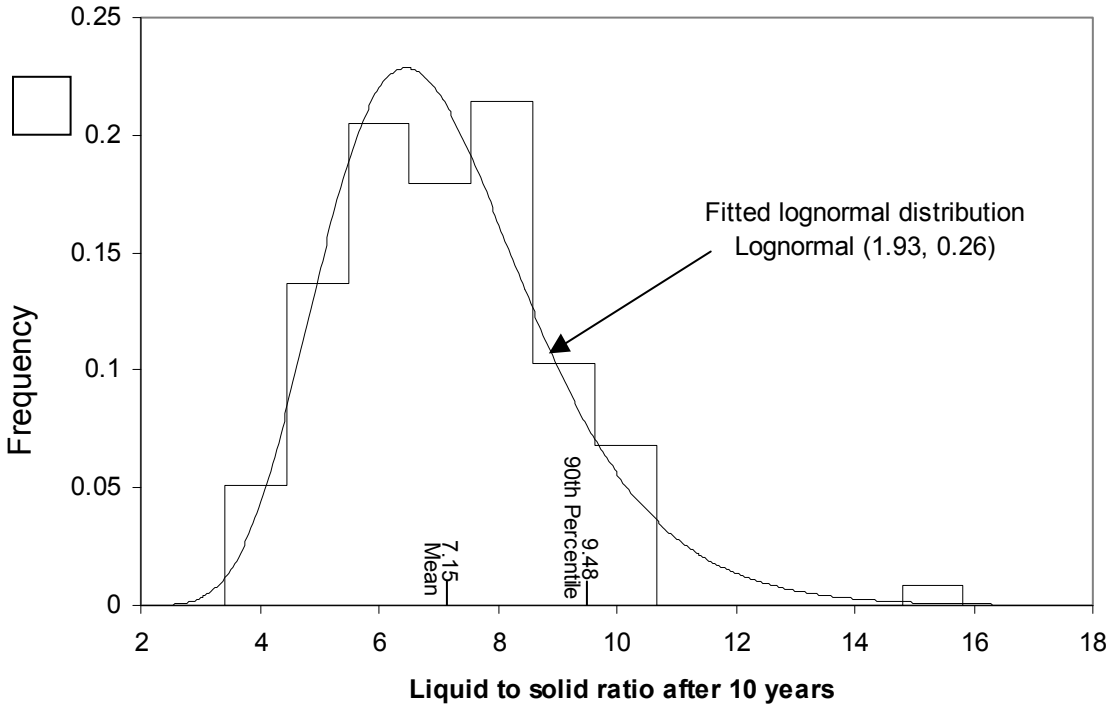

Figure 4.5 Histogram and fitted probability distribution for liquid to solid ratio after 10 years.

Leaching from Coal Fly Ash

The average percentage of initial available mass leached after 10 years, as observed 0.01 m below ash, was 0.21 $\pm$ 0.20 percent. As also suggested by the high value of the standard deviation, the probability distribution is skewed to the right (Figure 4.6). At the 90th percentile of uncertainty, the percentages of initial available mass leached are 0.02, 0.20, and 0.48 percent for one, five, and

ten years, respectively (Figure 4.7). No significant Cadmium fluxes were observed 0.25 m below the coal fly ash or at the groundwater table depth. After 10 years, the fraction of initial available mass leached was 5×10^{-6} percent at 0.25 m below the coal fly ash, and zero percent at the groundwater table depth (at the 90^{th} percentile of uncertainty).

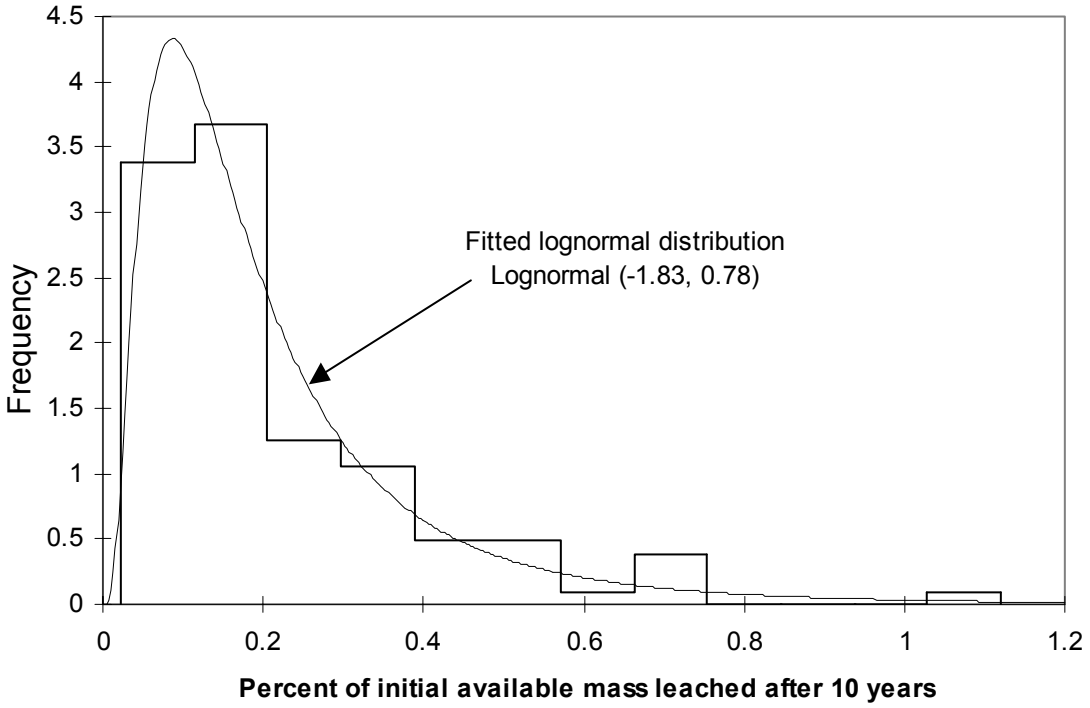

Figure 4.6 Histogram and fitted probability distribution for percent of initial available mass leached after 10 years (as observed 1 cm below coal fly ash).

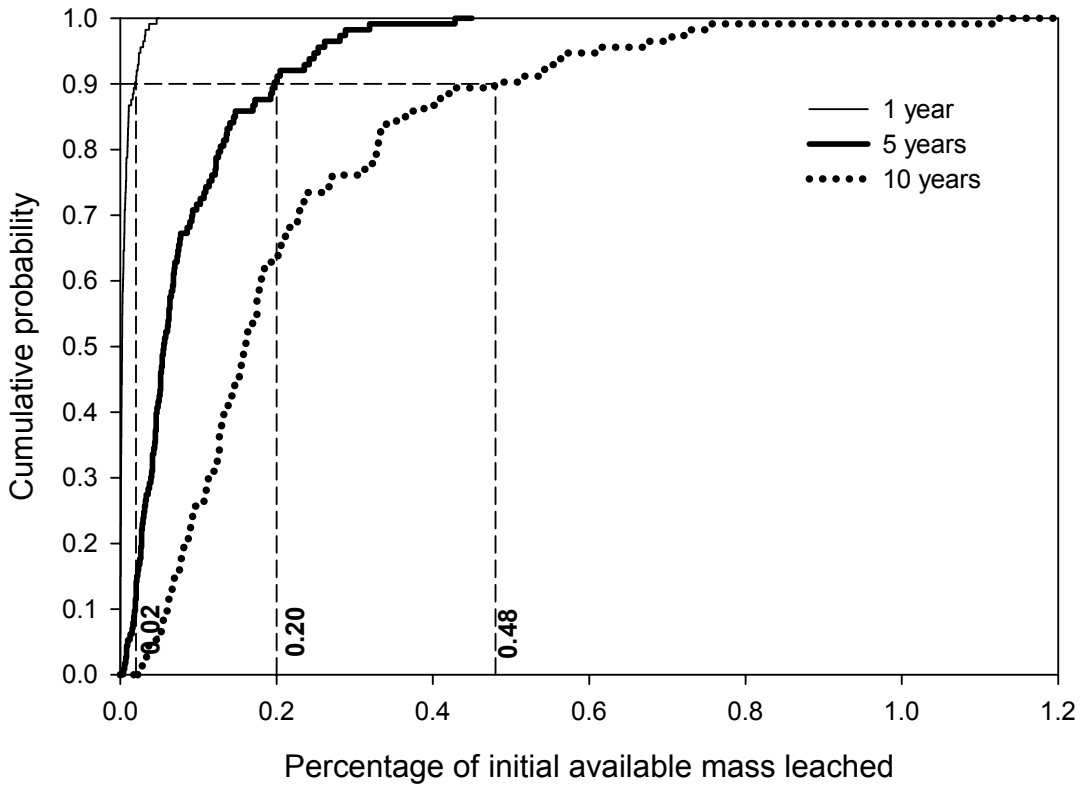

Figure 4.7 Cumulative probabilities of percentages of initial available mass leached (as observed 1 cm below coal fly ash) after 1, 5, and 10 years.

Results of HYDRUS2D simulations were so far expressed in percentage of initial available mass leached. These results can also be interpreted in mg/kg units by use of the following equation:

$$\text{Release (mg/kg)} = PL \times T_{Cd} \times MA \qquad [4.12]$$

where PL = percentage of initial available mass leached [-]

T_{Cd} = Total concentration of Cadmium in the sample [mg/kg]

MA = Maximum availability of Cadmium expressed as percentage of total contents [-]

Probability distributions were assigned to each term in equation 12. A lognormal distribution was fit to the percent leached data (Figure 4.6). The total Cadmium content in coal fly ash was modeled as a lognormal distribution ($\log(T_{Cd})$ ~normal(1.93, 0.26)) based on values reported for 96 coal fly ash sources reported in the literature (Alva et al., 1999a; Alva et al., 1999b; Brunori et al., 2001; Garavaglia and Caramuscio, 1994; Hassett et al., 2001; Khandekar et al., 1999; Mukherjee and Kikuchi, 1999; Schwab, 1993; Twardowska, 1999a; Twardowska, 1999b; van der Sloot et al., 1991; van der Sloot et al., 1992; Wu and Chen, 1987). The percentage of maximum observed availability of total content was modeled with a uniform distribution with minimum and maximum values of 5 percent and 36 percent, respectively (van der Sloot et al., 1992; Chaudhuri et al., 2003; Kim and Kazonich, 2001).

The cumulative release at the 90^{th} percentile of uncertainty, calculated using equation 12 and the appropriate probability distributions, was 2.65×10^{-3} mg Cd/kg ash after 10 years (Figure 4.8). The mean of the release estimate was 1.15×10^{-3} mg Cd/kg ash. Hjelmar (1990) measured Cadmium concentrations in coal fly ash lysimeters and reported below detection limit concentrations (<0.0001 mg/L) after 0.5, 2.6, and 2.6 years for three different lysimeters. To estimate total release of Cadmium in 5 and 10 years, I assumed detection limit concentrations for those times when Hjelmar's (1990) measurements were below detection limit. With this conservative approach, the total release measured by Hjelmar (1990) varies from 1.7×10^{-5} to 6.5×10^{-5} mg Cd/kg ash, in approximately

five years. If the estimates are extended to 10 years, the release varies from 6.3×10^{-4} to 6.7×10^{-4} mg Cd/kg ash. Thus, the mean of the HYDRUS2D simulation results were within one order of magnitude of the estimate from Hjelmar's (1990) field experiments when his results were extrapolated conservatively to 10 years.

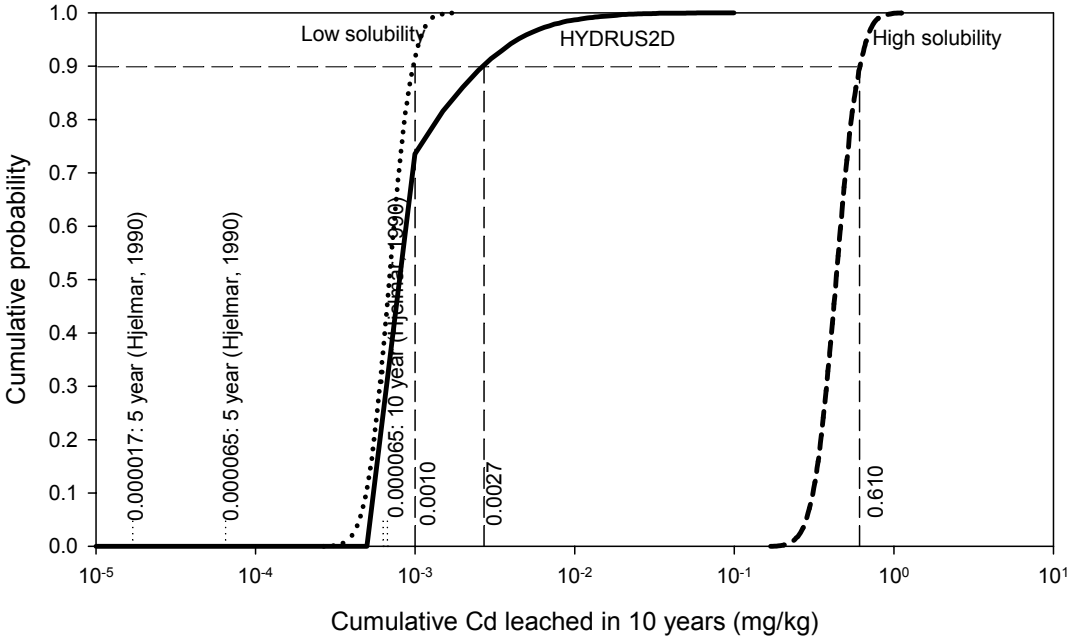

Figure 4.8 Cumulative probabilities of mass of Cd leached.

Comparison with the Percolation Equation Method

In the percolation equation suggested by Kosson et al. (1996) the cumulative mass released is calculated from the product of solubility of Cadmium and the cumulative liquid to solid ratio.

$$\text{Release (mg/kg)} = S_{Cd} \times \text{(Liquid to Solid Ratio)} \quad [4.13]$$

Where S_{Cd} is the solubility of Cadmium [mg/L].

The underlying assumption of this approach is that Cadmium will be transported at its solubility value and the advection rate is equal to the annual infiltration rate. Spatial and temporal scales are not explicitly considered in this equation; the release is assumed to be a point source with constant concentration transported at the infiltration rate. This approach is a simplified application of the HYDRUS2D simulations (Table 4.3).

Table 4.3 Comparison of deterministic applications of the two approaches for calculating release

	Percolation equation	HYDRUS2D simulations
Considers diffusion?	No	Yes
Considers dispersion?	No	Yes
Considers multiple layers?	No	Yes
Considers tortuosity?	No	Yes
Solubility assumption	Constant	Varies linearly with the partition coefficient
Infiltration	Obtained from other resources	Calculated
Source of release	Point source	Release throughout the material

The distribution assigned to the liquid to solid ratio for use in the percolation equation method was the lognormal distribution fitted to the

HYDRUS2D outputs (Figure 4.5). Leachate Cadmium concentrations from coal fly ashes can vary from 0.0001 to 0.063 mg/L as a function of pH and liquid to solid ratios (van der Sloot et al., 1992). When the low value of leachate Cadmium concentration was used, the release estimate from the percolation equation was within one order of magnitude of the release estimate from the HYDRUS2D simulation at the 90^{th} percentile of uncertainty (Figure 4.8). The release estimate from the high value of leachate Cadmium concentration was two to three orders of magnitude higher than the other estimates. Figure 4.8 shows that the release estimates predicted from Hjelmar's (1990) field lysimeters data are close to the HYDRUS2D results, and the percolation equation results estimated from the low Cadmium solubility value. Use of high solubility values results in a significant over predictions of Cadmium release.

CONCLUSIONS

In this research, the dynamics of the water content in a highway embankment was simulated using a probabilistic Bayesian updating approach for parameter calibration. Updated parameters and literature values were used to predict release of Cadmium from a hypothetical coal fly ash embankment using two different approaches. If a low solubility value is used for Cadmium, the release estimates are close to those measured by Hjelmar (1990) and also predicted from HYDRUS2D simulations. If high solubility is used, the percolation equation significantly over predicts the actual release. The use of the advection

dispersion equation for transport and retardation in unsaturated medium is a powerful method for predicting contaminant release, especially when it is coupled with probability. One implication of the use of the advection dispersion equation is the ability to extend the release estimates to two-dimensional systems where the percolation equation may no longer be applicable due to lateral flows and more complicated hydraulic regimes. The authors recommend application of the proposed approach to two dimensions to more realistically predict both the water flow and the contaminant release and transport processes in highway environments.

ACKNOWLEDGEMENTS

The authors would like to thank Jirka Simunek for his valuable help on the use of HYDRUS2D code. This work was funded through a cooperative agreement (DTFH61-09-X-00095) between FHWA and the University of New Hampshire.

REFERENCES

1. Alva, A.K., Bilski, J.J., Sajwan, K.S. and Clief, D.V. (1999a). Leaching of metals from soils amended with fly ash and organic byproducts. In K.S. Sajwan, A.K. Alva and R.F. Keefer, Eds., *Biogeochemistry of trace elements in coal and coal combustion byproducts.* New York: Kluwer Academic, pp. 193-206.

2. Alva, A.K., Paramasivam, S., Prakash, O. and Sajwan, K.S. (1999b). Effects of fly ash and sewage sludge amendments on transport of metals in different soils. In K.S. Sajwan, A.K. Alva and R.F. Keefer Eds., *Biogeochemistry of trace elements in coal and coal combustion byproducts*. New York: Kluwer Academic, pp. 207-222.

3. Apul, D. S., Gardner, K.H., and Eighmy, T.T. (2003). A probabilistic source assessment framework for leaching from secondary materials in highway applications. *Clean Techn. Environ. Policy.* **5**, 120-127

4. Brunori, C., Balzamo, S. and Morabito, R. (2001). Comparison between different leaching test for the evaluation of metal release from fly ash. *Fresenius J. Anal. Chem*, 371, 843-848.

5. Bigl, R. And Berg, R.L. (1996). *Testing of materials from the Minnesota cold regions pavement research test facility.* CRREL Special report 96-20.

6. Bin-Shafique, M. S., Benson, C.H., and Edil, T. B. (2002). *Leaching of heavy metals from fly ash stabilized soils used in highway pavements*. Geo Engineering Report No. 02-14, Madison, University of Wisconsin - Madison: 204.

7. Birgisson, B. and Roberson, R. (2000). Drainage of pavement base material: Design and construction issues. *Transport. Res. Rec.* **1709,** 11-18.

8. Birgisson, B. and Ruth, B. E. (2003). Improving performance through consideration of terrain conditions: Soils, drainage, and climate. *Transport. Res. Rec.* **1819**, 369-377.

9. Bowders, J., Usmen, M, and Gidley, J. (1987). Stabilized fly ash for use as low-permeability barriers. In R.D. Woods, Eds., *Geotechnical practice for waste disposal '87 (Geotechnical Special Publication No. 13).* New York: ASCE. pp. 320-333.

10. Chaudhuri, D., Tripathy, S., Veeresh, H., Powerll, M.A., and Hart, B.R. (2003). Mobility and bioavailability of selected heavy metals in coal ash- and sewage sludge-amended acid soil. *Environ. Geol.* **44**, 419-432

11. Creek, D. and Shackelford, C. (1992). Permeability and leaching characteristics of fly ash liner materials. *Transport. Res. Rec.* **1345**, 74.

12. De Haan, I. H. D., Fraaij, A. L. A., and Molenaar, A.A. (2003). Unsaturated water transport in secondary road building materials. In T.T. Eighmy, Eds., *Beneficial use of recycled materials in transportation applications*. Air & Waste Management, Washington, D.C., pp. 215-224.

13. Dijkstra, J. J., Van. Der Sloot, H. A., and Comans R. (2002). Process identification and model development of contaminant transport in MSWI bottom ash. *Waste Manage.* **22**, 531-541.

14. Fallman, A.-M. (2000). Leaching of chromium and barium from steel slag in laboratory and field tests - a solubility controlled process? *Waste Manage.* **20**, 149-154.

15. Ferre, T. P. A., Nissen, H.H., and Simunek, J. (2002). The effect of spatial sensitivity of TDR on inferring soil hydraulic properties from water content measurements made during the advance of a wetting front. *Vadose ZoneJ*. **1**, 281-288.

16. Frey, H. C. and Rhodes, D.S. (1996). Characterizing, simulation, and analyzing variability and uncertainty: an illustration of methods using an air toxics emissions example. *Hum. Ecol. Risk Assess.*. **2**(4), 762-797.

17. Ganguly, C., Matsumoto, M. R., Rabideau, A.J., and Van Benschoten, J.E. (1998). Metal ion leaching from contaminated soils: model calibration and application. *J. Environ. Eng.* **124**(12),1150-1158.

18. Garavaglia, R. and Caramuscio, P. (1994). Coal fly-ash leaching behaviour and solubility controlling solids. In J.J.J.M. Goumans, H.A.v.d. Sloot and T.G. Albers Eds., *Environmental aspects of construction with waste materials: Proceedings of the international conference on environmental implications of construction materials and technology developments, Maastricht, The Netherlands*. London: Elsevier, pp. 87-102.

19. Gardner, K.H., Theis, T.L. and Iyer, R. (2002). An experimental and analytical approach to understanding the dynamic leaching from municipal solid waste combustion residue. *Environ. Eng. Sci.* **19**(2), 89-100

20. Hassett, D., Heebink, L., Bloom, P. and Gustin, F. (2001). *Environmental evaluation for utilization of ash in soil stabilization*, Electric Power Research Institute, Palo Alto, CA.

21. Hjelmar, O. (1990). Leachate from land disposal of coal fly ash. *Waste Manage.* **8**,429-449.

22. Jacques, D., Simunek, J., Timmerman, A., and Feyen, J. (2002). Calibration of Richards' and convection-dispersion equations to field-scale water flow and solute transport under rainfall conditions*. J. Hydrol.* **259**,15-31.

23. Huber, W. C., Nelson, P.O, Eldin, N.N., Williamson, K.J., and Lundy, J.R. (2001). Environmental impact of runoff from highway construction and repair materials: project overview. *2001 TRB Annual Meeting*, Washington D.C.

24. Kalbfleisch, J.D. and Sprott, D.A. (1970). Application of likelihood methods to models involving large number of parameter. *J. R. Stat. Soc. Ser. B Stat. Methodol*. **32**,175-208.

25. Khandekar, M.P., Bhide, A.D. and Sajwan, K.S. (1999). Trace elements in indian coal and coal fly ash. In K.S. Sajwan, A.K. Alva and R.F. Keefer, Eds., *Biogeochemistry of trace elements in coal and coal combustion byproducts.* New York: Kluwer Academic, pp. 99-113.

26. Kida, A., Noma, Y. and Imada, T. (1996). Chemical speciation and leaching properties of elements in municipal incinerator ashes. *Waste Manage.* **16**(5/6), 527-536.

27. Kim, A.G. and Kazonich, G. (2001) In S.S. Tyson and G.J. Deinhart, Eds., Proceedings: 14th International symposium on management and use of coal combustion products (CCPs): Volume 1, EPRI, Palo Alto, CA, pp. 20.

28. Kosson, D.S., Van Der Sloot, H.A., and Eighmy, T.T., (1996). An approach for estimation of contaminant release during utilization and disposal of municipal waste combustion residues. *J. Hazard. Mater.* **47**, 43-75.

29. Kosson, D.S., Van Der Sloot, H., Sanchez, F., and Garrabrants, A.C. (2002). An integrated framework for evaluating leaching in waste

management and utilization of secondary materials. *Environ. Eng. Sci.* **19**(3),159-204.

30. Lambot, S., Javaux, M., Hupet, F., and Vanclooster, M. (2002). A global multilevel coordinate search procedure for estimating the unsaturated soil hydraulic properties. *Water Resour. Res.* **38**(11)**,** 6.

31. Ledieu, J., Deridder, P., Declerck, P., and Dautrebande, S. (1986). A method of measuring soil moisture by time-domain reflectometry. *J. Hydrol.* **88**, 319-328.

32. Li, Y. and Gregory, S. (1974). Diffusion of ions in sea water and in deep-sea sediments. *Geochim. Cosmochim. Ac.* **38**, 703-714.

33. Maxwell, R. M. and Kastenberg, W. R. (1999). Stochastic environmental risk analysis: an integrated methodology for predicting cancer risk from contaminated groundwater. *Stoch. Env. Research Risk A.* **13**,27-47.

34. Meima, J. A. and Comans, R. N. J. (1998). Application of surface complexation / precipitation modeling to contaminant leaching from weathered municipal solid waste incinerator bottom ash. *Environ. Sci. Technol*. **32**,688-693.

35. Millington , R. J. and Quirk, J.M. (1961). Permeability of porous solids. *Trans. Faraday Soc.* **57**, 1200-1207.

36. Mukherjee, A.B. and Kikuchi, R. (1999). Coal ash from thermal power plants in Finland: A review. In K.S. Sajwan, A.K. Alva and R.F. Keefer, Eds., *Biogeochemistry of trace elements in coal and coal combustion byproducts*. New York: Kluwer Academic, New York, pp. 59-75.

37. Pagotto, C., Bechet, B., Lanini, S. Descat, M., Paris, B., Piantone, P. and Raimbault, G. (2003). Environmental impact assessment of the use of municipal solid waste incineration bottom ash in roadwork. In G.O. d. Urbina and H. Goumans, Eds., *WASCON 2003: Proceedings of the Fifth international conference on the environmental and technical implications of construction with alternative materials*. San Sebastian, INASMET. pp. 3-12.

38. Park, J.-Y. and Batchelor, B. (2002). A multi-component numerical leach model copuled with a general chemical speciation code. *Water Res.* **36**,156-166.

39. Poeter, E. and Hill, M.C. (1997). Inverse models: a necessary next step in ground-water modeling. *Ground Water.* **35**(2), 251-260.

40. Rai, S. N., Krewski, D. And Bartlett, S. (1996). A general framework for the analysis of uncertainty and variability in risk assessment. *Hum Ecol. Risk Assess.* **2**(4), 972-989.

41. Sanchez, F., Gervais, C., Garrabrants, A.C., Barna, R, and Kosson, D.S. (2002). Leaching of inorganic contaminants from cement-based waste materials as a results of carbonation during intermittent wetting. *Waste Manage.* **22**, 249-260.

42. Schwab, A.P. (1993). Extractable and plant concentrations of metals in amended coal ash. In: R.F. Keefer and K.S. Sajwan, Eds., *Trace elements in coal and coal combustion residues*. Ann Harbor: Lewis Publishers, pp. 185-211.

43. Simunek, J., Sejna, M. and Van Genuchten, M.T. (1999). The HYDRUS-2D software package for simulating the two-dimensional movement of water, heat, and multiple solutes in variably-saturated media, version 2.0, U.S. Salinity Laboratory, Riverside, CA

44. Sohn, M.D., Small, M.J., and Pantazidou, M. (2000). Uncertainty in site characterization using Bayes Monte Carlo methods, *J. Environ. Eng*. **126**(10), 893-902.

45. Townsend, T. G., Jang, Y, and Thurn, L.G. (1999). Simulation of construction and demolition waste leachate. *J. Environ. Eng* **125**(11), 1071-1081.

46. Twardowska, I. (1999a). Environmental aspects of power plants fly ash utilization in deep coal mine workings. In K.S. Sajwan, A.K. Alva and R.F. Keefer, Eds., *Biogeochemistry of trace elements in coal and coal combustion byproducts.* New York; Kluwer Academic, pp. 29-57.

47. Twardowska, I., 1999b. Environmental behavior of power plants fly ash containing FGD solids utilized in deep coal mines. In K.S. Sajwan, A.K. Alva and R.F. Keefer, Eds., *Biogeochemistry of trace elements in coal and coal combustion byproducts***.** Kluwer Academic, New York, pp. 77-98.

48. U.S. EPA. (1999). *Understanding variation in partition coefficient, Kd, values Volume II: Review of geochemistry and available Kd values for cadmium, cesium, chromium, lead, plutonium, radon, strontium, thorium, tritium (3H), and uranium.* EPA 402-R-99-004B. Washington, D.C.

49. Valota, G., Giudici, M., Parravicini, G., Ponzini, G. and Romano, E. (2002). Is the forward problem of groundwater hydrology always well posed? *Ground Water.* **40**(5), 500-508

50. Van Der Sloot, H.A., Hoede, D., and Bonouvrie, P. (1991). *Comparison of different regulatory leaching test procedure for waste materials and construction materials.* ECN-C--91-082, Netherlands Energy Research Foundation (ECN), Petten.

51. Van Der Sloot, H.A., Van Der Hoek, E.E., De Groot, G.J. and Comans, R.N.J. (1992). *Classification of pulverized coal ash: Part 1 Leaching behavior of coal fly ash.* ECN-C--92-059, Netherlands Energy Research Foundation (ECN), Petten.

52. Van Genuchten, M.T. (1980). A closed-form equation for predicting the hydraulic conductivity of unsaturated soils. *Soil Sci. Soc. Am. J.* **44**, 892-898.

53. Vesperman, K., Edil, B, and Berthouex, P. (1985). Constant flow and constant gradient permeability on sand-bentonite-fly ash mixtures. In D. Daniel and S. Trauwein, Eds., *Hydraulic conductivity and waste contaminant transport in soil*. Philadelphia, ASTM STP 1142, pp. 521-545.

54. Vrugt, J.A., and Bouten, W. (2002). Validity of first-order approximations to describe parameter uncertainty in soil hydrologic models. *Soil Sci. Soc. Am. J*. **66**,1740-1751.

55. WU, E.J. and CHEN, K.Y., 1987. *Chemical form and leachability of inorganic trace elements in coal ash.* EPRI EA-5115, Electric Power Research Institute, Los Angeles, p. 160.

56. Young, S. C. (1993). Physical and hydraulic properties of fly ash and other by-products from coal combustion. Palo Alto, EPRI.

CHAPTER 5

SIMULTANEOUS APPLICATION OF DISSOLUTION/PRECIPITATION AND SURFACE COMPLEXATION/PRECIPITATION MODELING TO CONTAMINANT LEACHING FROM WEATHERED STEEL SLAG

ABSTRACT

This paper illustrates a new approach for modeling anion and cation leaching from complex matrices such as weathered steel slag. The novelty of the method is its simultaneous inclusion of sorption and solubility controls for multiple analytes. Thermodynamic equilibrium of As, Ca, Cr, Ba, SO_4, Mg, Cd, Cu, Mo, Pb, V, and Zn ions with aqueous complexes, soluble solids and sorptive surfaces were investigated; Al, Cl, Co, Fe, K, Mn, Na, Ni, Hg, and NO_3 were input in the model as background analytes. Saturation indices of minerals were used to identify possible soluble solids controlling the release of major ions. To estimate concentrations of sorptive surfaces, selective extractions of oxalate for aluminum silicates and ascorbate for hydrous ferric oxides (HFO) were used. Model calculations were based on the generalized double layer model and HFO sorption constants implemented in Visual Minteq. The developed model shows that leaching of SO_4, Cr, As, Si, Ca, Mg, and V are controlled by corresponding soluble solids. Leaching of Pb is controlled by $Pb(VO_4)_3$ solubility at low pHs and by surface precipitation reactions at high pHs. Leaching of Cd and Zn are controlled by surface complexation and surface precipitation, respectively.

INTRODUCTION

Steel slag is a by-product of steel making and has traditionally been used in road construction because of its good engineering properties. In the U.S., approximately 6.5 million tons of steel slag are produced annually, three quarters of which is used in road construction as asphaltic concrete aggregate (21%), as fill (21%), and as road base (37%). Other uses of steel slag are in railroad ballast, ice control, neutralization of industrial discharge and mine drainage, roofing granules, and landfill daily cover materials (Kalyoncu, 2001). Steel slag is formed at very high temperatures (1200-1700^{o}C). After it cools to atmospheric conditions, it becomes unstable and chemically weathers mainly due to oxic conditions, lower temperatures, and the presence of water. The secondary minerals that form are oxides of aluminum and iron, which may coat the surface of the steel slag grains (Luxan et al., 2000; Dorn and Meek, 1995; Bodurtha and Brassard, 2000). Amorphous oxide minerals of aluminum and iron may have a significant impact on the mobility of trace elements because of their large surface areas, microporous structures, and an abundance of binding sites (Jenne, 1968; Coughlin and Stone, 1995).

In this research, I investigated the leaching of 13 anions and cations from five-year old weathered steel slag by pH-stat experiments and geochemical modeling of the leaching system. Considering that aging reactions and formation of new minerals may affect release of contaminants by surface complexation,

surface precipitation, and dissolution / precipitation reactions, I considered all these chemical reactions in conjunction with aqueous contaminant complexation. Much of the investigation in similar types of work on residues focused on modeling dissolution / precipitation reactions of major elements in the residues (Eighmy et al, 1995). Two exceptions are the works of Meima and Comans (1998) and Dijkstra et al. (2000) who investigated the interactions of metals with hydrous oxides and successfully predicted the release of Cu, Mo, Pb, and Zn from MSWI ash. They used the surface complexation model (SCM) and the surface precipitation model (SPM) which have been extensively applied to various surfaces such as pure metal (Al, Si, Mn, Fe) hydroxides (Karthikeyan and Elliott, 1999; Tonkin et al., 2004; Csoban and Joo, 1999), carbonates (Zhu, 2002; Zachara et al., 1991), sulfides (Sun, 1991), natural soils (Gustafsson, 2001), sediments (Davis et al., 1998), and bacterial surfaces (Daughney and Fein, 1998). While SCM/SPMs have been used for many surfaces, most of these systems have been simpler, dual or tertiary systems unlike the conditions of leaching from residues where dozens of ions are present and competitively affect leaching.

The goal of this study was to develop a new modeling approach for anion and cation leaching from complex matrices such as weathered steel slag. The novelty of the method is its simultaneous inclusion of sorption and solubility controls for multiple analytes. I modeled leaching in the presence of multiple analytes as opposed to modeling each element in isolation from other species

because the nature of metal surface speciation on solid surfaces is a function of not only pH but also of surface coverage, specific surface complexes, ionic strength, and electrolyte type (Criscenti and Sverjensky, 2002). The steel slag sorptive surfaces were assumed to be characteristic of hydrous ferric oxides and the generalized double layer model and the SPM described in detail in Dzombak and Morel (1990) and Zhu (2002) were used. All reactions were modeled using Visual Minteq (version 2.15; http://www.lwr.kth.se/English/OurSoftware/vminteq/), which includes the HFO sorption constants from Dzombak and Morel (1990). Inputs for the model such as background analytes, sorbate and sorbent concentrations were obtained from pH stat leaching experiments, availability tests, and selective chemical extractions of the steel slag, respectively.

MATERIALS AND METHODS

Steel Slag and Laboratory Measurements

Steel slag was obtained from a Swedish electric arc furnace steel plant designed to produce low alloy steel from scrap steel. The slag is alkaline and dominated by Ca (22%), Al (2%), Fe (24%), Mg (4%), Cr (7%), Mn (4%), and Si (6%). The slag was placed in lysimeters at the Swedish Geotechnical Institute in Linköping, Sweden, in December 1992 and excavated in October 1997. Details of sample treatment and description of lysimeters and laboratory experiments are

given elsewhere (Fällman and Hartlén, 1994; Fällman, 1997; Fällman et al., 1999; Fällman et al., 2000) . Excavated samples were stored and sieved (4 mm sieve) under N_2/Ar to minimize the impact of O_2 or CO_2 on leachate characteristics. pH dependent leaching experiments were performed at room temperature, for 24 hours, and at a low liquid to solid (L/S) ratio of 5 L/kg which approximates interstitial water concentrations while still allowing for mixing to create homogenous solution. Neutral to alkaline pHs (6, 8, 10, and 12) were selected to bracket the pH between freshly produced slag (pH~12) and potential future pH values associated with carbonation (pH 7-8). The leachates were filtered through 0.2 μm filters and split into three samples. One split was preserved with HNO_3 for analysis of Al, As, Ba, Ca, Cd, Co, Cr, Cu, Fe, Hg, K, Mg, Mn, Mo, Na, Ni, Pb, S, Si, V, and Zn by AAS, GFAAS, or ICP-MS. The second split was left unpreserved and analyzed by IC for Cl, Na, K, and SO_4. The third split was analyzed for carbonates by high-temperature catalytic combustion and IR-analysis of CO_2. Metal concentrations available for sorption are needed for SCM/SPMs and were estimated from maximum potential leaching of the metals in the raw steel slag as described in Fällman and Hartlén (1994).

To determine mineral surface concentrations, XPS and “operationally” selective chemical extractions were used. For particle surface analysis using XPS, steel slag samples were ground to <250 μm to provide a homogenous and flat surface. Initially a broad scan at a pass energy of 150 eV was collected between 1,100 and 0 eV to identify photoelectron peaks of interest. Then

detailed, high resolution scans of photoelectrons of interest were collected at a lower pass energy (50 eV) to permit better resolution of spectral features. Element concentrations of C, O, Ca, Al, Si, and Fe, and their speciation were obtained from a statistical measure about the quality of the curve fitting exercise and the likely mineral phase identified using the National Institute of Standards and Technology (NIST) XPS database. The procedure for chemical extractions comes from Meima and Comans (1998). HFO extraction is based on the use of ascorbic acid as a solvent for the HFO as described by Kostka and Luther (1994). Amorphous aluminum (hydr)oxide extraction is based on the use of an acidic ammonium oxalate extraction of amorphous and partially crystalline aluminum phases as described by Blakemore et al. (1987). All extracted aluminum was attributed to amorphous aluminum (hydr)oxide.

Modeling

Modeling efforts were concentrated on As, Ca, Cr, Ba, SO_4, Mg, Cd, Cu, Mo, Pb, V, and Zn. The governing processes for Co and Ni leaching were not investigated because their leachate concentrations were below the detection limit at pHs greater than 8 and 6, respectively. Similarly, leaching of Hg was not described in the model because its concentration at pH of 10 was below detection limit and the availability test data for Hg was not available. Thus, in the model, Al, Cl, Co, Fe, K, Mn, Na, Ni, Hg, and NO_3 were treated as background analytes and their concentrations in the model were set to their measured

leachate concentrations at four different pHs. Equilibrium concentrations of the remaining components were investigated. Cu, Cd, Zn, and Mo input concentrations were obtained from the availability test of the raw steel slag (Table 5.1). Details of how Ca, Cr, Ba, SO_4, Mg, and Pb concentrations were input in the model are discussed in the results section. When I input all measured concentrations of ions and let Visual Minteq calculate the equilibrium concentrations of redox couples at the Eh values measured (Eh=360, 429, 327, and 166mV for pH 6,8,10, and 12 respectively), the speciation of Cr, As, V, and Fe were mainly dominated by their oxidized states except for Mn. Thus, in model calculations Mn^{+2}, CrO_4^{-2}, AsO_4^{-3}, VO_2^{+}, Fe^{+3} were used and redox calculations were not specified. Additions to the Visual Minteq database are given in Table 5.2.

Table 5.1 Availability, total composition and lysimeter losses (Fällman 1997). *Below detection limit, **oxidized availability, details given in (Fällman 1997).

	Total compositions	Availability	Availability (assuming L/S=5 L/kg)	Highest concentration leached and corresponding pH in pH stat experiments	Metal concentration released from December 1992 to June 1997 as collected from lysimeters
	mg/kg	mg/kg	mol/L	mol/L	mg/kg
As	5.26	1.75	$1.4\ 10^{-4}$	$1.6\ 10^{-7}$, pH=12	0.0051
Cd	0.45	0.06	$1.1\ 10^{-7}$	$2.3\ 10^{-7}$, pH=6	0.0002*
Cr	7760	5.42	$2.1\ 10^{-5}$	$1.2\ 10^{-6}$, pH=12	0.119
Cu	166	0.99	$3.1\ 10^{-6}$	$4.3\ 10^{-7}$, pH=12	0.0006
Mo	20.6	4.7	$9.8\ 10^{-6}$	$2.4\ 10^{-6}$, pH=10	0.0536
Pb	21.5	0.12	$1.2\ 10^{-7}$	$1.1\ 10^{-7}$, pH=6	0.0005
Zn	244	38.5	$1.5\ 10^{-4}$	$1.4\ 10^{-4}$, pH=6	0.0008

Table 5.2 Pure phase solids and solid solutions added to the Visual Minteq database

	Log K	Source
$Fe_2(MoO_4)_{3(s)}$	35.3	Meima and Comans (1998)
$Ba(S_{0.77},Cr_{0.23})O_4$	10.1	Rai et al. (1986)
$Cd(OH)_{2(ss)}$	-13.7	Meima and Comans (1998)
$Pb(OH)_{2(ss)}$	-8.2	Visual Minteq database
$Cu(OH)_{2(ss)}$	-10.7	Visual Minteq database
$Fe_2(MoO_4)_{3(ss)}$	35.3	Dijkstra et al. (2002)
$FeAsO_4{:}2H_2O_{(ss)}$	20.2	Visual Minteq database

Possible Controlling Solids

To determine solid phase control, measured leachate concentrations from pH dependent leaching experiments were entered into the model. pH was fixed at the controlled pH of the leachate sample. The Davies equation was used to calculate activity coefficients. Initially, no solids were allowed to precipitate and no sorption reactions were specified. The saturation indices in the output were used to determine possible solid phases present in the system. Once these solids were identified, simulations were repeated by inputting these solids as infinite solids and allowing surface complexation and surface precipitation reactions.

Sorbent Mineral Concentrations

As in Meima and Comans (1998) the sorbent concentration (sum of aluminum (hydr)oxides and HFO) was estimated from extractions and the HFO sorption constants were also applied to the alumino hydroxide surface. Meima and Comans (1998) justified the use of HFO as a surrogate for amorphous

aluminum oxides by noting that both the charge and coordination number of Fe(III) and Al(III) in these oxides were the same suggesting that aluminum and iron oxides may have a similar reactivity. An extensive database for sorption constants on aluminum hydroxides still does not exist. Limited measured data show that surface ionization constants are quite similar to those of HFO while the surface area may be three times smaller (210 m^2/g) (Karthikeyan and Elliott 1999). In the model, a different value for aluminum(hydr)oxides was not used because methods for estimating the area of a sorptive surface are debatable and can vary by up to five times (Dzombak and Morel, 1990). The HFO values recommended by Dzombak and Morel (1990) and also used by Meima and Comans (1998) were input in the model for specific surface area of HFO (600 m^2/g), concentration of binding sites (high and low affinity: 5 mmol/mol Fe, and 0.2 mol/mol Fe) and molecular weight of HFO and aluminum(hydr)oxides (89 g of sorbent/mol of Fe or Al).

Competitive Sorption

To accurately predict both sorbed and aqueous concentrations, ion competition on the sorptive surfaces needs to be considered. Incorrect estimation of the sorbed concentration of an ion may cause incorrect estimation of the sorbed concentration of other ions. For example, if a major sorbing ion is neglected in the system, the sorption of other ions may be overestimated. One method to overcome this problem is to pre-equilibrate the sites with existing ions

to determine the appropriate loading of the sorbent (Dijkstra et al., 2000). A different approach was taken in this study because an additional goal was to predict the aqueous concentrations of multiple ions. The most important major sorbing ions, Ca, Si, Mg, and Ba were modeled in the presence of soluble solids and the sorptive surface was allowed to equilibrate in these conditions.

Surface precipitation and estimation of T_s

The fraction of the adsorbent involved in the surface precipitation can vary from a few percent to the whole solid. The concentration of that fraction, T_s, was used as a fitting parameter in the model. In the model, T_s was iteratively estimated by fixing it to the concentration of solid material in solid solution (i.e. $T_s = Fe(OH)_{3(ss)}] + [Cd(OH)_{2(ss)}] + \ldots\ldots + [Cu(OH)_{2(ss)}] + [Pb(OH)_{2(ss)}]$). This modeling approach is consistent with two other definitions: (i) the activity of the sum of the solid solution precipitates is unity in an ideal solid solution ($\{Fe(OH)_{3(ss)}\} + \{Cd(OH)_{2(ss)}\} + \ldots\ldots + \{Cu(OH)_{2(ss)}\} = 1$), and (ii) the activity of a solid solution precipitate is its mole fraction on the surface (i.e. $\{Cd(OH)_{2(ss)}\} = [Cd(OH)_{2(ss)}] / T_s$). Since the solubility product, $K_{spMe} = \{Me^{2+}\} \times \{OH^-\}^2 / \{Me(OH)_{2(ss)}\}$, when the activity of $\{Me(OH)_{2(ss)}\}$ decreases from unity, surface precipitation occurs at metal and OH^- activities lower than those required for precipitation of pure solid phases.

RESULTS AND DISCUSSION

Sorptive Surfaces

The amounts of Al and Fe obtained from ascorbate and oxalic acid extractions from samples less than 4 mm in size were 895 mg/kg (0.00201 mol/L) and 3040 mg/kg (0.00683 mol/L), respectively. Amorphous ferric oxide concentrations estimated from individual Fe peaks of XPS on samples ground to 250 μm were about twice greater (6300 mg/kg) while amorphous aluminosilicate concentrations from all Al peaks were almost 30 times greater (29000 mg/kg). It is possible that Al was mainly locked up inside bigger particles; when the samples were ground to 250 μm, the Al inside particles were exposed and detected with XPS. The aluminum(hydr)oxide and HFO concentrations measured by extractions are 25 and 800 times lower than the total amount of Al and Fe in raw samples suggesting that only a small fraction of the Al and Fe in steel slag forms sorptive aluminum(hydr)oxide and HFO surfaces. Compared to MSWI bottom ash, the weathered steel slag has almost one order of magnitude less aluminum(hydr)oxide concentration and almost twice as great HFO concentration (Meima and Comans, 1998). Thus, any potential modeling errors introduced from use of HFO specific parameters for the aluminum(hydr)oxide surface would be less significant in weathered steel slag than in MSWI bottom ash.

Sorbate Concentrations

The mass available for surface complexation / surface precipitation was estimated from the availability test results from the raw samples. Potential leachability of metals in aged samples was not measured since lysimeter data suggested that very little release had occurred during aging (Table 5.1). Sorbate concentrations estimated from the availability test were within one order of magnitude of the highest concentrations measured in the pH stat experiments (Table 5.1). The only exception was As: availability test estimates were three orders of magnitude greater than the highest As concentration which was observed at pH 12. In accordance with expected low affinity of heavy metals for sorption at low pHs, the pH at which the heavy metal had highest concentration was 6 for Pb, Cd, and Zn.

Modeling

The phase rule constrains the number of soluble solids that can be input in the model. For some metals, there was more than one solid that had saturation indices close to zero. After trying various combinations of solids in the model it was found that the system as a whole was best modeled in the presence of the following five solubility controlling solids: $CaMg(CO_3)_2$, $BaHAsO_4{:}H_2O$, $Ba(S_{0.77}Cr_{0.23})O_4$, $Pb_3(VO_4)_2$, and SiO_2. Measured concentrations were input for CO_3, Ba, and SO_4 and zero concentrations for As, Ca, Mg, Si, V, Cr, and Pb. For

Cd, Cu, Mo, and Zn, the highest available concentrations were input as measured by availability test in the raw sample. Modeling of Cd, Cu, and Zn in the presence of $CdMoO_4$, $Cu(OH)_2$, and zincite (ZnO) pure solids were considered but not used in the final model as presence of these solids resulted in overestimation of measured concentrations. The T_s values fitted in the model were 0.00005 at pH 6 and 0.0002 at pH values of 8, 10, and 12.

An Overall Description of Leaching from Steel Slag

Leached concentrations of elements such as SO_4, Si, Ca, V, and Mg varied from 10^{-1}M to 10^{-6}M and were governed by the solubility of the minerals listed above and shown in Figure 5.1. Cr and As had relatively lower leached concentrations but were successfully modeled in the presence of solids controlling their solubility. The leachate concentrations of Cu, Pb, Mo, Zn, and Cd were lower than 10^{-4}M and mainly undersaturated with respect to their minerals included in the Visual Minteq database. Leaching of Pb, Zn, and Cd were well described by SPM whereas results of Cu and Mo leachate modeling were inconclusive.

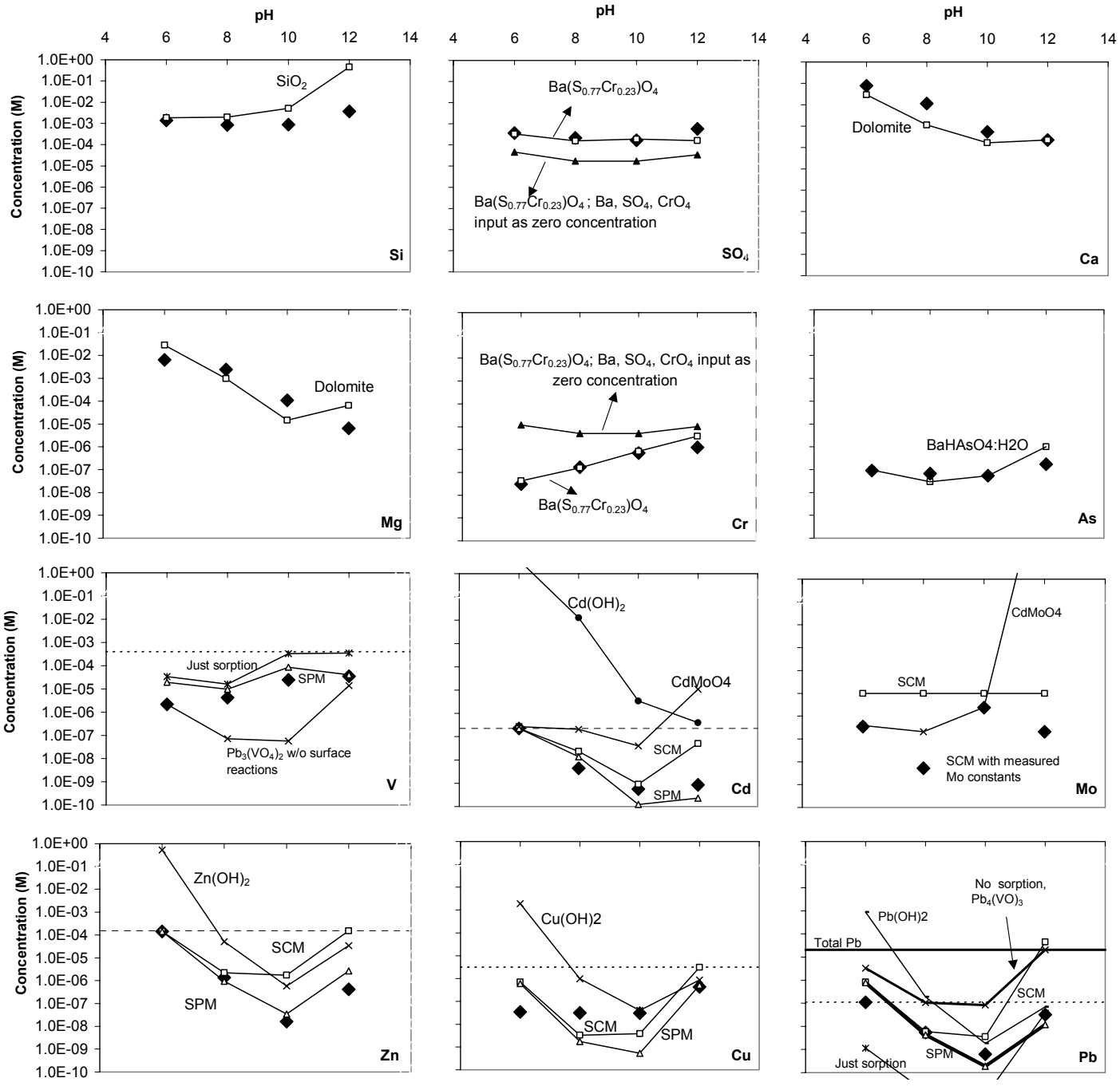

Figure 5.1 Measured leachate concentrations and model predictions (horizontal dashed lines indicate metal availability).

Speciation on Sorptive Surfaces

The high-affinity sites at the sorptive surfaces were mainly covered by Pb, Zn, and Ca, followed by Ba, Cd, Cu, and Si (Figure 5.2). CO_3 showed a high surface coverage at pH 6. On the weak affinity sites, Mg and V were also important (Figure 5.3). While present on the surface, Mo, Cr, As, SO_4, and Hg did not have high sorbed concentrations suggesting that for the weathered steel slag system that was modeled, accurate sorption modeling of these elements may not be significant in describing how the other elements are sorbed. Greater than 99% of the sites were occupied in the SCM and SPM indicating that competition is important. Experience with modeling the system at various available concentrations also pointed to the importance of competition in determining equilibrium concentrations.

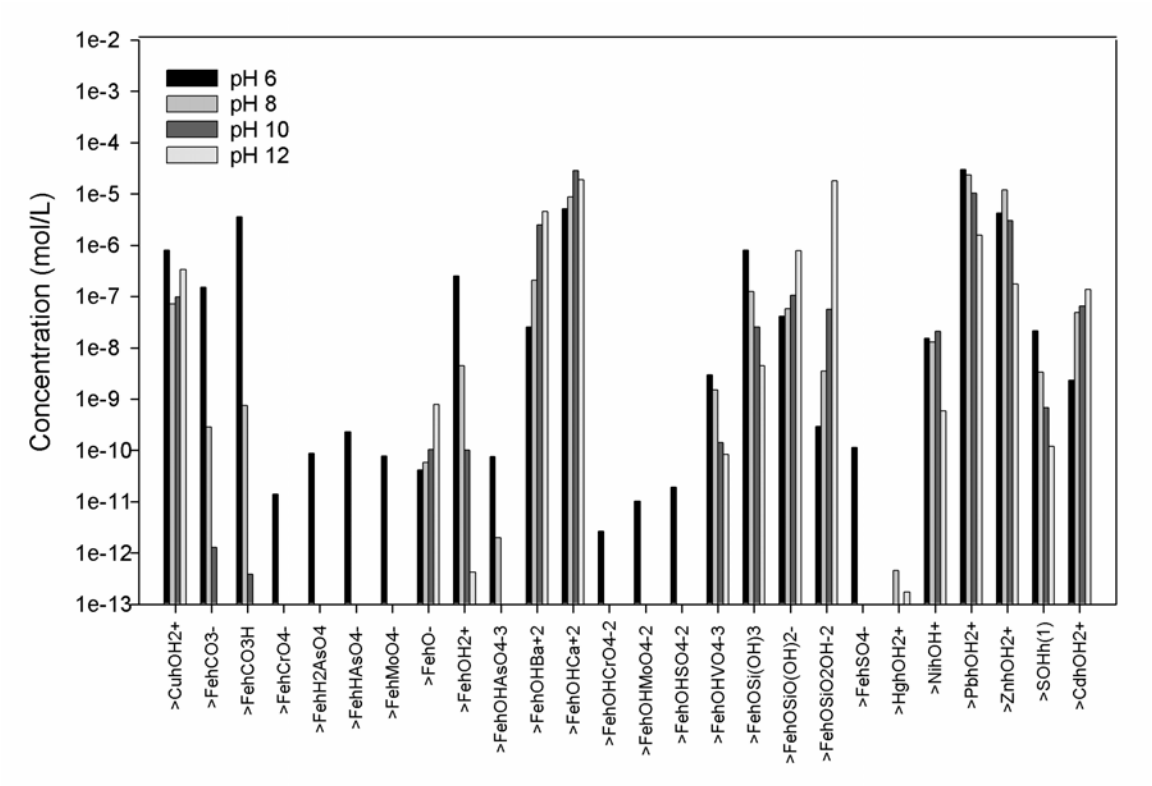

Figure 5.2 Concentration of surface complexes on high affinity surface sites at pH 6, 8, 10, and 12.

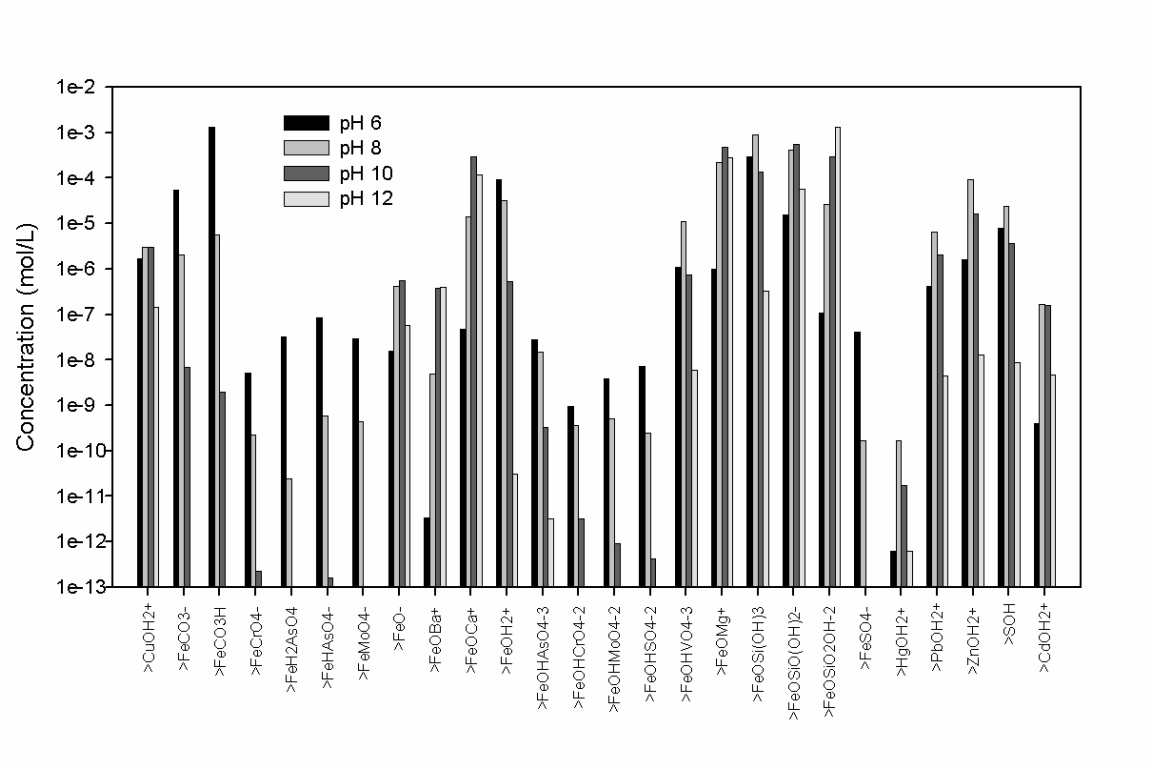

Figure 5.3 Concentration of surface complexes on high affinity surface sites at pH 6, 8, 10, and 12.

Calcium and Magnesium

Dolomite was selected based on its saturation index and its detection in the weathered steel slag sample using XPS. Ca-silicates ($MgCa_2Si_2O_7$, Ca_3SiO_5) detected by other authors in steel slag samples did not result in saturation indices close to zero (Kortbaoui et al.,1993; Monaco and Wu, 1994). Selection of dolomite as the solubility controlling solid for Ca and Mg is also in agreement with the literature. Luxan et al. (2000) identified calcite and dolomite in Spanish electric arc furnace steel slags using IR spectroscopy. Dolomite was also observed with XRD in ladle slag from an electric arc furnace steel production

plant (Shi, 2002). Zevenbergen et al. (1998) also reported dolomite as a secondary mineral resulting from weathering of MSWI bottom ash at high water infiltration rates. In the model, measured concentration of CO_3 was input in the model because it is possibly controlled by carbon dioxide solubility in the unsaturated conditions of the lysimeter steel slag. When measured concentrations of CO_3 are input in the model, dolomite solubility controls Ca and Mg concentrations within one order of magnitude from leachate measured values.

Silica

SiO_2 was detected in the weathered steel slag sample using XPS. Quartz (SiO_2) and amorphous silica have been observed in steel slag (Kortbaoui et al., 1993). Within the Visual Minteq database for Si solid species, amorphous SiO_2 had saturation indices closest to zero for all pHs modeled, yet it does not satisfactorily model leaching of Si at high pHs when sorption is included. The equilibrium predicted concentrations of Si are very high at high pHs. It is possible that the duration of leaching experiments were too short to allow such high concentrations of Si to dissolve and come to equilibrium in that period. The rapid release of Si to solution through the dissolution of glasses, quartz, and other silicates might have been slower than the precipitation of amorphous SiO_2 as has also been hypothesized for MSWI ash leaching (Kirby and Rimstidt, 1994).

Chromium, Barium, and Sulphate

Adsorption was not expected to control Cr concentrations because Cr(VI) adsorption to iron oxides is relatively weak and decreases in the presence of CO_3 and SO_4 (Zachara et al., 1987; Vangeen et al., 1994). Earlier evidence suggests that Cr solubility may be controlled by $Ba(S_{0.77}Cr_{0.23})O_4$ in steel slags (Fällman, 2000). Ba and SO_4 and Ba, SO_4, and Cr were found to be associated in naturally weathered archae-metallurgical slags (Carlier et al., 2000) and coal fly ash samples (Fruchter et al., 1990)

In the model, $Ba(S_{0.77}Cr_{0.23})O_4$ consistently resulted in low saturation indices across the pH range (SI=-0.11, -0.21, -0.41, -1.70 for pHs 6,8, 10, and 12, respectively). When initial concentrations of Ba, Cr, and SO_4 were input as zero in the presence of the $Ba(S_{0.77}Cr_{0.23})O_4$ solid, Cr was up to two orders of magnitude overestimated while SO_4 was underestimated and Ba was overestimated both within one order of magnitude. However, when measured Ba and SO_4 concentrations were input in the model, aqueous concentrations of Cr in the presence of both sorption and precipitation/dissolution equilibrium closely approximate the measured Cr concentration.

Cadmium

SCM overestimated and SPM underestimated the measured concentrations. While SPM provides a better estimate of the measured Cd

concentration than SCM the criteria set by Dzombak and Morel (1990) with regard to the likeliness of surface precipitation is not met. Dzombak and Morel (1990) suggested that as a rule of thumb SPM is likely to become significant when (i) the dissolved sorbate concentration exceeds one-tenth of its solubility or (ii) the dissolved sorbate concentration exceeds one-half of the total surface site concentration. The dominant complexes of Cd in the model were surface complexation and surface precipitation species as well as aqueous complexes with NO_3 and Cl at pH 6. High $CdNO_3$ concentrations are possibly due to the substantial amounts of HNO_3 added to the solution to lower the pH.

Zinc, Lead, and Vanadium

Pb was modeled with a finite concentration of $Pb(VO_4)_3$ because Pb release was under estimated in absence of the solid and both Pb and V were modeled well in the presence of the solid. If an infinite solid, as opposed to a finite solid equal to the total Pb ($2.07\ 10^{-5}$ M) was used, equilibrium concentration of Pb sorbed and co-precipitated on the surface was higher than the total Pb in unweathered samples. V concentrations are overestimated if only sorption is considered and underestimated if only solubility control without sorption is considered. Modeling of V in the presence of finite $Pb_3(VO_4)_2$ and SPM provides a close match. The modeling results suggest that leaching of Pb is controlled both by $Pb_3(VO_4)_2$ solubility at pHs 6 and 8 and by sorption / surface precipitation at higher pHs where the Pb in the solid phase is exhausted (i.e. the solid is

undersaturated) and the released Pb is in equilibrium with aqueous and surface complexes only. The importance of surface reactions in the release of Pb was anticipated as Pb is well known to have a high affinity for iron oxides (Violante et al., 2003). Carlier et al. (2000) also observed Pb in hydrous iron oxides in the archeo-metallurgical slags. The need for SPM for both Pb and Zn was also expected since the dissolved Zn and Pb concentrations were close to one-tenth of their solubility values (Dzombak and Morel, 1990).

Surface complexation provided good estimates of Zn and Pb except at high pHs where consideration of surface precipitation reactions were needed. While Zn and Pb formed aqueous complexes with the carbonate, nitrate, hydroxide, sulfate, and chloride, the speciation of Zn and Pb was predominantly in sorptive surfaces and solid solution as $Zn(OH)_2$ and $Pb(OH)_2$. Consideration of surface reactions for Pb and Zn is essential because the modeling results show that: (1) both Pb and Zn mainly speciate onto the surfaces, and (2) the surfaces are mainly occupied by Pb and Zn (Figures 5.2 and 5.3) where they compete for available sites on the surface.

Our modeling observation of surface precipitation at high pHs is consistent with literature data. Shuman (1977) proposed that Zn may form $Zn(OH)_2(s)$ upon sorption to hydrous Al oxide at pH values above 8. In a Zn-amorphous-silica system, Roberts at al. (2003) showed using X-ray absorption spectroscopy, the formation of an amorphous $Zn(OH)_2$ precipitate with tetrahedral coordination between Zn and O only at the highest pH that they studied which was 7.5.

Arsenic

Van der Hoek and Comans (1996) have shown that As leaching in coal fly ash was controlled by sorption onto HFO. However, they observed more than two orders of magnitude difference between the amounts leached between pHs 6 and 12 whereas in this work the amounts leached were almost the same across this pH range without any apparent increase in concentration with higher pH. These observations suggest that sorption may not be the major mechanism controlling the release of As. As modeled in presence of $BaHAsO_4$:H_2O as an infinite solid closely matched the measured concentrations when measured leachate concentration of Ba and zero concentration of As was input in the model. Evidence from modeling for presence of $BaHAsO_4$:H_2O as a secondary mineral in the weathered steel slag is in agreement with its occurrence in groundwater and drinking water systems (Orellana et al., 2000; Planer-Friedrich et al., 2001; Davis, 2000)

Copper

Based on saturation indices, $Cu(OH)_2$ was determined as the only solid species that could have controlled the release of Cu. Cu was significantly undersaturated with respect to $Cu(OH)_2$ at low pHs suggesting that interactions of Cu with sorptive surfaces and other aqueous complexes were the major processes controlling the release of Cu. SCM provided a reasonable fit with less

than one order of magnitude difference for each pH modeled and SPM underestimated the measured concentration at medium pHs. I would expect Cu concentrations to be higher if I had considered Cu complexation with dissolved organic carbon. However, the measured dissolved organic carbon was low at pHs 8 and 10 (2 and 3 mg/L) (where an increase in modeled Cu concentration would have fit the measured data better) and high at the end pHs (10 and 11 mg/L), suggesting that the release of Cu is possibly more complicated than what I included in the model. The major species of Cu in the model were sorbed (all modeled pHs) and co-precipitated Cu (at pH=12 and 10) followed by Cu complexation with CO_3 (at pH=6), NO_3 (at pH=6) (experimental artifact), and hydroxide (at pH=12).

Molybdenum

Modeling results for Mo are inconclusive. $CdMoO_4$ does not predict the release of Mo or Cd well. For the SCM, two different sets of parameters were tried. First, Dzombak and Morel's (1991) sorption constants estimated by linear free energy relationships were used which resulted in no adsorption within the pH range studied, in agreement with van der Sloot et al's (2001) observations on municipal solid waste residues. Second, Gustafsson's (2003) measured sorption constants were tried. Neither sets of sorption constants resulted in accurate predictions of Mo concentration. The prevalent speciation of Mo was in aqueous complexes of $CaMoO_4$ and $MgMoO_4$.

Limitations of the Modeling Approach

Some ion species that might have affected the modeling results were neither measured nor included in the model. For example, steel slag typically contains high concentrations of phosphorus (Kortbaoui et al., 1993; Murphy et al., 1997; Proctor et al., 1997), which might have competed for sorption sites (Li and Stanforth, 2000; Gustafsson, 2001). While fluoride was also not measured in this study, fluoride concentrations an order of magnitude greater than those of Cl have been observed to be leached from other steel slag samples (Rastovcan-Miac et al. 2000).

I only considered iron and aluminum sorptive surfaces and assumed aluminum sorptive surfaces had similar affinities to ions as iron surfaces. While Fe, Al, and Si are the major elements in steel slag, carbonates and hydrous manganese oxides may influence observed leaching behavior. Carbonates are likely to form during weathering reactions (Fällman et al., 1999). Manganese hydrous oxides may not be as abundant in steel slag but they have high affinity for ions and the surface complexation constants for cations have recently been reported (Tonkin et al., 2004). The component additivity approach (Davis et al., 1998) where all sorptive surfaces are treated separately with their appropriate sorption constants and measured surface site concentrations may provide useful insight into leaching in further studies.

Other uncertainties related to my model are that the availability of metals measured by the availability test or by pH 6 are operationally defined. For example, Gustafsson (2001) used oxalate extractable arsenate and phosphate as the total adsorbed + dissolved concentration of these ions. I also considered analyzing trace concentrations obtained from oxalate and ascorbate extractions and comparing them to modeled data but decided that was impractical considering that the total sorbed and dissolved concentrations change considerably as a function of pH.

I have shown that ions released from steel slag at trace and high concentrations can be modeled by simultaneous consideration of dissolution / precipitation and surface complexation / surface precipitation reactions and estimation of a single parameter, T_s. These types of reactions are relevant for other wastes as well. The modeling approach described in this paper is applicable to other complex secondary materials such as contaminated sediments, coal combustion byproducts, and MSWI ash.

ACKNOWLEDGEMENTS

I would like to thank Jon Petter Gustafsson for his helpful comments on the use of Visual Minteq software. This work was funded through a cooperative agreement (DTFH61-98-X-00095) between FHWA and the University of New Hampshire. The experimental part was financially supported by Swedish Waste Research Council under grants AFN Dnr 261/97 and the Swedish Geotechnical Institute, which is greatly acknowledged.

REFERENCES

1. Blakemore, L.C. Searle, P.L., and Daly, B.K. (1987) Methods for chemical analysis of soil. NZ Soil bureau scientific report 80, New Zealand

2. Bodurtha, P. and Brassard, P., (2000) Neutralization of acid by steel-making slags. Environmental Technology, 21: 1271-1281.

3. Carlier, C.M.-L., Veslud, C.L.C.d., Ploquin, A. and Royer, J.-J., (2000) L'alteration naturelle des scories de la metallurgie ancienne: un analgue de dechets vitrifies. Earth and Planetary Sciences, 330: 179-184.

4. Coughlin, B., and Stone, A. (1995) Nonreversible adsorption of divalent metal ions (Mn++, Co++, Ni++, Cu++, and Pb++) onto Geothite: Effects of acidification, Fe++ addition, and picolinic acid addition. Environmental Science and Technology, 29(9), 2445-2455

5. Criscenti, L.J. and Sverjensky, D.A., (2002) A single-site model for divalent transition and heavy metal adsorption over a range of metal concentrations. Journal of Colloid and Interface Science, 253: 329-352.

6. Csoban, K. and Joo, P. (1999) Sorption of Cr(III) on silica and aluminum oxide: experiments and modeling. Colloids and Surfaces A: Physicochemical and engineering aspects, 151: 97-112.

7. Daughney, C.J. and Fein, J.B., (1998) The effect of ionic strength on the adsorption of H+, Cd2+, Pb2+, and Cu2+ by bacillus subtilis and bacillus licheniformis: a surface complexation m odel. Journal of Colloid and Interface Science, 198: 53-77.

8. Davis, J.A., Coston, J.A., Kent, D.B. and Fuller, C.C., (1998) Application of the surface complexation concept to complex mineral assemblages. Environmental Science and Technology, 32(19): 2820-2828.

9. Davis, J. (2000) Stability of metal-arsenic solids in drinking water systems. Practice periodical of hazardous, toxic, and redioactive waste management, 4(1): 31-35.

10. Dijkstra, J.J., Sloot, H.A.van der and Comans, R.N.J., (2002) Process identification and model development of contaminant transport in MSWI bottom ash. Waste Management, 22: 531-541.

11. Dorn, R.I. and Meek, N. (1995) Rapid formation of rock varnich and other rock coatings on slag deposits near Fontana, California. Earth surface processes and landforms, 20: 547-560.

12. Dzombak and Morel (1990) Surface complexation modeling: Hydrous ferric oxide, John Wiley and Sons

13. Eighmy, T.T., Eusden, D.J., Krzanowski, J., Domingo, D.S., Stampell, D., Martin, J.R. and Erickson, P.M. (1995) Comprehensive approach toward understanding element speciation and leaching behavior in municipal solid waste incineration electrostatic precipitator ash. Environmental Science and Technology, 29: 629-646.

14. Fällman, A-M. and Hartlén, J. (1994) Leaching of slags and ashes – controlling factors in field experiments versus in laboratory tests. In Environmental Aspects of Construction with Waste Materials (Goumans, J.J.J.M., van der Sloot, H.A., Aalbers Th.G. Eds.) Studies in Environmental Science 60, pp 39-54. Elsevier, Amsterdam.

15. Fällman, A.-M. (1997). Characterization of residues: Release of contaminant from slags and ashes. Department of physics and measurement technology. Linkoping, Linkoping University.

16. Fällman, A.-M. (2000). “Leaching of chromium and barium from steel slag in laboratory and field tests - a solubility controlled process?” Waste Management 20: 149-154.

17. Fällman, A.-M., Eighmy, T.T., and Salaneck, W.R. (1999). Aging reactions in residues. Stochkholm, Swedish Environmental Protection Agency.

18. Fruchter, J.S., Rai, D. and Zachara, J.M., (1990) Identification of solubility-controlling solid phases in a large fly ash field lysimeter. Environmental Science and Technology, 24(8): 1173-1179.

19. Gustaffson, J.P. (2001) Modelling competitive anion adsorption on oxide minerals and an allophane-containing soil. European Journal of Soil Science, 52: 639-653.

20. Gustafsson, J.P. (2003) Modelling molybdate and tungstate adsorption to ferrihydrite. Chemical Geology. 200(1-2): 105-115

21. Jenne, E.A., (1968) in "Trace Inorganics in Water" (R.F. Gould, Ed.), pp. 337-387, Am. Chem. Soc., Washington, DC

22. Kalyoncu, R.S. (2001) Slag - iron and steel, Annual Review, Mineral Industry Surveys, U.S. Geological Survey: Reston, VA

23. Karthikeyan, K.G. and Elliott, H.A., (1999) Surface complexation modeling of Copper sorption by hydrous oxides of iron and aluminum. Journal of Colloid and Interface Science, 220: 88-95.

24. Kirby, C.S. and Rimstidt, D.D. (1994) Interaction of municipal solid waste ash with water. Environmental Science and Technology, 28(3): 443-451.

25. Kortbaoui, A., Tagnit-Hamou, A. and Aitcin, P.C. (1993) The use of stainless steel slag in concrete. Ceramic Transactions, 37: 77-90.

26. Kostka, J.E. and Luther III, G.W. 1994 Partitioning and speciation of solid phase iron in saltmarsh sediments. Geochimica Cosmochimica Acta 58:1701-1710

27. Li, L. and Stanforth, R. (2000) Distinguishing adsorption and surface precipitation of phosphate on goethite (alpha - FeOOH). Journal of Colloid and Interface Science, 230: 12-21.

28. Luxan, M.P., Sotolongo, R., Dorrego, F. and Herrero, E. (2000) Characteristics of the slags produced in the fusion of scrap steel by electric arc furnace. Cement and Concrete Research, 30: 517-519.

29. Meima, J. A. and R. N. J. Comans (1998). “Application of surface complexation/precipitation modeling to contmainant leaching from weathered municipal solid waste incinerator bottom ash.” Environmental Science and Technology 32: 688-693.

30. Monaco, A. and Wu, W.-K. (1994) The effect of cooling conditions on the mineralogical characterization of steel slag. In: P. Mahant, C. Pickles and W.-K. Lu (Editors), Proceedings of the international symposium on resource ceonservation and environmental technologies in metallurgical industries, Toronto, Ontario.

31. Murphy, J.N., meadowcroft, T.R. and Barr, P.V. (1997). Enhancement of the cementitious properties of steelmaking slag. Canadian Metallurgical Quarterly, 36(5): 315-331.

32. Orellana, F., Ahumada, E., Suarez, C., Cote, G. and Lizama, H. (2000). Thermodynamic studies of parameters involved in the formation of arsenic(V) precipitates with barium(II). Boletin de la sociedad chilena de quimica, 46(3): 415-422.

33. Planer-Friedrich, B., Armienta, M.A. and Merkel, B.J.(2001). Origin of arsenic in the groundwater of the Roverde basin, Mexico. Environmental Geology, 40: 1290-1298.

34. Proctor, D.M., Fehling, K.A., Shay, E.C., Wittenborn, J.L., Green, J.J., Avent, C., Bigham, R.D., Connolly, M., Lee, B., Shepker, T.O. and Zak, M.A. (2000). Physical and chemical characteristics of blast furnace, basic oxygen furnace, and electric arc furnace steel industry slags. Environmental Science and Technology, 34: 1576-1582.

35. Rastovcan-Mioc, A., Cerjan-Stefanovic, S. and Curkovic, L. (2000) Aqueous leachate from eletric furnace slag. Croatica chemica acta, 73(2): 615-624.

36. Rai, D., Zachara, J.M., Schwab, A.P., Schmidt, R.L., Girvin, D.C., and Rogers, J.E. (1986). Chemical attanuation rates, coefficients and constants in leachate migration. Volume 1: A critical review. EPRI EA-3356, Electrical Power Research Institute. Palo Alto

37. Roberts, D.R., Ford, R.G. and Sparks, D.L. (2003) Kinetics and mechanisms of Zn complexation on metal oxides using EXAFS spectroscopy. Journal of Colloid and Interface Science, 263: 364-376.

38. Shi, C., (2002) Characteristics and cementitious properties of ladle slag fines from steel production. Cement and Concrete Research, 32: 459-462.

39. Shuman, L.M. (1977) Adsorption of Zn by Fe and Al hydrous oxides as influenced by aging and pH. Soil Science Society of America, 41(4): 703-706

40. Sun, S.X., Forsling, W. and Ronbren, L. (1991) Surface reaction in aqueous metal sulfide systems, 1. Fundamental surface reactions of hydrous PbS and ZnS. Int. J. Miner. Proc., 33: 83-89.

41. Tonkin, J.W., Balistrieri, L.S. and Murray, J.W. (2004) Modeling sorption of divalent metal cations on hydrous manganese oxides using the diffuse double layer model. Applied Geochemistry, 19: 29-53.

42. van der Sloot, H.A., Kosson, D.S. and Hjelmar, O. (2001) Characteristics, treatment and utilization of residues from municipal waste incineration. Waste Management, 21: 753-765

43. Vangeen, A., Robertson, A.P. and Leckie, J.O. (1994) Complexation of carbonate species at the goethite surface - implications for adsorption of metal ions in natural waters. Geochimica et Cosmochimica Acta, 58: 2073-2086

44. Violante A, Ricciardella M, Pigna M. (2003) Adsorption of heavy metals on mixed Fe-Al oxides in the absence or presence of organic ligands. Water Air and Soil Pollution, 145(1), 289-306

45. Zachara, J.M., Cowan, C.E. and Resch, C.T. (1991) Sorption of divalent metals on calcite. Geochimica et Cosmochimica Acta, 55: 1549-1562.

46. Zachara, J.M., Girvin, D.C., Schimdt, R.L. and Resch, C.T. (1987). Chromate adsorption on amorphous iron oxyhydroxide in the presence of major groundwater ions Environmental Science and Technology, 21(6), pp. 589-594.

47. Zevenbergen, C., Reeuwijk, L.P.v., Bradley, J.P., Comans, R.N.J. and Schuiling, R.D. (1998) Weathering of MSWI bottom ash with emphasis on the glassy constituents. Journal of Geochemical Exploration, 62: 293-298.

48. Zhu, C., (2002). Estimation of surface precipitation constants for sorption of divalent metals onto hydrous ferric oxide and calcite. Chemical Geology, 188: 23-32

CHAPTER 6

MODELING HYDROLOGY AND REACTIVE TRANSPORT IN ROADS: THE EFFECT OF CRACKS, THE EDGE, AND CONTAMINANT PROPERTIES

ABSTRACT

The goal of this research was to provide a tool for regulators to evaluate the groundwater contamination from the use of virgin and secondary materials in road construction. A finite element model, HYDRUS2D was used to evaluate generic scenarios for secondary material use in base layers. Use of generic model results for particular applications was demonstrated through a steel slag example. The hydrology and reactive transport of contaminants were modeled in a two-dimensional cross section of a road. Model simulations showed that in an intact pavement, lateral velocities from the edge towards the centerline may release and advect the contaminants in the base layer. The dominant transport mechanisms are advection closer to the edge and diffusion closer to the centerline. A shoulder joint in the pavement allows 0.03 to 0.45 m^3/day of infiltration per meter of joint length as a function of the base and subgrade hydrology and the rain intensity. Scenario simulations showed that salts in the base layer of pavements are depleted within the first year whereas the metals may never reach the groundwater if the pavement is built on adsorbing soils.

INTRODUCTION

Traditional materials and secondary materials used in road construction can both contain metals, which if released may contaminate soil and groundwater. Potential contamination from road construction materials is especially a concern for regulators when evaluating the use of alternative base materials which can include steel slags, blast furnace slags, non ferrous slags, glass and ceramics, construction and demolition debris, municipal solid waste incinerator ashes, reclaimed asphalt and concrete pavements, contaminated sediments and coal ashes. The complexity of the accurate prediction of long-term contaminant leaching and transport in a road environment arises from the interaction of multiple factors such as the condition of the pavement, the climate, contaminant properties, and pavement material matrix. Contaminant properties and material matrices have been studied in detail by laboratory leaching tests and by modeling the release of contaminants under equilibrium conditions (Kosson et al., 1996; Fallman, 2000; Dijkstra et al., 2002). What may occur in the field on larger spatial and temporal scales, and as a function of the climate and road condition, is relatively less well known.

Contaminant release and transport is directly affected by the presence and flow of water in pavements. While pavements are often considered impervious structures, roads constructed with Portland cement concrete or

asphalt concrete surface courses can experience water entry to the base layer from the sides (de Haan et al. 2003) and through cracks (Ridgeway 1978, Ahmed 1990). The extent and rate of infiltration into the pavement structure also depends on rain intensity. If the infiltration capacity of the cracks is exceeded, then some of the rain becomes runoff and does not influence the mobility of the contaminants in pavements. The current literature on pavement hydrology is missing a discussion on the spatial differences in water flow regimes in the pavement influenced by rain intensity, the edge effect, and presence of cracks.

The overall goal of this research was to provide a tool to help evaluate the environmental impacts of virgin and secondary road construction materials on groundwater contamination. As opposed to a site specific investigation, I aimed to provide information applicable to numerous secondary materials and investigated the extreme cases to determine the acceptable and unacceptable bounds for impacts on groundwater from use of secondary materials in base layers. More specifically, the objectives of the research were to develop a quantitative description of long term contaminant release and transport from pavement base layers. Towards this goal, the hydrology and reactive transport of contaminants were modeled in a two-dimensional cross section of a road and the effects of the edge, the cracks/joints, and contaminant reactivity were studied.

APPROACH

Model Description

One half of a hypothetical two-lane highway section was modeled with the assumption that the other half would yield similar results due to symmetry. The cross section of the modeled half-highway extended to 6.6 meters (Figure 6.1). The surface layer was assumed to be a 3.6 m wide Portland cement or asphalt concrete along the lane with a 1 m wide asphalt concrete shoulder, both of which were 20 cm thick. The slope of the lane was two percent and that of the shoulder was four percent. A 13 cm thick, 4.6 m wide base material underlay the lane and the paved shoulder. The embankment extended for two meters from the edge of the shoulder at ten percent slope. Both the embankment and the subgrade were assumed to be sandy soil.

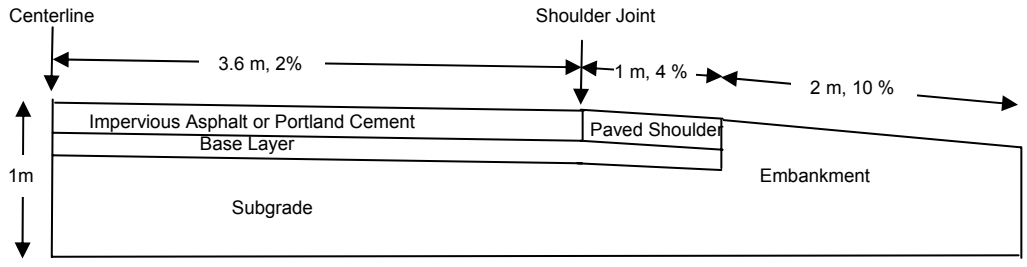

Figure 6.1 Geometry of the model

Three different conditions of the road surface were investigated: a fully intact pavement, a pavement with a 1.4 cm wide centerline joint and shoulder

joint, and a totally damaged pavement. In the totally damaged pavement scenario, the initially impervious surface layer was assumed to have become permeable and was assigned the same hydraulic properties as the base. In the fully intact pavement and the intact pavement with two joints, the surface layer of the pavement including the shoulder was assumed to be impervious (Apul et al., 2003) and thus not included in model calculations. The groundwater table was set at 1m deep from the surface at the centerline. The shallow groundwater is representative of a worst case scenario since in many instances and locations, the groundwater table is much lower.

A finite element model, HYDRUS2D was used for all simulations (Simunek et al., 1999). The meshes generated for different scenarios all had more than 6800 elements. The advection-dispersion equation with retardation was solved for contaminant transport calculations. Lateral dispersivity was input in the model as one tenth that of the thickness of the base (0.01 m) and subgrade materials (0.07 m) and the transverse dispersivity was assumed to be one tenth of the lateral dispersivity (0.001m and 0.007m) (Fetter, 1999). No flow and constant head (zero pressure head) boundary conditions were assigned on the sides and at the bottom of the model, respectively. The contaminant was placed in the base layer only. The absolute value of the initial concentration assigned is not important since the concentration term appears throughout the advection dispersion equation. In all simulations, a unit aqueous concentration assigned in

the base layer was equilibrated with the sorbed concentration and the simulation results were later normalized to initial total contaminant mass.

Aqueous diffusion was modeled using the molecular diffusion coefficient and the tortuosity factor. The tortuosity factor was calculated within HYDRUS2D's routine as a function of water content using Miller and Quirk's (1961) equation. Molecular diffusion coefficients of cations and anions are in the order of 10^{-4} and 10^{-5} m^2/day depending on the charge and radius of the ions and conditions of the solution including electro neutrality, ionic strength, temperature, and pressure (Sato et al., 1996; Li and Gregory, 1997). The molecular diffusion coefficient of cadmium (6.25 10^{-5} m^2/day) was input in the model as an average parameter.

Precipitation from Maplewood, MN was input in the model in 15 minute intervals for from the 1998 entire year of observations and this input was afterwards repeated for 20 years. The annual precipitation input in the model at 72 cm/year is a median precipitation rate considering that most of the areas in the U.S. have an average annual precipitation between 20 cm and 152 cm, with some extreme locations less than 10 cm and more than 400 cm. For all scenarios, precipitation was input as a time-varying flux boundary condition along the embankment. In modeling the fully damaged pavement, precipitation was also input along the width of the lane and the shoulder. In modeling a pavement with two joints, precipitation was also allowed to infiltrate through the joints but the flux of the precipitation input into the shoulder joint was adjusted to take into

account the lateral runoff from the centerline towards the edge of the pavement. This adjustment of the flux was necessary because lateral runoff could not be explicitly modeled using HYDRUS2D. The width (3.6 m) of the lane upslope of the shoulder joint was divided by the width of the crack (1.4 cm) to scale up (257 times) the intensity of the flux that was forced into the shoulder joint. If the joint's infiltration capacity was exceeded, the excess water was removed from the model domain. To avoid crashing HYDRUS2D due to high fluxes input into the shoulder joint, the mesh was discretized in and around the joints at 0.3 cm whereas the rest of the mesh resolution varied between 4-7 cm.

Hydraulic Parameters

Richards' equation was used for modeling the unsaturated water flow. To describe the relation between water content and pressure and between hydraulic conductivity and pressure, Van Genuchten's (1980) closed form equation was used. The hydraulic parameters of agricultural soils for the van Genuchten (1980) model have been studied in detail (Schaap et al., 2001). HYDRUS2D has its own database for parameters taken from Carsel and Parrish (1988). Database values were used for sand to describe the hydraulic properties of the subgrade and embankment (Figure 6.2).

There is very little information available for hydraulic properties of traditional and secondary pavement materials. Bigl and Berg (1996) have measured the soil moisture characteristic curve and the hydraulic conductivity

curve for aggregate base materials used in Minnesota. In this research, the "Class 5" Minnesota aggregate base material was used as a generic base layer. The hydraulic conductivity curve for "Class 5" material was fit to the van Genuchten's model using RETC (van Genuchten et al., 1991). The fitting parameters were α and n while the measured values were used for residual volumetric water content, volumetric saturated water content, and saturated hydraulic conductivity (Figure 6.2). The saturated hydraulic conductivity of "Class 5" material is on the lower end of the range of hydraulic conductivities reported for other pavement base materials (Apul, et al., 2004).

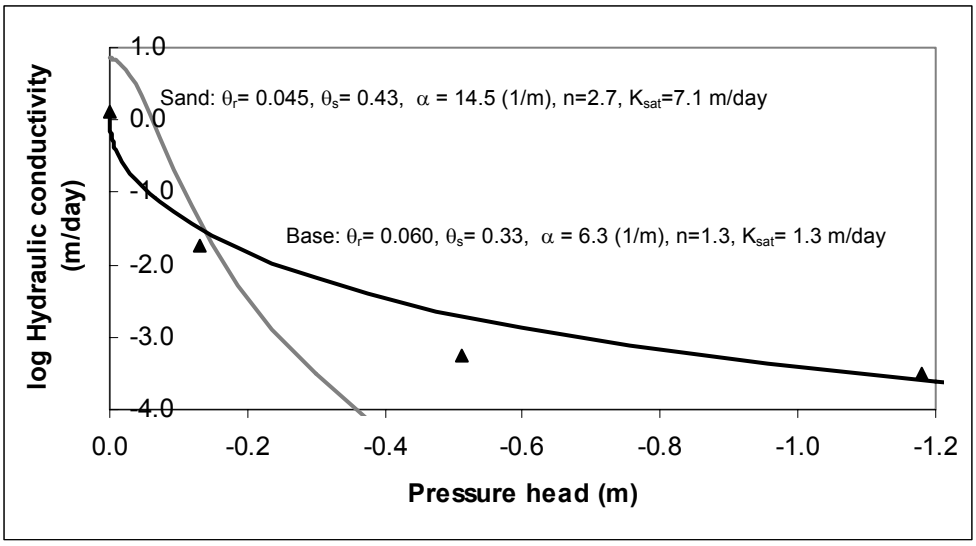

Figure 6.2 Hydraulic properties of the pavement base and sand embankment / subgrade. Bigl and Berg's (1996) measured data points for Class 5 base material are shown in triangles.

Contaminant Transport

Total metal content of a material may be higher than the total available metal concentration as some of the contaminant may be locked up inside the

particle matrix and never be available for release (Fallman, 1997). Ideally, the unavailable fraction should be excluded from model calculations. However, the available fraction of contaminants varies significantly (0.2 to 72.6 %; Fallman, 1997) in steel slags and possibly in other secondary materials. In the absence of a direct method for estimating availability for different contaminants, total contents were used in this research as a conservative and generic approach.

Once in contact with water, the available fraction of the contaminant may form aqueous complexes, surface complexes, surface precipitates, and pure precipitates. The detailed information necessary for modeling these reactions for secondary materials and soils is not readily available though some promising advances have been made (Meima and Comans, 1998; Davis et al., 1998; Apul et al., submitted, Fruchter et al., 1990). Unknowns and uncertainties of such a complex approach are often also problem specific making it difficult to extrapolate results to other scenarios. For these reasons, for the contaminant release and transport part of the model, a more general approach based on widely reported data was selected.

The linear distribution coefficient, K_d was used for describing the partitioning of an ion between the solid and aqueous phases. Using a lumped-K_d approach, mobility of salts and metals were grouped for attenuating and non-attenuating conditions. While K_d values can vary by orders of magnitude as a function of pH, liquid to solid ratio, and soil type, they have been extensively reported and provide a convenient way for regulators to interpret leaching

scenarios. In addition, considering the extent of uncertainty in accurate predictions of release and transport from pavement materials in field conditions, errors on the order of one or two magnitudes may be acceptable.

K_d values used in the model were based on reported literature values. Measured and estimated K_d values for metals partitioning in soils have been compiled from hundreds of sources (USEPA 1999; RTI 2000; USEPA 2003). While the data shows several orders of magnitude of scatter from 0.1 L/kg to 100000 L/kg for a variety of metals and conditions, a significant correlation was obtained between pH and K_d values for cadmium across a range of 1 to 12600 L/kg and 3 to 10 pH. In this research, a K_d value of 1 L/kg was assumed to be broadly representative of the retardation of a metal in highly acidic, non-attenuating or non-adsorbing soils (Table 6.1). Similarly, such a low K_d value was also assumed to be representative of salts such as Cl^-, K^+, NO_3, and SO_4, which have high mobility both in secondary materials and soils. A K_d value of 1000 L/kg was used to represent the reactivity of metals in the base layer; and K_d values of 50 L/kg and 2500 L/kg were used to represent the reactivity of metals in moderately attenuating and highly attenuating soils, respectively.

Table 6.1 Categories of contaminant reactivity

K_d in base (L/kg)	K_d in soil (L/kg)	Representative of	Additional assumptions	Scenario numbering for different pavement conditions	
				Damaged pavement	Intact Pavement
1	1	Salts	Readily released and transported	1	13
1	50	Salts	Moderate attenuation in the soil	2	14
1000	1	Metals	Very low attenuation in the soil	4	16
1000	50	Metals	Moderate attenuation in the soil	5	17
1000	2500	Metals	High attenuation in the soil	6	18

RESULTS AND DISCUSSION

Effect of Pavement Edge

A snapshot of the velocity profiles during a rain event shows that in the embankment the velocities are predominantly vertical as expected (Figure 6.3). However, close to the edge and in the base layer, lateral velocities were observed. Vertical velocities as high as 0.2 m/day developed in the embankment close to the surface. Pressures increased from the centerline towards the embankment (Figure 6.3) and near the edge, the pressures were consistently lower than -0.15 m throughout the simulation period. At these pressures, the hydraulic conductivity of the base material is greater than that of the sand (Figure 6.2). Higher pressures in the embankment direct the water laterally into the base layer towards the centerline. Close to the edge, lateral velocities towards the centerline can be as high as 0.04 m/day due to sharp pressure gradients and high hydraulic conductivities. Laboratory and modeling studies of De Haan (2001) also showed that water may enter below the surface layer of a pavement through later flow from the edges.

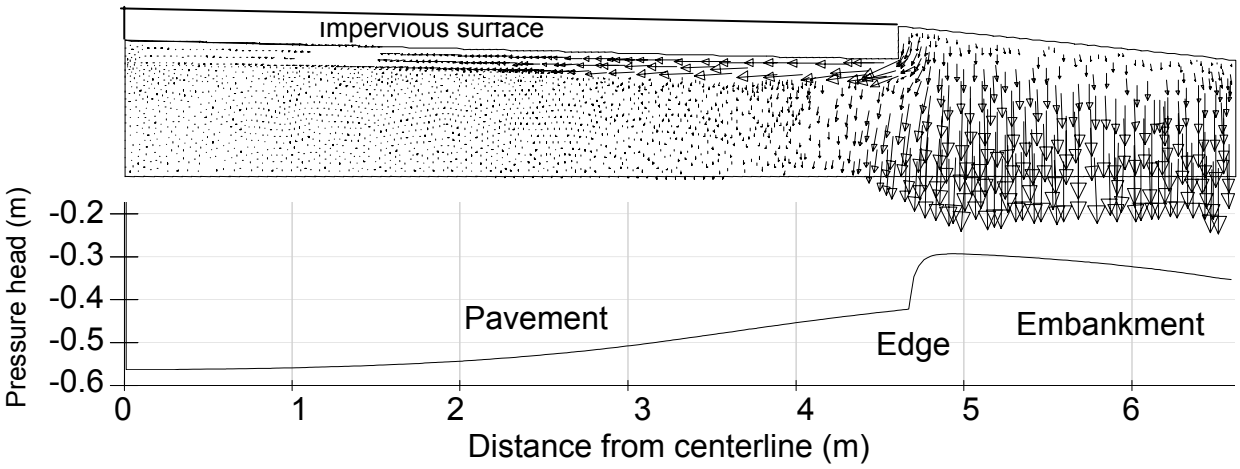

Figure 6.3 Velocity vectors and the pressure distribution during a rain event. A horizontal cross section 0.33 m below from the centerline was taken to show the pressure distribution in the base layer and in the embankment.

The effect of the edge on mobility of salts (Scenario 1) is shown in Figure 6.4. Influx of water into the base layer from the edge mobilizes and flushes the salts close to the edge. After one year, the aqueous concentrations under the shoulder have decreased to 10 percent of the initial value close the edge and to 70 percent of the initial value close to the lane. After 10 years the salts under the shoulder close to the edge are completely depleted and the concentrations at the intersection of the shoulder and the lane are 20 percent of the initial values. After 20 years, the edge effect reaches half of the pavement length and more than 99 percent of the salts under the shoulder have been depleted

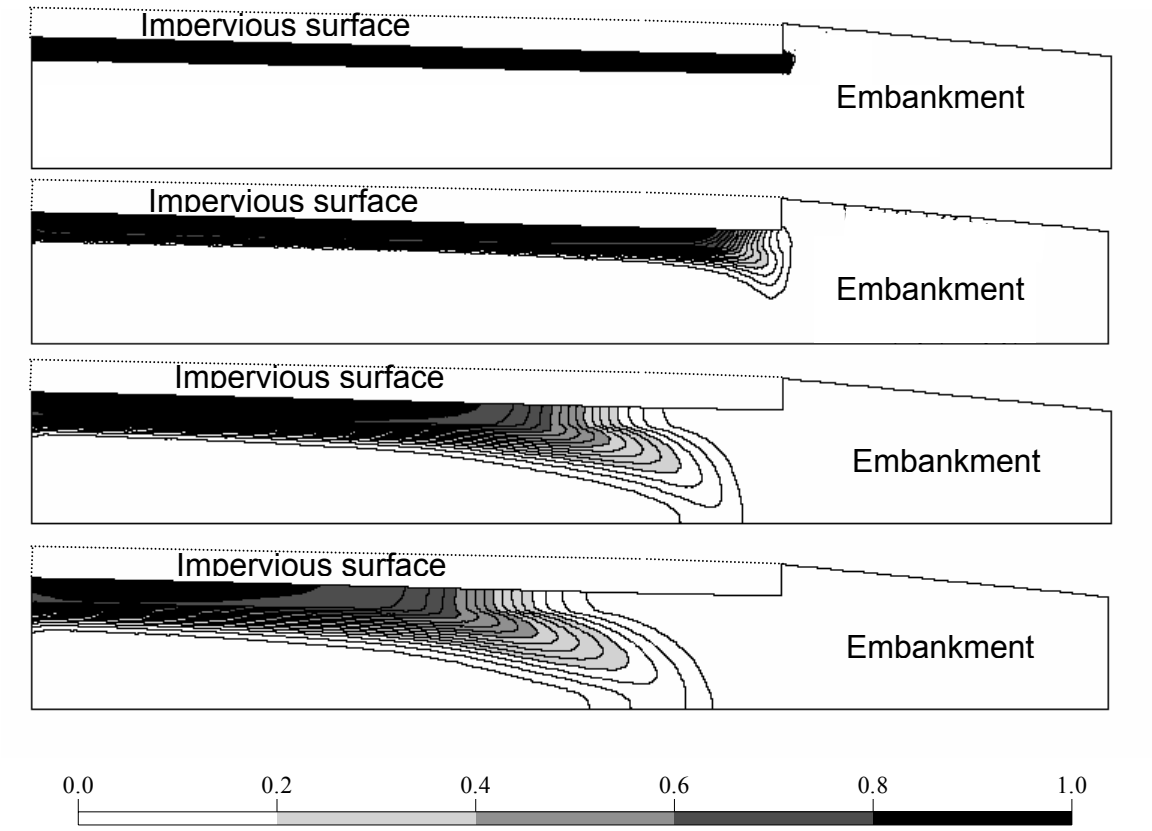

Figure 6.4 Aqueous salt concentrations in an intact pavement initially, after 1 year, after 10 years and after 20 years. Concentrations are normalized to initial aqueous concentration in the base layer.

Closer to the edge, downward transport of salts is faster than in the vicinity of the centerline because of higher vertical velocities close to the embankment (Figures 6.3 and 6.4). The mobility of salts under the shoulder in the base layer is dominated by advection since concentration profiles from simulations with and without diffusion show no difference in this region (Figure 6.5). However, downward velocities in the base layer under the lane are low enough that the contribution of diffusion to transport of salts can be observed.

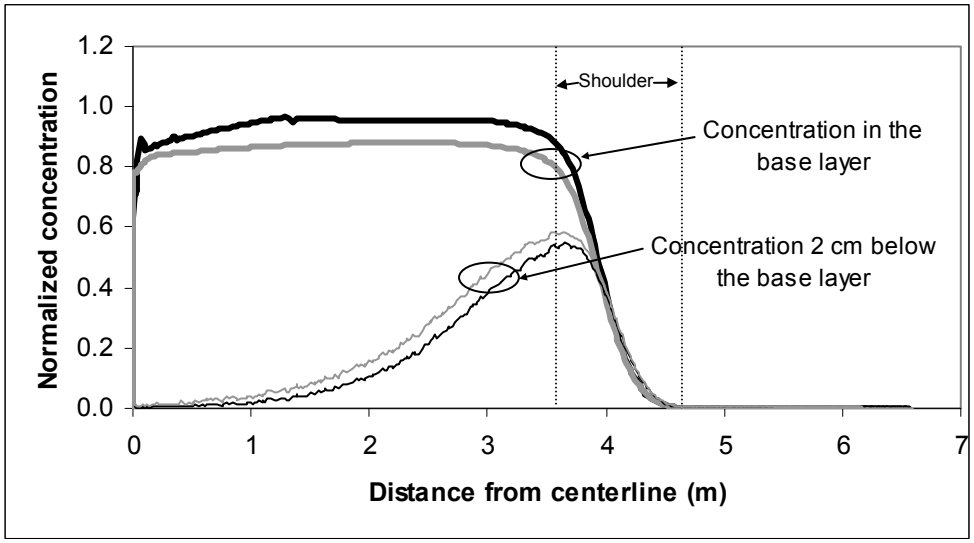

Figure 6.5 Cross section profile of concentration in (thicker lines) and below (thinner lines) the base layer after 3.6 years for two different simulations: with diffusion (gray line) and without diffusion (black line).

If neither diffusion nor advection had been occurring, the normalized aqueous concentration across the width of the pavement (i.e. zero to 4.6 m away from the centerline) would have a value of one in the base layer and zero below the base layer. Depletion of salts in the base layer within less than a meter from the edge causes higher concentrations right below (Figure 6.5). Closer to the edge there is no significant difference between concentration profiles when diffusion is not considered in calculations. Further away from the edge, there is clear difference between simulations that considered diffusion and omitted it from calculations: in the latter case, concentrations are higher in the base layer and lower in the subgrade. While spatial distribution of Peclet numbers were not calculated in the model domain, Figure 6.5 clearly demonstrates that diffusion

may play a significant role under the lane whereas advective velocities determine the mobility of the salt under the paved shoulder.

Effect of a Centerline and a Shoulder Joint on Hydrology and Contaminant Release

Water movement and contaminant transport under a centerline joint and a shoulder joint are significantly different. Located at the highest elevation, the centerline joint receives only the precipitation that falls directly on top of it and is thus not a major water influx route for the pavement. The precipitation that falls on the impervious lane becomes runoff and moves from the centerline towards the edge due to the two percent slope. Therefore, the shoulder joint is exposed to much greater amounts of water than any other crack upslope of it. HYDRUS2D simulations showed that over a period of 20 years, the infiltration capacity of the shoulder joint allowed ten percent of the precipitation upslope of it to infiltrate into the pavement. The infiltration rate of the shoulder joint varied from 0.03 to 0.45 m^3/day per meter of joint length as a function of the base and subgrade hydrology and the rain intensity. Measured infiltration rates reported by Ridgeway et al. (1976) (0.005-1.5m^3/day per meter of crack length) and Birgisdottir et al. (in preparation) (0.05 m^3/day per meter of crack length) were similar.

Large influxes of water through the shoulder joint are dissipated both vertically and laterally under the crack. At the initial stages of the precipitation

the water is distributed laterally (Figure 6.6a) to both sides in the base layer. As precipitation continues, the edge effect interferes with the velocity profile around the shoulder joint and most of the water is directed towards the centerline (Figure 6.6b).

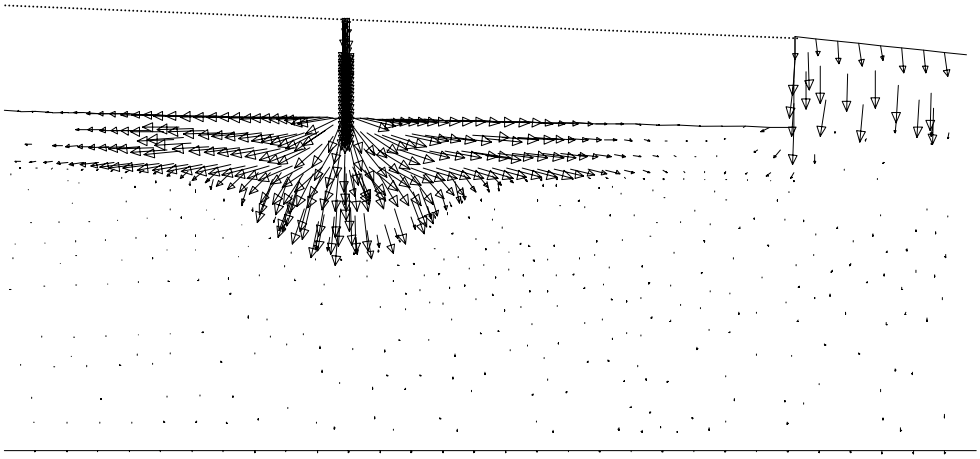

(a)

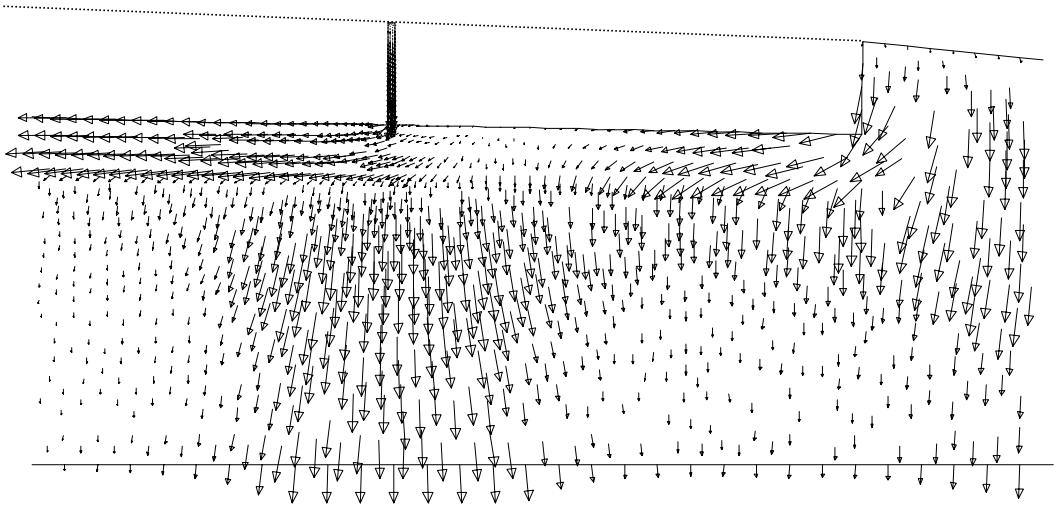

(b)

Figure 6.6 Velocity vectors around the shoulder joint at the early (a) and later (b) stages of a rain event.

In presence of a shoulder joint, the salts in the base layer are washed out fastest at the edges and the region under the shoulder joint (Figure 6.7). The low aqueous concentration zone formed under the shoulder joint expands to almost one meter within one year.

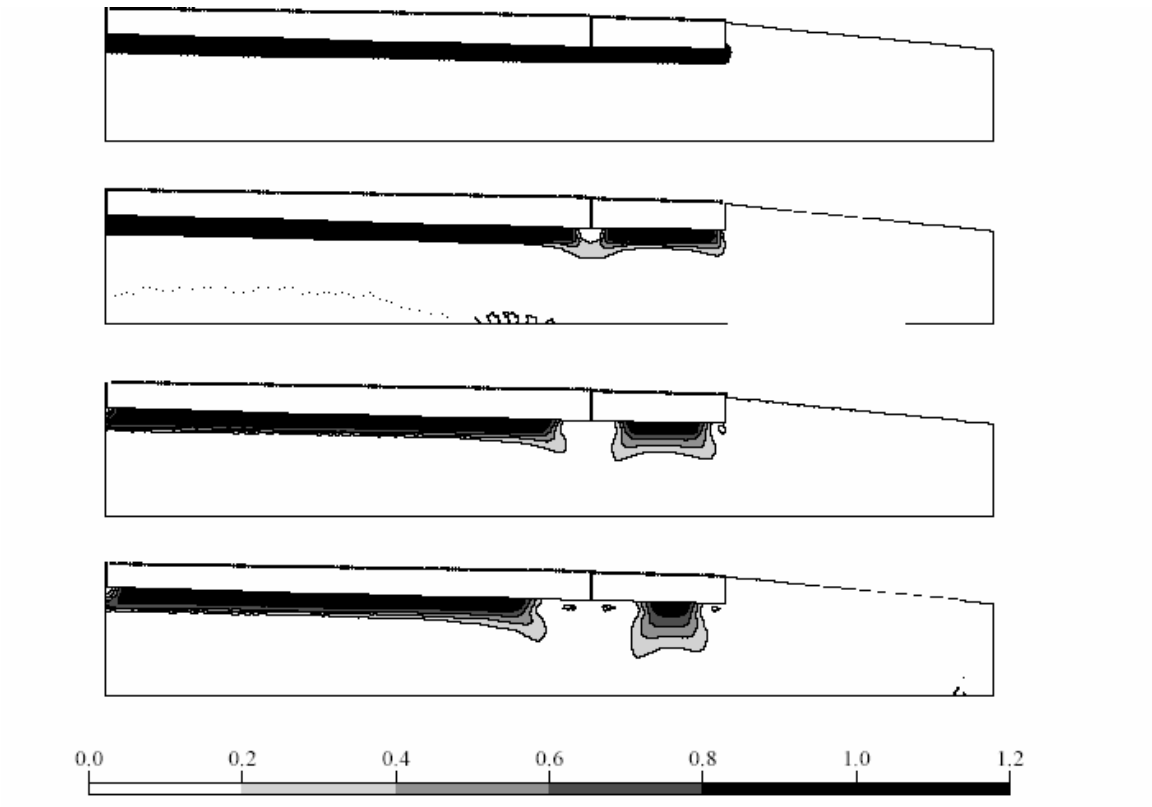

Figure 6.7 Normalized salt concentrations in a pavement with two cracks. Progression of salt depletion under the shoulder joint is shown for time zero, after one month, after six months, and after one year.

Percentage of Initial Mass Reaching Groundwater

Regulators might be interested in knowing the total mass of contaminant that has reached the groundwater at a given time. A generic way of presenting this type of information is shown in Figure 6.8 which indicates that less than 10 % of the initial mass of contaminant in the base layer reaches the groundwater after 20 years for all scenarios except scenario 1. Scenarios 6 and 18 were not included in the figure because the fractions of initial mass reaching groundwater for these two scenarios were less than 10^{-21} and 10^{-30}, respectively. To convert the fractions into more common units of mg contaminant released per kg of material, the fraction can simply be multiplied by the total mass of contaminant in the material. A calculation of this type also allows comparison of results from this modeling approach with other methods, such as the percolation/equilibrium model (Apul et al., in press).

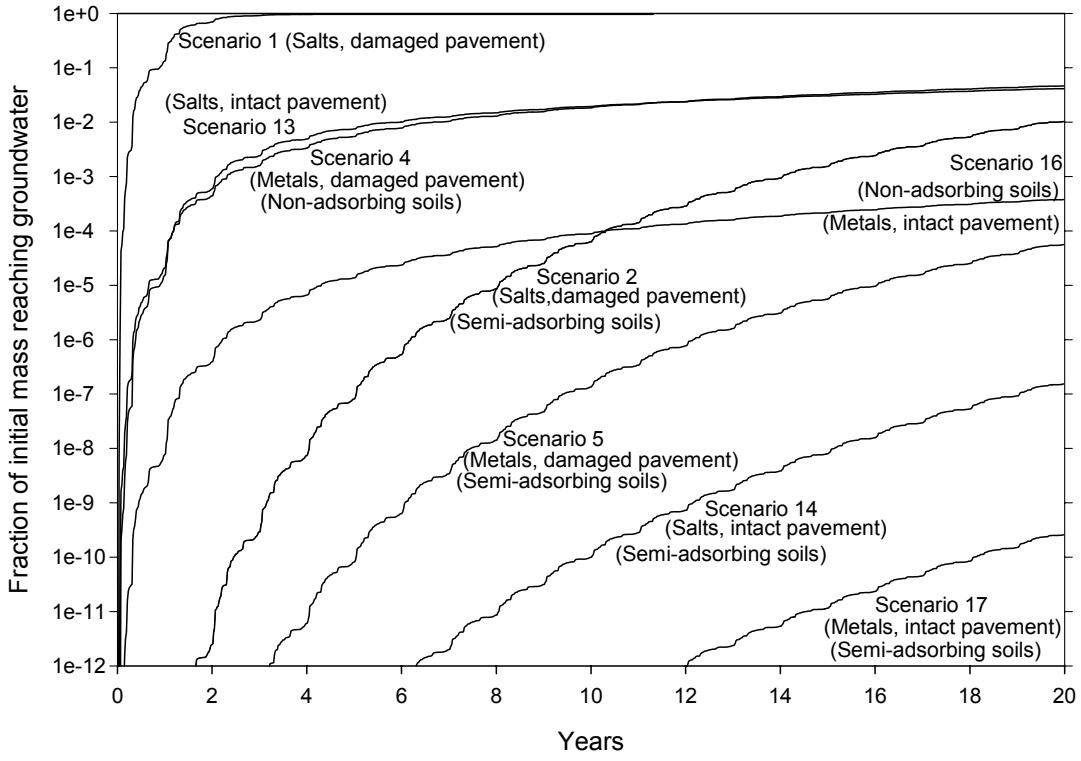

Figure 6.8 Fraction of initial total mass reaching groundwater for different scenarios.

In a totally damaged pavement, salts in the base layer are completely exhausted if they are not attenuated in the soil below (Scenario 1). However, only four percent of the salts reach the groundwater after 20 years if the pavement is intact (Scenario 13). The spatial distribution of remaining salts clearly indicate that the four percent of initial mass that has reached the groundwater have originated from the section under the shoulder (Figure 6.4). The time series for the fraction of metals reaching groundwater in a damaged pavement (Scenario 4) is very similar to the results obtained for salts in an intact pavement (Scenario 13). While the end result is the same, the release and

transport patterns are completely different because of differences in contaminant reactivity and pavement. conditions of the two scenarios. In the former, metals in the entire base layer are slowly advected towards the groundwater table in presence of strong retention; in the latter, salts are eroded from the edge without any significant retardation

Pore Water Concentrations Immediately above the Groundwater

Pore water concentrations immediately above the groundwater were normalized to initial contaminant contents to be able to express the results in a generic way. The normalized concentrations are given in Figure 6.9 for completely intact and totally damaged pavements. Concentrations represent average values for the model width. In other words, high concentrations reaching below joints and edges, low concentrations below other sections of the pavement, and zero concentrations below the embankment were spatially averaged. Concentrations fluctuate for intact pavement scenarios because of spatial averaging. The concentrations from intact pavements show a greater response to individual rain events because of localized high strength fluxes around the edge. Damaged pavements' responses are not as fluctuating because of more uniform transport of the contaminant from the pavement towards the groundwater.

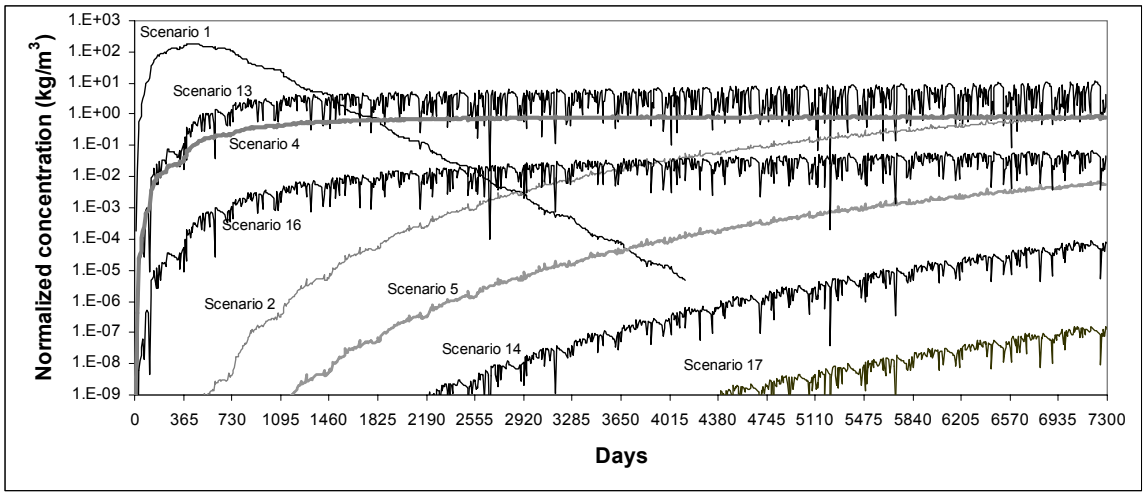

Figure 6.9 Average normalized pore water concentrations immediately above the groundwater.

In a totally damaged pavement built on non-adsorbing soils, concentrations of salts immediately above the groundwater increase until the first year after which they decrease because the center of mass of the plume has already reached the groundwater (Scenario 1). If the pavement is intact, the average normalized concentrations immediately above the groundwater increases until three years and then becomes steady (Scenario 13). The reason for steady concentrations in the intact pavement is the edge effect: erosion of salts from the edge towards the centerline supplies a constant flux of salts to the groundwater.

Steady state concentrations are observed also for metals in both damaged (Scenario 4) and intact (Scenario 16) pavements if the soil is non-adsorbing. The reason for steady state concentrations for these scenarios is different than the edge effect. When the soil is non-adsorbing and metals are strongly retained in the base layer, the release of metals from the base layer is the rate limiting step

for transport of metals towards the groundwater. As soon as the metal reaches the soil, it is easily transported in the subgrade with minimal retardation. The release rates of metals from the base layer are slower than their advection in the soil below resulting in steady state flux of metals into the groundwater.

The effect of adsorptive soils on concentrations above the groundwater is consistent across metals, salts, intact, and damaged pavement scenarios (Scenarios 2, 5, 14, and 17). Retardation in the subgrade causes contaminants to be transported very slowly and any continuous supply of contaminants from the base layer take a long time to reach groundwater. As a result concentrations reaching groundwater continue to increase during the 20 year period.

Example Calculations for Steel Slag

Example calculations are provided in this section to demonstrate how the model results can be applied to a secondary material. Steel slag was selected as the secondary material for the example because data was available for steel slag and its use in the U.S. may continue to grow.

The model calculations were based on the hydraulic properties of “Class 5” material. Therefore, model results are most applicable to those secondary materials that have similar hydraulic properties. Considering that the hydraulic conductivity curve for many pavement materials does not exist, particle size distribution is an alternative method for comparison. Model results can be applied to the use of electric arc furnace (EAF) steel slags in the base layer with

the justification that the size gradation of EAF steel slags is within the specifications for “Class 5” base material (Figure 6.10).

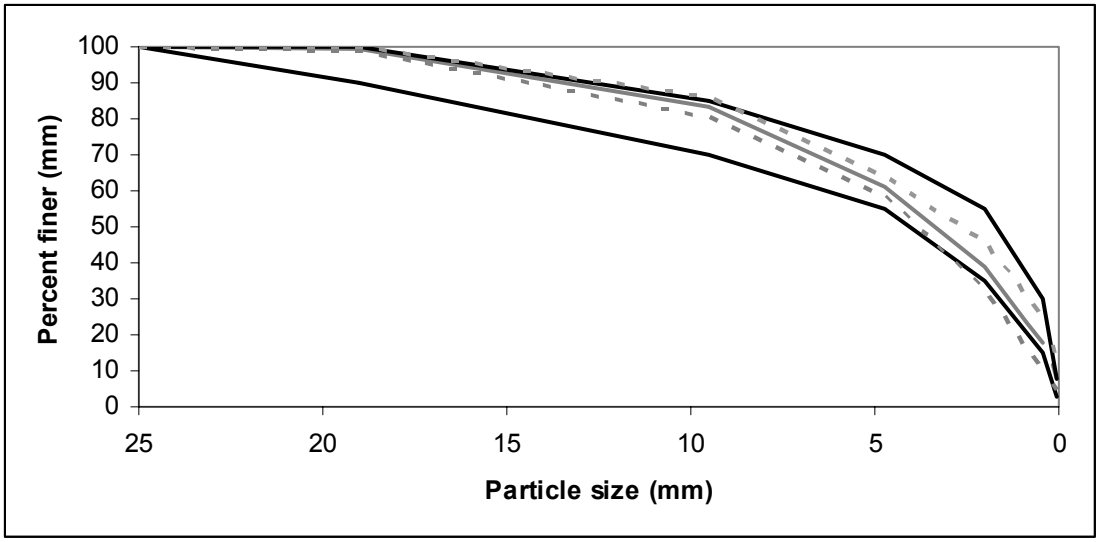

Figure 6.10 Particle size distribution for EAF steel slags from 48 different steel plants (Proctor et al., 2000) and class 5 specification. The mean value for steel slag and plus and minus one standard deviation are shown in gray. The range for class 5 specification is shown in black.

Proctor et al. (2000) measured K_d values for electric arc furnace steel slags under neutral conditions using the ASTM distilled water leachate test (ASTM Method D 3987) and reported that most of the metals (i.e. aluminum, antimony, barium, beryllium, cadmium, copper, iron, lead, manganese, molybdenum, nickel, selenium, silver, thallium, tin, vanadium, and zinc) had K_d values greater than 1000 L/kg with values in the order of 20-30 thousand for cadmium and lead. Aqueous extraction of arsenic and mercury were within the same order of magnitude but slightly lower with K_d values 819 L/kg and 900 L/kg, respectively. Therefore, a K_d value of 1000 L/kg used in the model for the base

layer is a “conservative” representation of the partitioning of metals in EAF steel slags. The results from the model should be within the same order of magnitude or higher than what would be expected in the field.

One way to interpret model estimates is to convert normalized concentrations to appropriate metals concentrations which can then be compared to EPA’s maximum contaminant levels (MCL). Such a comparison is conservative considering that the concentrations immediately above the groundwater as estimated in the model will be diluted further once they enter the aquifer. In this steel slag example, the dilution of the concentrations was not included in the comparison as the extent of dilution is site specific.

The worst case example is the completely damaged pavement underlay by non-adsorbing soils. The normalized concentration for this scenario gradually increases from 0.5 kg/m^3 to 0.8 kg/m^3 from the third year until the 20^{th} year (Figure 6.9). As an example, the maximum total arsenic content of steel slags is 5.8 mg/kg (Proctor et al., 2000); multiplied by the higher end of the normalized concentration (0.8 kg/m^3), the pore water concentration of arsenic immediately above the groundwater would be 0.005 mg/L which is lower than the arsenic MCL (0.01 mg/L).

If the pavement was maintained well such that it remained intact throughout the 20 year period, the highest normalized concentration reaching groundwater would be at least a magnitude lower at 0.05 kg/m^3. For such a

scenario, the corresponding aqueous arsenic concentration is 0.00029 mg/L, which is at least two orders of magnitude lower than the MCL.

Other example calculations for EAF steel slags are presented in Table 6.2. Both the maximum and the minimum metal contents reported in Proctor et al. (2000) were used in calculations. Comparison of damaged and intact pavement results show that the condition of the road may affect the concentration estimates by less than two orders of magnitude. The value of K_d used in simulations has a greater affect on the concentrations reaching groundwater.

Concentrations within one order of magnitude of the MCL are shown in bold in Table 6.2. If the pavement is built on highly adsorbing soils, the concentrations reaching groundwater are more than several orders of magnitude lower than the MCLs.

Moderately adsorbing soils can also attenuate the metal concentration reaching groundwater to much lower values than the MCLs. Estimates from the damaged pavement and any of the other worse case scenarios are higher than the MCLs for total chromium and manganese. However the K_d value of the base layer (1000 L/kg) used in the model was more than two orders of magnitude lower than the reported K_d values for these two metals (544105 L/kg and 14953635 L/kg). It is possible that the simulation results overestimated the concentrations reaching groundwater by many orders of magnitude for chromium and manganese.

Non-adsorbing soils are not expected to be encountered frequently and they represent the extremely cautious viewpoint of a regulator. If the groundwater dilution-attenuation effect is not considered, all the metals analyzed except for mercury, may reach concentrations within one order of magnitude proximity to the MCL after the third year of pavement construction. If such an extreme scenario may be considered to be relevant, a site specific assessment may be necessary.

Table 6.2 Concentrations immediately above the groundwater calculated from maximum values of normalized concentrations and maximum metal contents

	Max. metal content (mg/kg)	Min. metal content (mg/kg)	MCL (mg/L)	Damaged pavement, non-adsorbing soils		Intact pavement, non-adsorbing soils		Damaged pavement, semi-adsorbing soils		Intact pavement, semi-adsorbing soils		Damaged pavement, highly adsorbing soils		Intact pavement, highly adsorbing soils	
				Max	Min	Max	Min	Max	Min	Max	Min	Max	Min	Max	Min
Normalized max. conc. reaching groundwater				0.8 kg/m^3		0.05 kg/m^3		0.0064 kg/m^3		1.3E-7 kg/m^3		3.87E-20 kg/m^3		7.42E-27 kg/m^3	
As	5.8	0.5	1.0E-02	**4.6 E-03**	4.E-04	2.9E-04	3.E-05	3.7E-05	3.E-06	7.5E-10	7.E-11	2.2E-22	2.E-23	4.3E-29	4.E-30
Ba	1800	160	2.0	**1.4E+00**	1.E-01	9.0E-02	8.E-03	1.2E-02	1.E-03	2.3E-07	2.E-08	7.0E-20	6.E-21	1.3E-26	1.E-27
Be	6.3	0.6	4.0E-03	**5.0E-03**	**5.E-04**	**3.2E-04**	3.E-05	4.0E-05	4.E-06	8.2E-10	8.E-11	2.4E-22	2.E-23	4.7E-29	4.E-30
Cd	19	0.1	5.0E-03	**1.5E-02**	8.E-05	**9.5E-04**	5.E-06	1.2E-04	6.E-07	2.5E-09	1.E-11	7.4E-22	4.E-24	1.4E-28	7.E-31
Cr total	6200	320	1.0E-01	**5.0E+00**	**3.E-01**	**3.1E-01**	**2.E-02**	**4.0E-02**	2.E-03	8.1E-07	4.E-08	2.4E-19	1.E-20	4.6E-26	2.E-27
Cu	540	62	1.3	**4.3E-01**	5.E-02	2.7E-02	3.E-03	3.5E-03	4.E-04	7.0E-08	8.E-09	2.1E-20	2.E-21	4.0E-27	5.E-28
Pb	220	4.5	1.5E-02	**1.8E-01**	4.E-03	**1.1E-02**	2.E-04	1.4E-03	3.E-05	2.9E-08	6.E-10	8.5E-21	2.E-22	1.6E-27	3.E-29
Hg	0.1	0.1	2.0E-03	8.0E-05	8.E-05	5.0E-06	5.E-06	6.4E-07	6.E-07	1.3E-11	1.E-11	3.9E-24	4.E-24	7.4E-31	7.E-31
Se	36	7.5	5.0E-02	**2.9E-02**	**6.E-03**	**1.8E-03**	4.E-04	2.3E-04	5.E-05	4.7E-09	1.E-09	1.4E-21	3.E-22	2.7E-28	6.E-29
Zn	690	31	5.0*	**5.5E-01**	2.E-02	**3.5E-02**	2.E-03	4.4E-03	2.E-04	9.0E-08	4.E-09	2.7E-20	1.E-21	5.1E-27	2.E-28
Mn	63800	18900	5.0E-2*	**5.1E+01**	**2.E+01**	3.2E+00	**9.E-01**	**4.1E-01**	**1.E-01**	8.3E-06	2.E-06	2.5E-18	7.E-19	4.7E-25	1.E-25

*Secondary contaminant level

CONCLUSIONS

I developed a scientific generic approach for regulators to evaluate the impacts of virgin and secondary materials on groundwater contamination. HYDRUS2D simulation results for various scenarios showed that contaminants with high K_d values (1000 L/kg in base layer and 2500 L/kg in underlying soil) are retained in the base layer, while contaminants with low K_d values (1 L/kg in the base and underlying soil) are easily released and can reach the groundwater within a few years. This work also showed that the magnitude and spatial distribution of contaminant fluxes depend on the condition of the surface of the pavement. Model results expressed for various scenarios as normalized concentrations immediately above the groundwater and fraction of initial mass reaching groundwater can be used for any type of recycled material with the assumption that the hydraulic properties will not be significantly different.

REFERENCES

1. Ahmed, Z., White, T.D., and Kuczek, T. (1997). Comparative field performance of subdrainage systems. Journal of Irrigation and Drainage Engineering. 123(3):194-201

2. Apul, D.S., Gardner, K.H. and Eighmy, T.T. (2004) "Implications of roadway water movement for beneficial use of recycled materials," in *The Handbook of Environmental Chemistry, Water Pollution Series (Volume 5): Environmental Impact Assessment of Recycled Hazardous Waste Materials on Surface and Ground Waters: Chemodynamics, Toxicology, Modeling and Information System*, T. A.T. Aboul-Kassim and K.J. Williamson, Editors, Springer-Verlag (In Press).

3. Apul, D.S., Gardner, K., Eighmy, T., Linder, E., Frizzell, T., and Roberson, R. (in press) "Probabilistic modeling of one dimensional water movement and leaching from highway embankments containing secondary materials," *Environmental Engineering Science.*

4. Apul, D.S., Gardner, K., Eighmy, T., Comans R., and Fallman A-M. "Simultaneous application of dissolution/precipitation and surface complexation / precipitation modeling to contaminant leaching from weathered steel slag," submitted to Environmental Science and Technology.

5. Bigl, S. R. and R. L. Berg (1996). Testing of Materials from the Minnesota Cold Regions Pavement Research Test Facility, CRREL: 38.

6. Birisdottir, H., Apul, D., Christensen, T., Gardner, K, and Eighmy, T. A spreadsheet model for water movement in highways, in preparation for Waste Management.

7. Carsel, R.F. and Parrish, R.S. (1988). Developing joint probability distributions of soil water retention chacateristics. Water Resources Research, 24, pp. 755-769

8. Davis, J.A., Coston, J.A., Kent, D.B. and Fuller, C.C., (1998) Application of the surface complexation concept to complex mineral assemblages. Environmental Science and Technology, 32(19): 2820-2828.

9. De Haan, I. H. D., Fraaij, A. L. A., and Molenaar, A.A. (2003). Unsaturated water transport in secondary road building materials. In T.T. Eighmy, Eds., *Beneficial use of recycled materials in transportation applications*. Air & Waste Management, Washington, D.C., pp. 215-224.

10. Dijkstra, J.J., van der Sloot, H.A., and Comans, R. (2002) Process identification and model development of contaminant transport in MSWI bottom ash. Waste Managements. 22, pp. 531-541.

11. Fallman, A.-M. (2000). Leaching of chromium and barium from steel slag in laboratory and field tests – a solubility controlled process? Waste Management. 20, pp 149-154

12. Fallman, A-M. (1996) Characterization of residues: Release of contaminants from slags and ashes. Department of Physics and Measurements Technology. Linkoping University, S-581 83. Linkoping Studies in Science and Technology, Dissertation No. 486. Linkoping, Sweden.

13. Fetter, C.W. (1999) Contaminant Hydrogeology, 2nd Edition, Prentice Hall, Upper Saddle River, NJ

14. Fruchter, J.S., Rai, D. and Zachara, J.M., (1990) Identification of solubility-controlling solid phases in a large fly ash field lysimeter. Environmental Science and Technology, 24(8): 1173-1179.

15. Kosson, D.S., van der Sloot, H., and Eighmy, T.T. (1996). An approach for estimation of contaminant release during utilization and disposal of municipal waste combustion residues. Journal of Hazardous Materials. 47, pp 43-75.

16. Lie, Y-H., and Gregory, S. (1974) Diffusion of ions in sea water and in deep-sea sediments. Geochimica et Cosmochimica Acta. 38, pp. 703-714

17. Meima, J. A. and R. N. J. Comans (1998). “Application of surface complexation/precipitation modeling to contmainant leaching from weathered municipal solid waste incinerator bottom ash.” Environmental Science and Technology 32: 688-693.

18. Millington, R.J. and Quirk, J.M. (1961). Permeability of porous solids. Trans. Faraday Soc. 57, 1200-1207

19. Proctor, D. M, and Fehling, K.A., and Shay, E.C., Wittenborn, J.L., Green, J.J., Avent, C., Bigham, R.D., Connolly, M., Lee, B., Shepker, T.O., and

Zak, M.A. (2000) Physical and chemical characteristics of blast furnace, basic oxygen furnace, and electric arc furnace steel industry slags, Environmental Science and Technology, 2000, 34(8), pp. 1576-1582

20. Ridgeway, H. (1976) Infiltration of water through the pavement surface. Transportation Research Record. 616:98-101

21. Sato, H., Yui, M., and Yoshikawa, H. (1996) Ionic diffusion coefficients of Cs:, Pb^{2+}, Sm^{3+}, Ni^{2+}, SeO_4^{2-} and TcO_4^{-} in free water determined from conductivity measurements. Journal of Nuclear Science and Technology. 33(12), pp. 950-955

22. Schaap, M.G., Leij F.J., van Genuchten M.T. (2001) ROSETTA: A computer program for estimating soil hydraulic parameters with hiererchical pedotransfer functions. Journal of Hydrology. 251(3-4)163-176

23. Simunek, J., Sejna, M. and Van Genuchten, M.T. (1999). The HYDRUS-2D software package for simulating the two-dimensional movement of water, heat, and multiple solutes in variably-saturated media, version 2.0, U.S. Salinity Laboratory, Riverside, CA

24. van Genuchten (1980) A closed-form equation for predicting the hydraulic conductivity of unsaturated soils. Journal of Soil Science Society of America. 44, pp. 892-898.

25. van Genuchten, M.T., Leij, F.J., and Yates, S.R. (1991) The RETC Code for Quantifying the Hydraulic Functions of Unsaturated Soils, Version 1.0. EPA Report 600/2-91/065, U.S. Salinity Laboratory, USDA, ARS, Riverside, California.

26. U.S. EPA. (1999). *Understanding variation in partition coefficient, Kd, values Volume II: Review of geochemistry and available Kd values for cadmium, cesium, chromium, lead, plutonium, radon, strontium, thorium, tritium (3H), and uranium.* EPA 402-R-99-004B. Washington, D.C.

27. Research Triangle Park (RTI) (2000). Risk assessment for the listing determinations for inorganic chemical manufacturing waste: Background document. RTI Project Number 92U-7780.001.022. EPA Contract Number 68-W-98005

28. U.S.EPA (2003) Multi-media, multi-pathway, multi-receptor exposure and risk assessment (3MRA) model. http://www.epa.gov/ceampubl/mmedia/3mra/